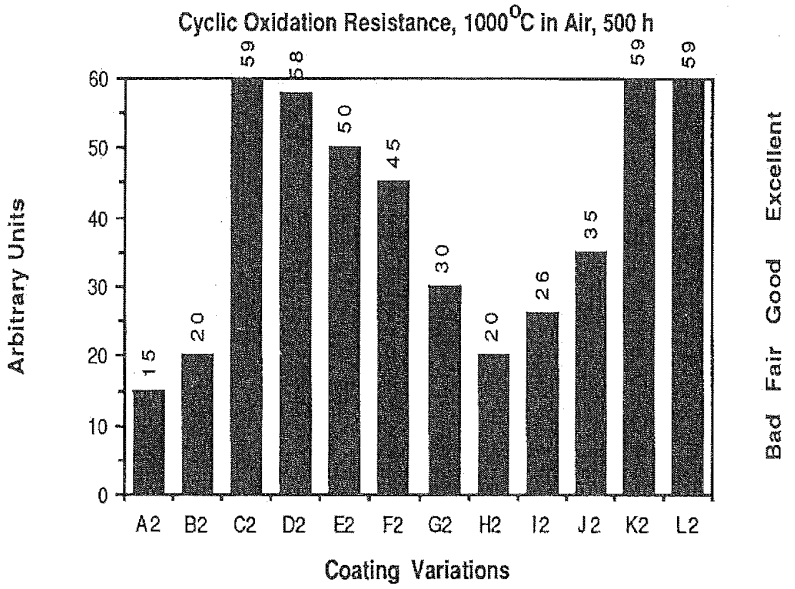

Fig.8-13

Legend	Substrate	Coating & Conditions
A2	*	CrAl
B2	*	CrTiSi
C2	*	CoNiCrAlY
D2	Co17Cr12Al0.8Y	
E2	Co25Cr6Al0.5Y	
F2	*	Co26Cr11AlY
G2	*	CoCrAlTaY
H2	*	NiCrAl
I2	Ni17Cr11Al0.5Y	
J2	*	NiCrAlSiY
K2	*	NiCrAlY + Pt(PVD-sputtered)
L2	*	NiCrAlY + Al (PVD +pack)

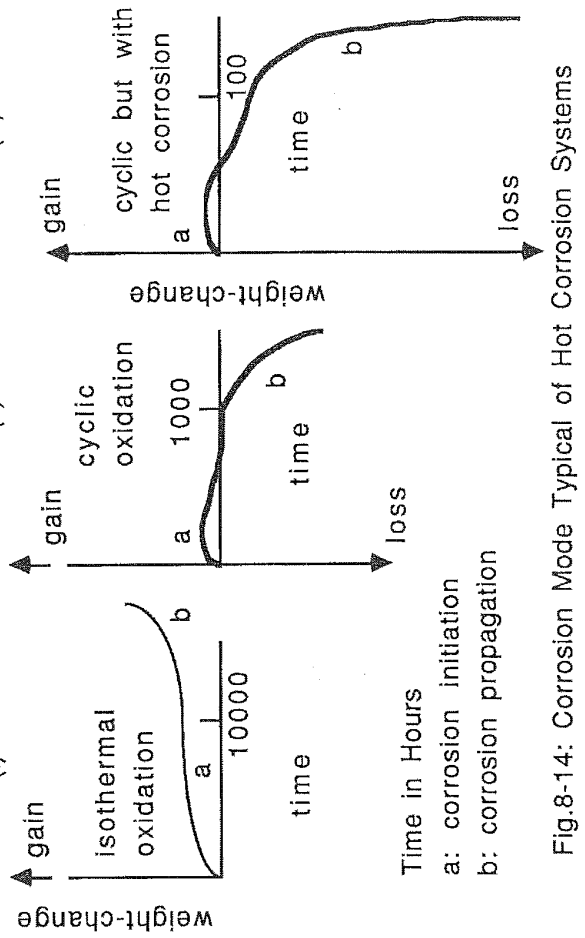

Fig.8-14: Corrosion Mode Typical of Hot Corrosion Systems

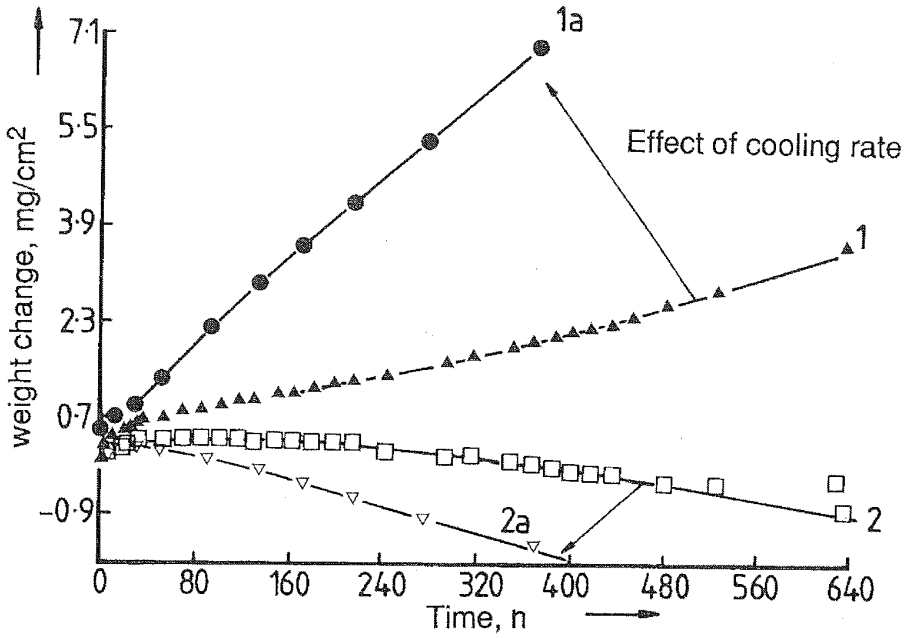

Fig.8-15: Cyclic Oxidation of CoCrAl & NiCrAl Alloys. Cooling Rate Effect.
(Nicoll 1984)

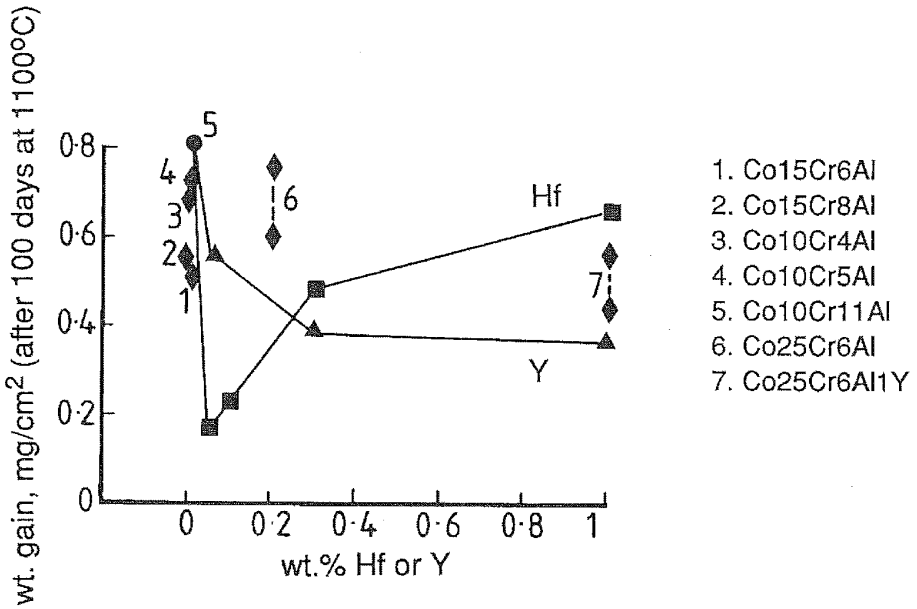

Fig.8-16: Co-10Cr-11Al at 1000°C for 100 h in Air. Effects of Hf & Y.

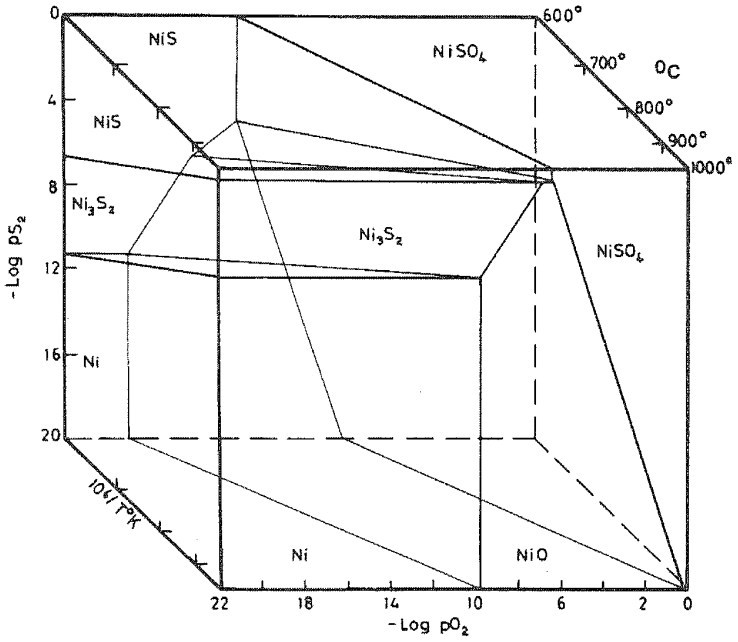

Fig.8-17a: Existence Diagram for the System Ni-S-O

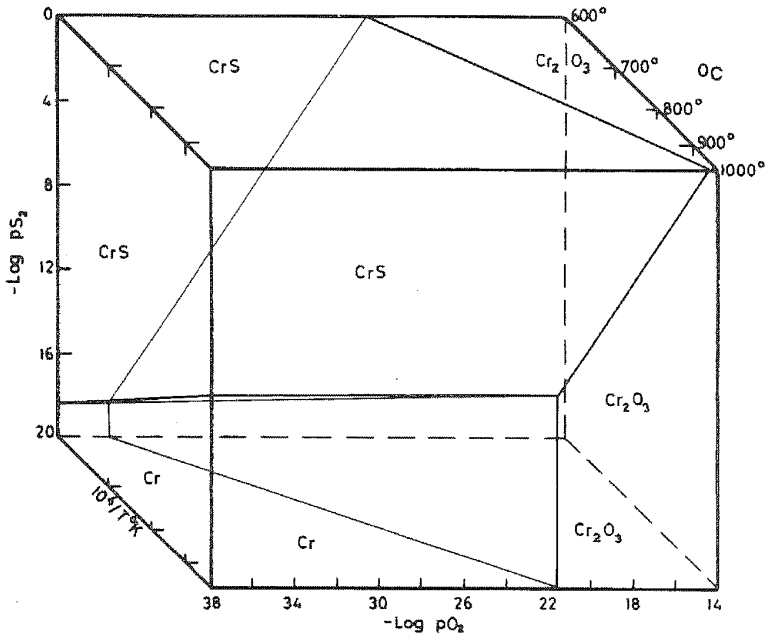

Fig.8-17b: Existence Diagram for the System Cr-S-O

600° - 1000°C

8.5. OXIDATION & HIGH TEMPERATURE CORROSION

Oxidation is often used to refer to corrosion in general, in addition to expressing degradation as a result of reaction with oxygen. Many of the early concepts, e.g. the classic Wagner model for diffusion and the Pilling and Bedworth ratio of scale to substrate molecular/atom volume ratio, evolved using oxides as examples. However, high temperature reactions have become quite complex and the simple framework indicated in the previous section has to be considered with respect to many systems undergoing corrosion simultaneously. The outcome of a reappraisal may indicate the several features which need to be addressed for scale growth, composition and stability (Rahmel et al 1985):

1. Adsorption, nucleation and initial stages of oxidation (Grabke 1985).
2. Complex defects in metal oxides and sulphides; their nature and transport mechanism (Hobbs 1985).
3. Lattice, line defect and grain boundary transport mechanism (Atkinson 1985).
4. Transport of gaseous species in growing oxide scales (Mrowec 1985).
5. Atomistics of scale growth at the scale/gas interface (Rapp 1985).
6. Lateral growth in oxide scales (Smeltzer 1985; 1987).
7. Adhesion mechanisms - the reactive element effect (Stringer 1985; Moon & Bennett 1987).
8. Key mechanical properties of oxidising components in maintaining scale integrity (Manning 1985).
9. Interaction between oxidation, sulphidation, carburization and creep (Ilschner & Scutze 1985).
10. Internal and intergranular oxidation of alloys (Yurek 1985).
11. Influence of impurities such as sulphides on the transport properties and nature of oxide scales (Wagner 1985).
12. Faults,fissures and voids in scales (Graham 1985).
13. Role of chlorides in high temperature corrosion (Hancock 1985).
14. Hot corrosion (Pettit 1985).
15. Role of oxides in abrasion, erosion and wear (Stott 1985).
16. Oxidation of compounds (Schmalzreid 1985).
17. New methods for studying high temperature corrosion, particularly in situ methods (Rahmel 1985).

It is beyond the scope of this review even to summarise the outcome of the above appraisal; coatings are an integral part of a high temperature system as more and more high temperature structural components are coated. Many of the available studies are conducted on individual candidate materials with a view to their utility as coatings, and later followed up by both corrosion and mechanical property studies in a substrate/coating mode. Information condensed herein must be viewed as such.

Oxide layers are not always protective although they predominate scale morphology in most respects. They are liable to damage, non-stoichiometry, mixed phases and stresses and present a complex diffusion pattern depending on scale morphology. Thus oxidation has to be viewed in many aspects w.r.t. scale growth, where plasticity is affected (Douglass 1969), where stresses generated in columnar scales lead to pit formation (Louat & Sadananda 1987), or lamellar stresses which occur in plasma spray coatings affect its adhesion and transport properties (Knotek & Elsing 1987) . Defects in oxide scales influence transport properties, and at intermediate temperatures short-circuit diffusion paths can take over and become the predominant mode (Gesmundo 1987; Moon & Bennett 1987; Moon 1987; Atkinson 1985; Gesmundo et al 1985; Chadwick & Taylor 1984, 1982). The marked influence which elements like Y and Ce have has been argued on the basis of pegging (Stringer 1987; Pendse & Stringer 1985). But increasing evidence appears to come from effects of grain boundary diffusion and nucleation (Moon & Bennett 1987; Smeggil 1987). Oxides of Ce, La and Y exert a strong influence on oxide composition, adhesion and the scale growth direction of Cr_2O_3-formation; the effect is more pronounced on Ni-25Cr than the Co-25Cr (wt.%) alloys at 1000^{o} and $1100^{o}C$, and in this case the 'peg' theory does not apply (Hou & Stringer 1987). A similar effect was observed on stainless steels doped with Y, Ce and La enhancing oxidation resistance while Hf and Zr offered no benefit (Landkof et al 1984).

Dispersed oxides of Mg, La and Y and element Y in plasma sprayed NiCrAl coatings at $1150^{o}C$ and $1225^{o}C$ showed that yttrium oxide gave the best oxidation resistance which was influenced by the size and distribution of the oxide particles (Luthra & Hall 1986). La was ascribed to provide a diffusion barrier layer as Cr^{3+} diffused 40 times slower in $LaCrO_3$ than in Cr_2O_3 in Cr-La alloys (Tavadze et al 1986). Y_2O_3 dispersoids were found to influence the microstructure rather than providing oxide nucleation sites for Ni-20Cr in low pO_2 of 10^{-19} to 10^{-24} at $1000^{o}C$. It reduced Cr-evaporation, the oxide grain size and porosity (Braski et al 1986). A small amount of impurities enriched at grain boundaries may greatly affect the deformation characteristics and influence the mechanical and transport properties of the growing scales (Kofstad 1985). Implanted Y in chromia-forming Co-45 wt.% Cr alloys exhibited a x100 reduction in oxidation rate at $1000^{o}C$ in pure O_2, with the mechanism of chromia growth changing from cation to anion diffusion, and Y-segregation at Cr_2O_3 fine-grain boundaries. A solute-drag effect is proposed as the mechanism (Przybylski et al 1988a,b; Przybylski & Mrowec 1984).

Embrittlement, break-away oxidation, internal oxidation are a few other detrimental effects. Hydrogen embrittlement is a well-recognised form of corrosion in aqueous systems. Water vapour can play a large part in high temperature embrittlement as also H_2 and O_2. Thus pre-oxidation, envisaged as a means of prolonging the initiation stage of hot corrosion may not always be beneficial. Ni undergoes oxygen-embrittlement at high temperature; the

onset of embrittlement is dependent on the pO_2. Results on Inconel 718 seemed to indicate that the first stage oxidation process occurs at the grain boundaries before chromia formation influenced embrittlement (Andrieu & Henon 1987). An inverse phenomenon can occur in alloys prone to break-away oxidation. In 9Cr-1Mo steels, general oxidation occurs at 500-600°C and above 700°C Cr_2O_3 is the dominant oxide (Khanna et al 1986). Such preferential temperature-dependent scale development is not uncommon in Ni- and Co-base superalloys.

A side-step development of a 20Cr/25Ni/Nb steel precluding Al in the Fe-base alloy is reported. The wt.% steel composition was 19.9Cr , 24.6Ni, 0.7Nb, 0.6Mn, 0.56Si, 0.04C, balance Fe, which was first selectively oxidised in a 20% cold worked condition in a 50:1 H_2:H_2O for 2 hours at 800°C or 1hour at 930°C. The scales which developed were Fe- and Ni- free, with an average of 0.4 - 0.8 microns of Cr_2O_3. The alloy showed improved resistance to oxidation and carburization. Its sulphidation resistance is not reported (see Fig.8-19) (Bennett et al 1984). Implantation of Ce and Y reduced the oxidation rate consistently by more than 50% at 750°-950°C (Bennett & Tuson 1988/89). Alloying Ce (0.001-1.00 wt.%) and CeO_2 had a similar beneficial effect on Fe-(10-20)Cr alloys at 1000°C, pO_2 0.13 bar (Rhys-Jones 1987). Ceria dispersion added by jet injection to carbon steel was beneficial to oxidation of carbon steel (Tiefan et al 1984).

Ni- and Co-base superalloys generally are formulated to be preferential chromia- or alumina-forming variety. The degradation modes of MCrAl-coatings will be summarized later in this chapter. There are many studies on their oxidization behaviour (Wood & Whittle 1967; Wood & Hobby 1969; Wood et al 1970, 1971; Benard 1964; Kubaschewski & Hopkins 1961). Co effect on the oxidation of Ni-base alloys was found to lower the cyclic oxidation resistance on high-Cr alloys and was to be an optimum 5% to be effective in Al-containing alloys when tested in static air at 1000°, 1100° and 1150°C. The ratio Cr/Al decides the Cr_2O_3/chromite spinel (Cr/Al>3.5) or the Al_2O_3/aluminate spinel (Cr/Al <3.0), with the latter having a better resistance to cyclic oxidation. Refractory metal additions (Ta, Nb, W and Mo) were beneficial, with Ta the most effective. In all cases, any factor which promoted NiO formation resulted in scale breakdown (Barrett 1986)

Ti, as a light , high temperature metal is a prime candidate for aerospace vehicle systems. The metal oxidizes readily and also is prone to embrittlement (Shenoy et al 1986; Strafford et al 1983; Datta et al 1983; Strafford 1983; Datta et al 1984). It is found to manifest a moving boundary parallel to the interface as the two oxides change in proportion (Unnam et al 1986). Coatings of Al by EB, sputtered SiO_2, and CVD silicate via silane and borane, and mixed coatings of Al with the latter two were tested on Ti-6Al-2Sn-4Zr-2Mo foils and oxidized. Al+SiO_2 presented the best barrier layer performance with no effect on its mechanical properties (Clark et al 1988). Amorphous metals are not widely studied for their high temperature characteristics. Ti, Zr and Hf

affected void formation at the interface in a Ni_3Al-0.1B alloy. Hf addition was the most effective in promoting a protective oxide layer (Taniguchi & Shibata 1986). Studies on a rapidly solidified Ta-Ir alloy at 500 and 700°C are also reported. Ta was selectively oxidized, while the Ir coalesced into platelets of Ir-rich crystalline alloy oriented roughly parallel to the oxide-alloy interface. Although the unoxidized core remained in the glassy state, dissolved oxygen and the oxidation process had embrittled it (Cotell & Yurek 1986). Spectacular stratified oxidation layers develop on Ti (760°, 960°), Ta (900°) and Nb (450°, 600°C), in pure oxygen as demonstrated by Rousselet et al (1987).

8.6. HOT CORROSION

Hot corrosion has been variously defined but always involves the presence of sulphur species in the environment. Hot corrosion attack is recognized by the fact that a protective layer loses its resistance characteristics to shield the system it covers and this may lead to catastrophic failure. In general, the useful life of a coating in a corrosive atmosphere is very much a factor of time. There is a period over which it develops a protective scale; once the protective coating forms, its endurance to stress and temperature changes decides the subsequent breakdown of the scale. Coating degradation can be rapid or restrained, depending on the coherence, plasticity and shock proof qualities of the outer scale, the stability and compactness, free of voids of the intermediate scale, and, the stress and embrittlement accommodation and adherence of the scale/metal interface. Hot corrosion aggravates the scale breakdown mode and occurs in two recognizable stages, and it is particularly severe where a liquid phase is involved, irrespective of whether it is a fluid product or a fluid reactant.

Monitoring coating life thus can be considered in two stages:

Stage 1 - Scale initiation, retention and repair;
Stage 2 - Scale damage, weak repair, and rapid deterioration.

Stage 1 is termed the initiation stage and stage 2 is the propagation stage. Fig.8-14 (iii) (p.412) shows the two stages in environments ranging from mild to severe.

8.6.1. FACTORS AT THE INITIATION STAGE OF HOT CORROSION:

The overall factors which govern the onset of hot corrosion are (Giggins & Pettit 1979; Condé et al 1982):

1. Coating condition and its composition;
2. Gas composition and velocity;
3. Reactive particle/salt composition, its deposition rate and

existence state;
4. Temperature - isothermal/cyclic;
5. Non-reactive particle inclusion, deposition and impact;
6. Component geometry.

Hot corrosion is always a secondary reaction in the degradation process. It originates at the initiation stage, reduces the scale coherence and thus its protective life time there itself and follows it up with a catastrophic attack at the propagation stage. There have been several discussions on it which are available in the various references cited. Several contributory factors appear at the initiation stage; opinions differ about the definition, the factors of importance and the mechanism. One of the very common featurs is that a liquid phase is involved. Although in carburization this does not occur a liquid phase involvement is common with reactants where sulphur- or chloride media are present and also certain oxides, e.g. oxides of V. Gaseous oxide formation such as CrO_3, SiO, oxides of W , Mo etc., are also to be considered as promoters of catastrophic corrosion. The role of a coating then is to prolong the initiation stage, under isothermal and cyclic hot corrosion conditions by developing stable scales with adequate creep and rupture strength.

8.7. CARBURIZATION/OXIDATION DEGRADATION

A typical situation of carburization occurs in coal gasification and fluidized-bed combustion processes. Fe-base alloys are the most widely used in this field and hence documented (Hsu 1987; Tachikart et al 1987; Debruyn et al 1987; Ramanarayanan 1987; John 1986; Kofstad 1984; Terry et al 1987).

The 4-step kinetics involved in carburization may be seen as follows:

1. Transport in the gaseous environment by flow or diffusion. Uncombusted hydrocarbons, CO, CO_2 or CH_4 can induce carbide formation in the matrix;

2. Transfer of carbon to the metal matrix by phase boundary and/or reduction reactions which result in carbon atoms;

3. The dissolved carbon diffuses inwards;

4. Reaction of carbon with any or all of the alloy constituents which have the free energy for carbide-forming at the available carbon activity, is accompanied by diffusion of these constituents to the precipitate.

Oxide layers can be destroyed if graphite (or coke) deposits or gets trapped in the growing scale, or if reducing conditions prevail. High carbon activities are possible as the pCO/pCO_2 ratio links to the metal/oxide equilibrium. The metal matrix

itself and the oxide that grows preferentially on it determine the growth of the graphite reductant. For instance, graphite grows much faster on Fe than on Ni, but in the presence of H_2S, the growth is accelerated on Ni, while on Fe it is retarded. Internal carbide formation in alloys such as Fe-Ni-Cr is called 'metal dusting'. Often, the formation of the same oxide can allow or arrest carburization. Naturally formed oxide on a Fe-12Ni-20Cr alloy caused local carburization of the alloy by impurities present in a N_2-H_2 atmosphere, while the material was fully resistant under the same conditions once the oxide was sandblasted. At higher than 1100°C, the protective Cr_2O_3 can undergo reduction by CO to form Cr_3C_2 and/or Cr_7C_3, especially if coke deposition is in significant amounts, and the oxide is buried under it. Internal carbide precipitation can also occur in CO-H_2-H_2O atmosphere.

In the absence of a protective scale, carbon ingress into a Fe-Ni-Cr alloy is by phase boundary reaction and diffusion controlled. The presence of sulphur retards the transfer of carbon, but to curtail the solubility and diffusion, a high Ni/Fe ratio is needed and additives like Si. If the oxide is coherent, dense and adherent carbon cannot penetrate since it has no solid solubility in oxides, but if there are fissures and cracks or pores, then carburization is possible. The integrity of the scale could be hampered by creep fatigue or thermal cycling. Any factor which induces stress is thus conducive to carburization. Additions of Nb, Ce, Si etc., would control in this case. Formation of higher oxides, spinels or mixed oxides lower the resistance to carburization. Fig.8-18 shows the oxide failure modes by carburization (Grabke & Wolf 1987; Ramanarayanan 1987; Hsu 1987).

The following carbon pick-up was recorded for various Fe-Base alloys in Argon-5%H_2-5%CO-5%CH_4 environment (Rothman et al 1984): (ranking in order of increase of carbon pick-up)

925°C, 215 h:
Cabot 214 < Cabot 800H < Multimet < Cabot 600 < Hastelloy S < Hastelloy X < Inconel 610 < Haynes 230 < Inconel 617 < 310 stainless steel;

980°C, 55 h:
Cabot 214 < Cabot 800H < Multimet < Hastelloy S < Haynes 230 < Hastelloy X < Cabot 600 < Inconel 601 < Inconel 617

The influence of selective oxidation on 20/25/Nb stainless steel at 650° and 700°C is given in Fig.8-19a,b. On electropolished surfaces of chromia-forming Fe-Cr-Ni and Cr-Ni alloys, the oxidation layer appears to form non-uniformly, while cold worked samples undergo uniform oxidation in H_2-CH_4 with very low pO_2 of 10^{-30} at 825°C with carbon activity at 0.8. Removal of alpha-chromia during nucleation of the carbide M_7C_3 occurred followed by internal carbide precipitation. (Smith et al 1985a,b). At low pO_2 heat resistant steels are completely under the influence of carbides wth M_7C_3 developing beneath Cr_3C_2 and are not affected

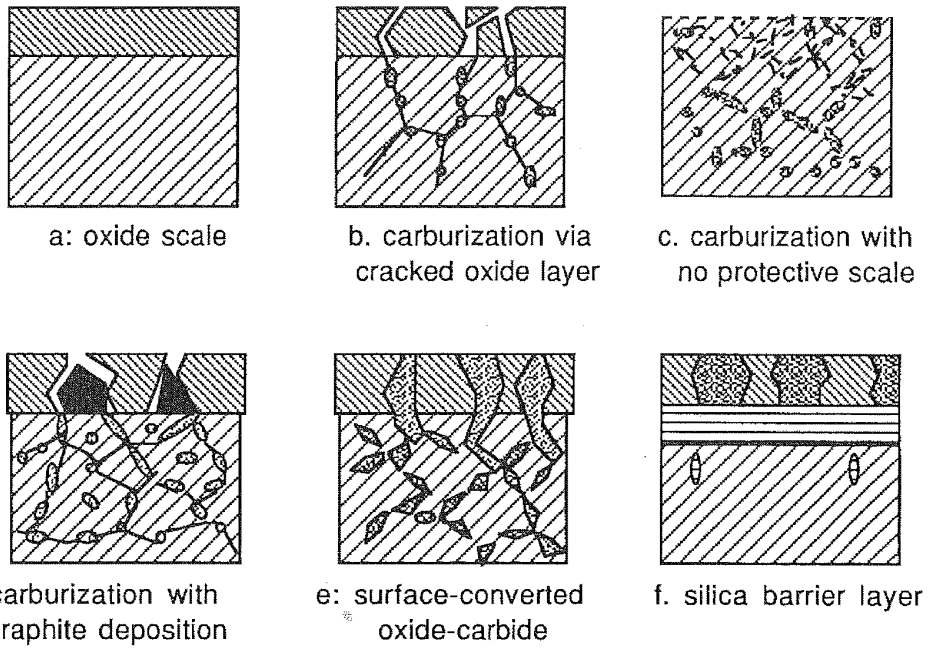

Schematic diagram of carburization with oxidation & barrier layers

FIG.8-18

by brief periods of oxidation (Kinniard et al 1986). Breakaway oxidation and laminated structure morphology were observed at 600°C on Fe-9Cr-1Mo steel in a high pressure CO_2/CO atmosphere (Newcombe & Stobbs 1986).

SiO_2 coatings by PAVD on IN 800H provided excellent resistance to carburization in H_2-CH_4 mixtures at 825°C, but were totally ineffective at 1000°C where the SiO_2 was converted to SiC by a gas phase reduction. Partial degradation was found to occur even at 825° as Ti, Mn and Al additives in the alloy reduced the silica (Lang et al 1987). Silicide coatings are not protective on steels and if they are produced via a methyl-silane, carburization was found to set in at the coating stage itself (Southwell et al 1987). Ferritic steels with 6 wt.% Al showed good resistance to cyclic oxidation-carburization in H_2-H_2O-CO-CO_2 atmospheres with carbon activity 0.2, and Ti and Zr had very favourable effects in catalyzing the alumina phase transformation from the early theta- to the alpha-phase. They also increased the sintering rate and fracture toughness, while suppressing grain growth. None of these benefits were realized in the austenitic series tested with 4%Al, and Y also did not improve oxide adherence. Instead it caused grain boundary embrittlement. In creep tests the oxide layer cracked with subsequent intergranular oxidation and carburization (Wambach et al 1987).

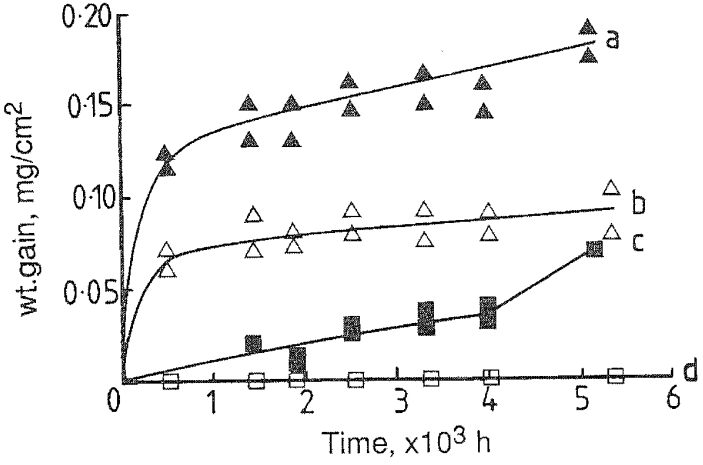

Fig.8-19a: a. 20/25/Nb steel at 700°C
b. selectively oxidised 20/25/Nb steel at 700°C
c. 20/25/Nb steel at 650°C
d. selectively oxidised 20/25/Nb steel at 650°C

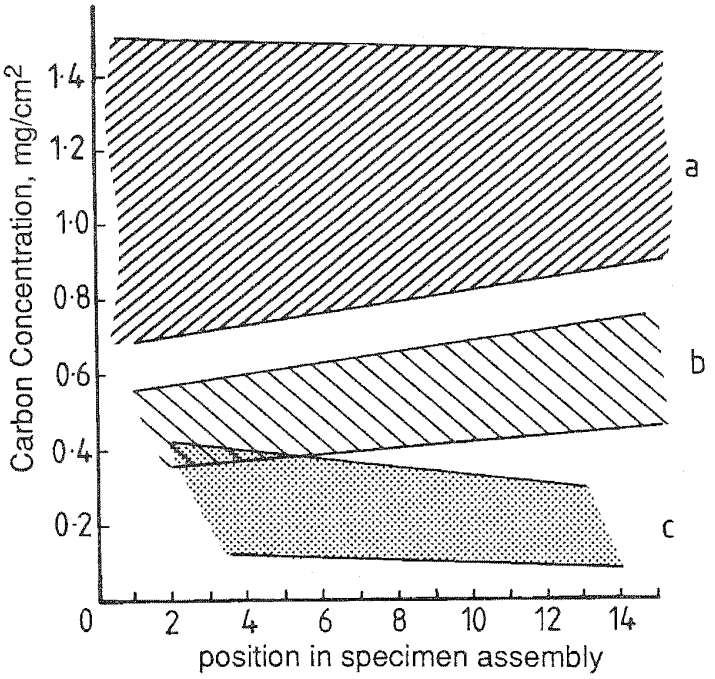

Fig.8-19b: a.20/25/Nb stainless steel; a. no treatment
b. selectively oxidised; c. selectively oxidised.

Fig.8-19: Effects of Selective Oxidation. 20/25/Nb Stainless Steel in $CO/CO_2/H_2/H_2O/CH_4$

In the above case the alloys were pre-oxidized prior to exposure to reactive atmosphere. Pre-oxidation has been found to be a deterrent, but not with sustained efectiveness. A coating of 63%Al-33%Cr-4%Hf on Incoloy 800 performed well at 980°C in coal char environment after pre-oxidation (Douglass & Bhide 1981). MA956, the mechnically alloyed product, yielded good mechanical stability of the alumina scale (Sheybany & Douglass 1988).

8.7.1. CARBURIZATION IN THE PRESENCE OF SULPHIDATION:

Carburization conditions are not encountered on their own in coal-derived atmospheres, but along with gases such as H_2-H_2S, and H_2-H_2O. The oxide layer which is perfectly resistant otherwise, is then exposed to conditions which render it unstable. In the previous section the 'inhibiting' effect of sulphur to carburization was briefly mentioned. A number of environmental variations have been studied: CO_2, CO, H_2 (introduced as forming gas), H_2S, with and without CH_4, chloride etc., with pO_2 variation brought in from the equilibrium CO/CO_2 and/or H_2/H_2O. Temperature appears to exercise a critical control on the degree of carburization. At carbon activity 0.8 in H_2-CH_4, H_2S at 100 ppm at $pS_2=2.2x10^{-12}$ to $5.5x10^{-11}$, at 1000°C, carbide M_7C_3 on Fe-Ni-Cr alloys exhibited a preferred growth orientation in the [001] direction, and in commercial alloys surface carbides of M_7C_3 and $M_{23}C_6$ nucleated with MnS buried underneath, in contrast to subscale $M_{23}C_6$ and surface M_7C_3 embedded in surface alpha-Cr_2O_3 in sulphur-free atmospheres. An apparent reduction of 75% in weight gain occurs when pS_2 is introduced at $1.4x10^{-10}$, with significant decrease of internal carburization. However, sulphide scales are formed and the overall corrosion increases with corrosion at 950° greater than at 1000° and 1050°C (Barnes et al 1985,1986).

The inference from the above would be that although 'metal dusting' by internal carbide precipitation and external carbide formation can be arrested in the presence of sulphur, no ultimate benefit is obtained as one form of corrosion is exchanged for another. Internal precipitation reflects in material degradation by physical and mechanical factors such as creep and stress, and a marked loss in constituents will also result in chemical degradation. Surface scales formed by chemical reaction, on the other hand need to be plastic, stable and coherent; adverse factors will destroy them. Attack by sulphur manifests in catastrophic corrosion in the majority of cases, and such corrosion is often associated with a liquid phase. The effect of H_2-H_2S has been extensively studied and reported in literature. A few papers are listed here:- Weber & Hocking 1985; Majid & Lambertin 1985; Strafford et al 1983,1985; Floreen et al 1981; Gibb 1983; Grabke 1984; Norton 1984; Grabke et al 1980; Hemmings & Perkins 1977; Mrowec 1976; Mrowec & Werber 1975. The principal aspect of attack by sulphur-media is that one or more liquid phases are often involved.

8.8. THE LIQUID PHASE EFFECT

8.8.1. LIQUID PHASE FROM THE ENVIRONMENT:

In the marine gas turbine, sodium is picked up as NaCl, which reacts with sulphur and oxygen from the fuel + air mixture to form Na_2SO_4:

$$4NaCl + S_2 + 4O_2 = 2Na_2SO_4 + 2Cl_2.$$

The melting points of NaCl and Na_2SO_4 are 800° and 884°C respectively. The two salts however, form low melting eutectics and can exist in a solid + liquid state over a range of composition and temperature (Fig.8-20a). The deposits which arrive at the hot turbine blade are composed of NaCl, Na_2SO_4, carbon (from the fuel) and perhaps dust/sand . They do not cover the entire blade but are deposited at discrete areas in the leading edge or at a middle concave (suction) region. The brunt of the deposition is taken by the first stage vanes and blades operating at 900 - 1150°C. In coal gasifiers $CaSO_4$+CaO provides a deposit and sulphidizing conditions and vanadium participates in the formation of molten oxides (Fig.8-20b). The eutectic $NaSO_4$+$NaVO_3$ forms at 610°C.

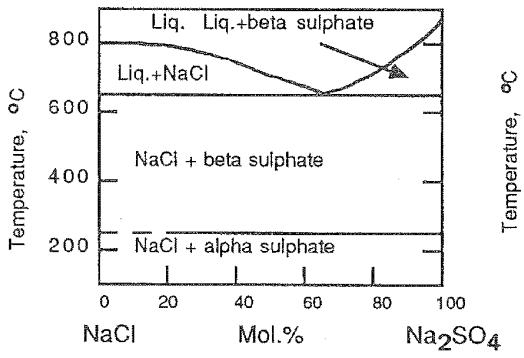

The Sodium Chloride - sulphate system

Fig.8-20a

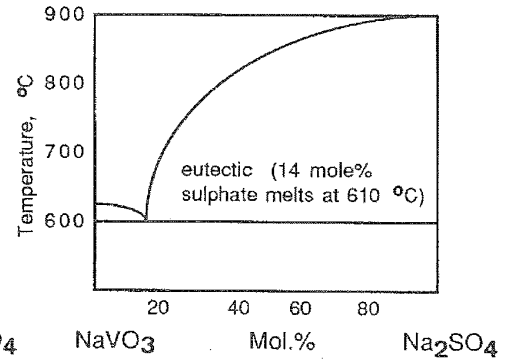

The Sodium Vanadate - Chloride system

Fig.8-20b

8.8.2. LIQUID PHASE FROM ALLOY + GAS REACTIONS:

The gas enviroment in a turbine is O_2 predominant with a trace of sulphur which arrives as SO_2. The presence of metals can catalyse the reaction to give a mixture of O_2, SO_2 and SO_3. The metal / SO_2, SO_3, O_2 reaction mechanisms have been discussed elsewhere (Alcock et al 1969; Birks 1975; Kofstad & Akesson 1979; Seybolt & Beltran 1967). It suffices here to say that oxides, sulphides and

sulphates form as reaction products under specific conditions. A few examples of the melting points of metal + metal sulphides of turbine and coal gasifier alloys are given below:-

Eutectic Ni + Ni_3S_2, m.p. = 645°C; Ni_3S_2, m.p. = 810°C;

Eutectic Co + CoS, m.p. = 879°C; CoS, m.p. = 1070°C;

Eutectic Fe + FeS, m.p. = 965°C

The more reducing environment in coal gasifier environments promotes Fe sulphide eutectics and in Ni-additive steels Ni-sulphides can appear as a liquid phase.

Liquid Phases from Alloy & Environment Reaction Product Interaction; a few examples :-

CoO or Co_3O_4 + SO_3 = $CoSO_4$; $CoSO_4$ + Na_2SO_4 ; m.p. = 565°C

NiO + SO_3 = $NiSO_4$; $NiSO_4$ + Na_2SO_4 ; m.p. = 670°C

$2NaVO_3$ + 2NiO = $Ni_2V_2O_7$ + Na_2O ; m.p. = 850°C,

$Ni_2V_2O_7$ + NiO = NiV_2O_8 ; m.p. >1000°C,

$2NaVO_3$ + NiO = $Ni(VO_3)_2$ + Na_2O ; m.p. 750°C,

$2NaVO_3$ + 3NiO = $Ni_3(VO_4)_2$ + Na_2O ; m.p. = 1210°C,

Al_2O_3 + $2NaVO_3$ = $2AlVO_4$ + Na_2O; $AlVO_4$ decomposes at 625°C.

Cr_2O_3 + $2NaVO_3$ = $2CrVO_4$ + Na_2O; $CrVO_4$ melts between 810° and 900°C.

8.8.3. THE EFFECT OF THE LIQUID PHASE:

The emergence of a liquid phase during a corrosion reaction will result in:

(i) drastic effects on diffusion control parameters, transport and mobility,
(ii) create electrochemical conditions - bimetallic cell situation between different metals and different phases,
(iii) dissolve protective reaction product oxides via acidic and/or basic fluxing,
(iv) facilitate fast transport of reactant species to the alloy /scale interface hitherto barred by coherent scales,
(v) physically undermine scale coherence by mass flow.

Products which vaporize, or react to form a vapour product and deposit in a more stable form on the cooler parts are well known. For instance in a chloride-containing environment reactive species can form chlorides which later oxidize. Mass spectrometric

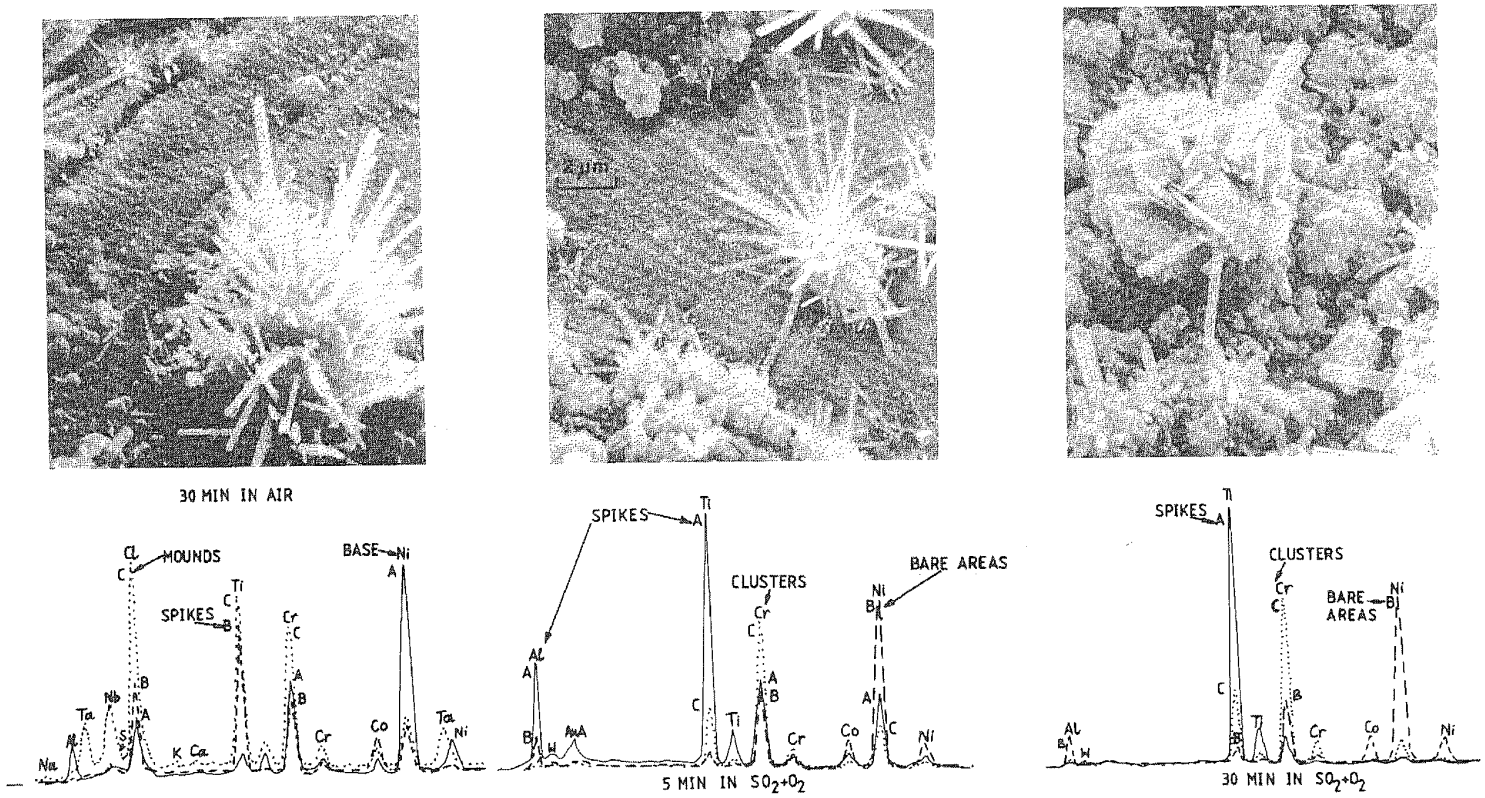

Fig.8-21: Pre-Oxidised IN 738 Exposed to Sea Salt Melt at 750°C

studies by the authors (Hocking & Vasantasree 1976) showed formation of volatile TiS_2; needles of TiO_2 growing out of the Cr_2O_3 barrier layer may be expected to have formed via a vapour deposition mode (see Fig.8-21). Fig.8-22a,b show another needle-forming system where liquid sulphide eutectic pipes up a column of $Ni-Ni_3S_2$ to be rapidly covered by NiO (Hocking & Vasantasree 1976, 1982).

The catastrophic effect of Na_2SO_4 would have been confined to temperatures just around 900°C except for the chloride effect first recognised in UK laboratories in the sixties. Much of turbine hot corrosion was shown to fall into two categories - the low temperature degradation in the region of 620-750°C and the high temperature corrosion over 850 - 950°C. Sulphides and sulphates largely responsible for hot corrosion of Ni - and Co-base alloys are unstable or do not form beyond these temperature regions. Aggravated corrosion occurs well above 900°C if a floating potential of SO_2 is allowed to prevail in the reactant (Vasantasree & Hocking 1976).

NaCl itself is completly converted to Na_2SO_4 within 3 minutes (Conde et al 1977), but its continuous arrival and its stability in solution with Na_2SO_4 at lower temperatures well below its melting point mostly in a solid + liquid state and sometimes liquid state is an important factor in low temperature hot corrosion. Co-base alloys are vulnerable to Na_2SO_4 itself as the $CoO - CoSO_4 - Na_2SO_4$ reaction and solution progresses. Volatile chlorides are often intermediate products in hot corrosion, which enhance the corrosion rate to result in more stable products and also to form more stable reactants. Chloridation of Fe, Ni and Fe-Ni alloys in pCl_2 10^{-3}, 10^{-5} and 10^{-7} with pO_2 range 10^{-11} to 10^{-15} indicates that the aggressive effect of the chloride medium on Fe is greater between 800 and 1000°C, except for pCl_2 10^{-7}. A limiting content of 50%Ni in the Fe-Ni system provided excellent chloridation resistance; above 1000°C Ni was inert in pCl_2 10^{-5} (Strafford et al 1987).

Vanadic melts form the molten salt media encountered in low grade fuel combustion and residual fuel oil ash hot corrosion (Johnson & Littler 1963). The deposit-forming reaction may be of the type

$$wNa + xO_2 + yV + zS + aCl \text{ -----> deposit (Halstead 1973)}$$

in which Na, O_2, V, S and Cl are in the vapour phase, and can be involved in several reaction systems.

8.9. FLUXING MECHANISMS IN HOT CORROSION

Thermochemical diagrams give a direction on corrosion in melts (Pourbaix 1987) and the eletrochemistry of molten salt corrosion is reviewed by several workers: Rapp (1987); Rahmel (1987); Pourbaix (1987); Hocking & Sequeira (1982).

b: Stub & Needle in SO_2, 3 h exposure

a: Needle 7mm long at 700°C

Fig.8-22: Ni_3S_2 Core Within a Case of NiO Clusters. Needle & Stub Growth.
Ni-0.1%Cr Alloy

8.9.1. THE Na_2SO_4 MODEL:

The oxy-anionic Na_2SO_4 melt has been a model on which most of the acidic and basic-fluxing concepts have been developed. The concept can be extended to all molten salt metal product reactions as long as ion-exchange reactions can be applied validly to the reaction system. Thus sulphates, carbonates, nitrates and vanadates can be included in oxy-anionic reactions at high temperature (Johnson & Laitinen 1963; Cutler 1971). The primary factor in viewing molten salts with respect to hot corrosion is that of the availability of the melt and not its mass. An attack will be self-sustaining as long as the melt can participate in the exchange and remain as the intermediate means by which alloy component elements will eventually react to solid corrosion products. In the turbine operating conditions melt can form as and when the component particles are deposited. Products can remain in solution with the melt, form a eutectic, precipitate out or form a solid complex with the total mass of available melt.

The following reactions will clarify the various points noted above:

$$Na_2SO_4 \text{ ----------> } Na_2O + SO_3$$

$$SO_4^{=} \qquad\qquad O_2^{=} + SO_3$$

Acidic Basic Acidic

$$1/2S_2 + (3/2)O_2$$

8.9.2. ACIDIC FLUXING:

Hot corrosion reactions occur where $SO_4^{=}$ participates with the S_2, SO_2 and SO_3 species from the gas or dissociated melt in converting the alloy to corrosion products either by chemical thermodynamic reaction or electrochemically transported as an ion for a subsequent reaction with the gaseous medium. Thus for an alloy AB,

(i) $A \text{ (alloy)} + SO_3 + (1/2)O_2 = A^{++} + SO_4^{=}$

For a continuous solution of ASO_4 in Na_2SO_4, SO_3 and O_2 must be available, e.g. $CoSO_4 + Na_2SO_4$,

(ii) $\underset{\text{alloy}}{A^{2+}} + \underset{\text{melt}}{SO_4^{=}} + (1/2)O_2 = \underset{\text{solid}}{AO} + SO_3$

(iii) AO can remain in solution with Na_2SO_4 melt if there is a negative solubility gradient [note this cannot happen in a small mass or thin layer of melt].

(iv) $B\ (alloy) + SO_4^{=} + (3/2)O_2 = BO_4^{=} + SO_3$

or

$$A(alloy)B(alloy) + 2O_2 = A^{2+} + BO_4^{=}\ (solution\ in\ melt)$$

$$A^{2+} + BO_4^{=} = AO + BO_3$$

The melt remains as a via media; very small amounts of Na_2SO_4 can permit a substantial alloy-to-alloy metal oxides conversion.

In practical systems virtually all alloys are susceptible to acidic fluxing depending on the level of pSO_3 or the amount of V_2O_5 formed or deposited. The condition is prevalent when chloride is present and induces alloy depletion in gas turbine environment and in carburizing conditions when oxygen starvation occurs. Alloys containing Mo, W or V are very vulnerable because they can be auto-generative to acidic oxides, e.g. B-1800, IN 100, Mar M-200 etc. High-chromium alloys present a reasonably good resistance, as well as silica-formers. IN 738 and some Hastelloys are found to out-perform the above listed alloys. Refractory metal additions has to be restricted to avoid acidic degradation. Hot pressed Si_3N_4 performs well in acidic fluxing conditions (Giggins & Pettit 1979).

8.9.3. BASIC FLUXING:

Basic fluxing of the reaction product occurs when the alkali Na_2O or the $O^{=}$ part of the oxy-anionic melt participates in the reaction process.

(i) $A\ (alloy) + O^{=} + (1/2)O_2 = AO_2^{=}$

Na_2SO_4 is converted to Na_2AO_2 and ceases unless fresh melt Na_2SO_4 is available.

(ii) $A\ (alloy) + O^{=} + (1/2)O_2 = AO_2^{=} = AO\ (solid) + O^{=}$.

Melt can act as a transport - precipitation reaction medium as long as it is balanced by an SO_3 supply; else, it will stifle the reaction when sufficiently basic. This means, that for this reaction to be possible there should be a negative solubility gradient of the oxide in the melt (Stroud & Rapp 1978).

Viewing melt fluxing in the context of protective oxide scale formation it may be generalized that:

Cr_2O_3 is more resistant under low pSO_3 conditions, i.e.basic conditions,

SiO_2 has minimal solubility in high pSO_3, i.e. it is good to resist acidic fluxing,

Al_2O_3 has a lower solubility at low pSO_3 than Cr_2O_3.

Degradation due to basic fluxing can be resisted effectively by promoting continuous scale growth of Al_2O_3 under Cr_2O_3. Since it requires an oxygen gradient for promotion, the best means of counteracting it is by formation of oxide scales which grow at a slow rate and need very low pO_2. In Ni-Cr-base superalloys it is better not to have any Al at all than Al in a low level since the chloride effect is particularly marked in low-Al Ni-Cr-Al-alloys. Deposits of carbon are observed to hasten the onset of basic fluxing as it creates local reducing conditions while a 5 micron surface top coat of Pt inhibits basic fluxing.

Susceptibility to basic fluxing occurs with Ni and Co and their alloy systems, binary e.g. Ni-Al and Co-Al, ternary Ni-Cr-Al, or multi-element systems where Cr and Al levels are lower than is required to form their stable oxides. Alloys with 20Cr or more and 10-12 Al with reactive elements such as Y have good resistance in basic fluxing media. If Al has to be lowered for mechanical purposes, then the preference is given to a CoCrAl system rather than a NiCrAl alloy. Alloy depletion caused by chloride reactions and carbon induced oxygen depletion are, once again, the contributory factors (Giggins & Pettit 1979).

8.9.4. STUDIES IN MELT SYSTEMS:

8.9.4.1. Sulphate-Chloride Systems:

Several workers have studied the molten salt as an electrochemical system and corrosion medium since the early studies on fluxing effects (DeCrescente & Bornstein 1968; Bornstein & DeCrescente 1969, 1971; Goebel & Pettit 1970, 1973). The sulphate - chloride provides a molten salt system over a wide range of temperatures relevant to gas turbine conditions. The binary eutectic of the sodium salt (Hocking & Sequeira 1980, 1981,1982) and the ternary system with Mg- and Ca- sulphates have been studied (Swidzinski et al 1978; Swidzinski 1980; Carew 1980; Hocking et al 1984; Rapp & Goto 1979; Gupta & Rapp 1982; Shores & Fang 1981; Shivakumar et al 1985; Kameswari 1986; Rapp 1987; Rahmel 1987).

Although alloy composition can be formulated for degradation by melts, it is more difficult to resist gas-induced acid fluxing. Both the temperature and a high pSO_3 (hence pS_2) favour this mode of degradation and attack is inevitable at low temperatures (700^oC) or high, as long as a stable phase of liquid is generated. Cr_2O_3 and SiO_2 give the most favourable durations of resistance. Acidic and basic fluxing can succeed one another as is shown in an attack on B-1900 and IN 738 by Na_2SO_4 (Fryburg et al 1982, 1984). Alloy induced acidic fluxing is generated from elements like Mo, W and V and aggravated by chloride and carbon from the reactant environment.

Na_2SO_4 melt caused basic fluxing of alpha-alumina on alloy B1900 which was followed by a catastrophic attack and acidic fluxing by a Na_2MoO_4-MoO_3 molten phase that had formed underneath the oxide layer. In the case of Na_2SO_4 induced hot corrosion on IN738 at 975°C the protective Cr_2O_3-TiO_2 scale was basic fluxed in the first 10 hrs. A long slow, linear oxidation rate ensued over the next 50 hrs and gave over to a rapid corrosion which decelerated as reactant availability was reduced considerably. MoO_3-WO_3 formed at the oxide - alloy interface during the slow stage; the fluxed Na_2CrO_4 and Na_2O $(TiO_2)_n$ reacted with MoO_3 to form the low melting Na_2MoO_4 and Na_2WO_4 which lowered the melting point of the MoO_3-WO_3 areas by fluxing and resulting in catastrophic attack. The difference from an earlier work (Giggins & Pettit 1981) is that the liquid phase is argued to be Na_2MoO_4/ MoO_3-WO_3 not the Na_2SO_4-acidified MoO_3-WO_3.

A number of solubility and stability studies of oxides, sulphates, sulphides and chromates in a Na_2SO_4 melt have generated activity diagrams w.r.t. to the Na_2O activity at 900°C and above (Rapp 1987). Fundamental treatments for the corrosion potential and rate calculations can be referred to in the literature (Rahmel 1987). NaCl itself can enhance stainless steel corrosion at its melting point and above (800°C) (Shinata et al 1987), but even in the solid state it can affect scale coherence (Hancock 1985). Because it can form low temperature eutectics with sulphates, sodium sulphate in particular, it is important to monitor melt effects at lower temperatures. The effect of NaCl has been examined by corroding alloys in melts of Na_2SO_4-NaCl and ternary sulphates of Mg-, Ca-and Na, to which additions of NaCl were made. These allow observation of melt attack at low temperatures in the range 650°C and above (Swidzinski et al 1978; Swidzinski 1980). Products such as cobalt oxides and $CoSO_4$, form eutectics with Na_2SO_4 at 575°C and lower at 535°C with sodium and potassium sulphates for which the stability regions have been shown (Luthra & Leblanc 1987).

Tests at 850°C show how the sulphate-chloride has significant detrimental effect on creep and fatigue behaviour of both IN 738 and Udimet 500 (Pieraggi 1987). Coated Hastelloy X and Haynes 188 fuel injector tips were tested in 95-5 sodium sulphate-chloride for cyclic oxidation at 982° and isothermal oxidation at 1150°C. NiCoCrAlY-YSZ (Yttria stabilized zirconia) showed poor adherence and spalling at 1150°. YSZ was the most resistant and Pt-aluminide the least; in the cyclic tests in the melt, the MCrAlY overlay was the best and the YSZ was the least resistant with the Pt-aluminide in-between. Vitreous ceramics failed in both the melt tests (van Roode & Hsu 1987). Low alloy steels (Kraft recovery boiler alloys) develop chromia scales which are not stable in the oxo-basic carbonate added sulphate-chloride melt at 800°C. Ni-rich alloys 600 and 800 presented the best resistance (Petit & Rameau 1987). A transition from ductile to local corrosion cracking occured in AISI 304L stainless steels at 570°C in a NaCl-$CaCl_2$ melt, leading to intergranular fracture (Atmani & Rameau 1987). Chloride pollution of a (Na,K)- nitrite and nitrate

melt mixture used as coolant in solar thermal electric power plant was detrimental to chromia scales on low alloy steels at temperatures as low as 450°C. The hottest part at 500°C was well resisted by AISI 316L stainless steels (Spiteri et al 1987).

Non-protective scales form on alloys due to several processes, and where a molten phase is involved exchanges via donation to the 'acid' or acceptance from the 'basic' oxide part of the melt will occur, neither of them requiring an actual dissoluiton and precipitation of the oxide product (Pettit 1985). Work quoted above gives a cross section of the sulphate-chloride effect on the stability of coatings developed at high temperature, over an entire range as low as 450°C and as high as 1100°C. The chloride effect is particularly detrimental to creep and fracture resistance of prospective scales which has been summarized with its corrosion effect (Hancock 1985).

8.9.4.2. Studies in Molten Vanadates:

Vanadic melts as oxy-anionic melts, are much more aggressive as the oxides can exist in multiple valency and form a number of oxides as products, decompose and re-react. The vanadate melting points range from 750° to 1210°C for the NiO-Na-vanadate reactions alone and are much lower in oxide melts. The vanadic melt attack is more self-sustaining and stable and therefore more harmful (Vasu 1964; Richard 1971). In Na-vanadate melts non-protective $CrVO_4$ forms and Al was detrimental in Na_2SO_4 + $NaVO_3$ melts for Ni-base alloys (Sidky & Hocking 1987). In a simple system of Ni in V_2O_5 at 900°C, the increase in corrosion by a factor of 3 has been explained as due to enhanced cationic diffusion along defective grain boundaries and pores of NiO in which (Ni,V) oxide is located (Chassagneux et al 1987). CoCrAlY coating alloy exhibited a retardation in sulphate - SO_3 attack at 700°C in the presence of V_2O_5. $Co_2V_2O_7$ developed as a surface layer seemed to act as a barrier layer for the inward diffusion of SO_3 and O_2. The effect is deemed to be temporary until the vanadate is decomposed and yields to the eutectic sulphate attack mechanism (Jones & Williams 1987). Vanadate attack occurred on Ni and MCrAlY on IN 600 with pre-formed vanadate deposits. Ni content at >75% produced a $Ni_3(VO_4)_2$ layer which retarded vanadic attack (Seirsten & Kofstad 1987). Aluminosilicates are easily fluxed by both sodium and vanadium oxides over a range of 600 - 1300°C, with the effect more pronounced at the higher end, while the effect of SO_3 was found to be higher up to 900°C (Mascolo & Marino 1987). Fig.8-23 illustrates vanadic attack on Ni-20Cr with and without protection of a Si coating.

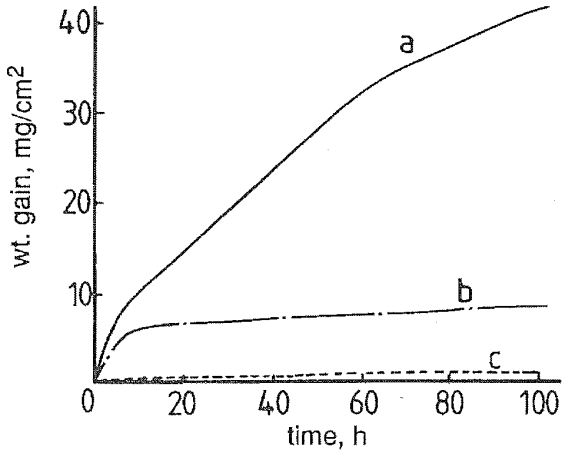

a: Uncoated Vanadic attack; b: Silicon Coating in Vanadic Slag; c: oxidation with and without coating

Fig.8-23: Vanadic Corrosion & Oxidation Kinetics for Ni20Cr With & Without Silicon Coating at 900°C.

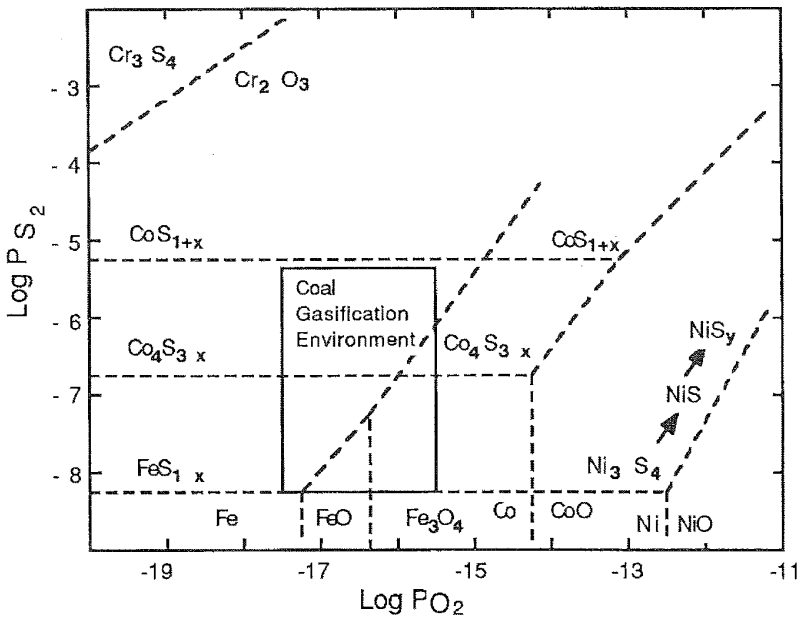

Fig.8-24 a: Sulphide-Oxide Existence Diagram for Fe, Ni & Co at 871 °C , & the Coal Gasification Regime

434

8.10. HOT CORROSION IN S_2 & SO_2 ENVIRONMENTS

8.10.1. COAL GASIFIER CONDITIONS:

Sulphides and oxides predominate as corrosion products although the coal gasification environment appears to be mainly reducing with prevailing H_2/H_2S and CO/CO_2 potentials. The sulphur content of coal is identified to be in sulphatic, organic and pyritic forms, the latter two present in nearly x10 that of the sulphatic variety (Raask 1988). Sulphur is known to have a strong poisoning effect, and is disruptive to the formation of protective oxide layers on the surfaces of many metals (Oudar 1980; Grabke 1980; Strafford 1982; Hocking 1981). Adsorbed sulphur or oxygen at a constant available activity can inhibit carburization (and nitrogenation). The synergetic action of a sulphur-containing environment is its ability to sustain reactions to produce oxide, sulphide and sulphate products from the scale/environment surface to the metal/scale interface and subsurface internal sulphides. The presence of H_2S, H_2O, SO_2, SO_3, CO and CO_2 thus result in oxide/sulphide existence at various sulphur and oxygen potentials over a wide range of temperature. Fig.8-19 shows the existence diagram for sulphides and oxides of Al, Co, Cr, Fe, Mn and Ni at 871°C (Perkins & Vonk 1979; Hemmings & Perkins 1977; Natesan 1983; Natesan & Delaplane 1978; Weber 1986). Fig.8-25 indicates the relative sulphide stability to oxide at 900°C.

Above 4% Al an alloy can form a continuous layer of alpha-alumina at 900°C, because the pO_2 needed is almost five orders of magnitude lower than most other constituents, but it has very poor adhesion. Formation of a protective Cr_2O_3 is possible at a given temperature and sulphur activity if the oxygen activity is maintained at least five orders of magnitude higher than that needed for the Cr_3S_4-Cr_2O_3 and CrS-Cr_2O_3 systems. Ni-base alloys with low Al% (<5%) are susceptible to sulphur induced degradation. MCrAl systems with >10-12% Al (M=Fe, Ni, Co) are in general resistant as are, TD-NiCr, X-40, Hastelloy X, 304 stainless steel and CoCrAlY systems (Giggins & Pettit 1979).

A number of investigations have been done on candidate coating and substrate materials which can be seen in references quoting co-workers with Birks, Condé, Hancock, Hocking, Hsu, Kofstad, Mrowec, Natesan, Nicoll, Perkins, Rahmel, Strafford and others. A brief account is given here on degradation of FeCrAl and additive alloys.

A series of studies have been done in the authors' laboratory in H_2, H_2O, H_2S, HCl, CO, CO_2 and N_2 mixtures over a wide temperature range from 450-1150°C (Hocking & Sidky 1987; Hocking & Weber 1986). Cast FeCrAl-base alloys with additives such as Si, Zr, Hf, Ta, Mn and Y, and mechanically alloyed FeCrAl with Y_2O_3 have been studied. In the cast alloy series the corrosion was higher in some alloys at 450°C than at 850°C where more compact oxide scales of Fe and Al formed and additive effect was more evident. At 450°C multilayered scales with $Fe_{(1-x)}S$ and (Fe,Cr) spinels

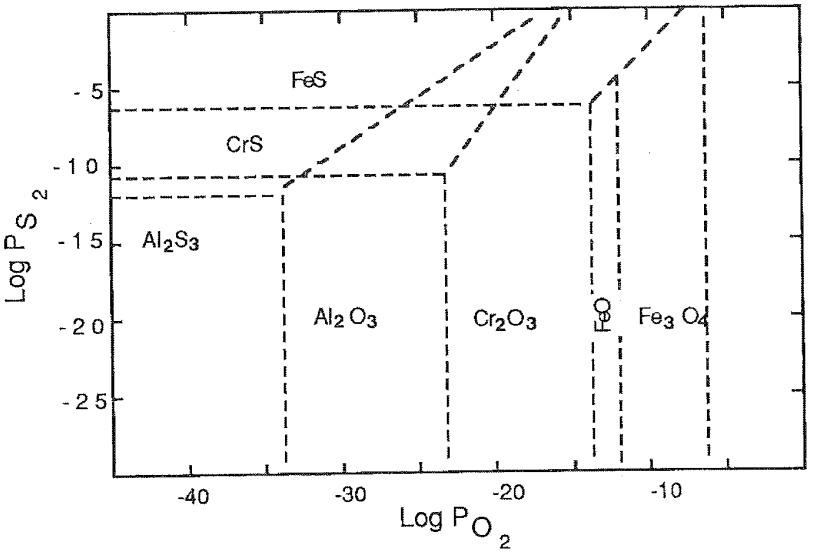

Fig. 8-24b: Fe-Cr-Al Existence Diagram in Gasifier Environment at 1050 °C

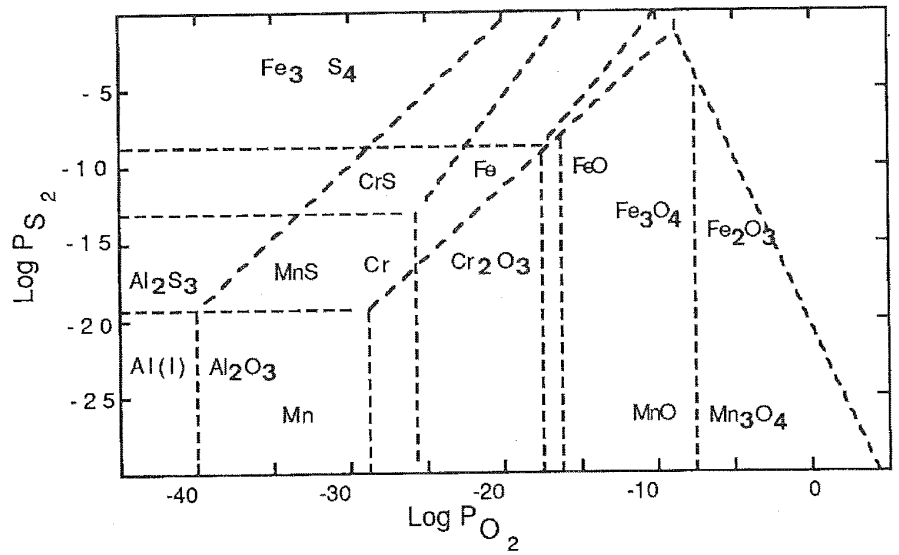

Fig.8-24c: Superimposed Existence Diagrams for Fe-Cr-Al-Mn in Gasifier Environment at 871 °C

with traces of Al and Si formed together with alumina whiskers.

Gas potentials were at pS_2=4.1x10^{-5},pO_2=2.4x10^{-18} and pHCl=9x10^{-6} atm. ; scale spalling was greater at 450^{o}C than at 850^{o}C (Sidky & Hocking 1984). Pre-oxidation of these alloys were beneficial to a large extent, especially at 450^{o}C, where no protective layer formed otherwise (Hocking & Sidky 1987). In Yttria-dispersed FeCrAl mechanical alloy series two distinct types of corrosion have been identified dependent on the pS_2 and the temperature. At 850^{o}C, thin adherent alpha-alumina forms with a slight negative deviation from parabolic behaviour when pS_2 is 3.4x10^{-8} atm. But at pS_2 7.3x10^{-7} atm. severe sulphidation occurred with a duplex scale pyrrhotite $Fe_{(1-x)}S$ outer layer covering a multiphase spinel inner layer. The negative deviation in parabolic kinetics is reasoned to be due to alumina 'laths' in the inner layer reducing the cross section for outward cation diffusion. Alloys pre-oxidized in air at 1100^{o}C were shown to retard sulphidation by up to 500 h. At pS_2 8.1x10^{-6} atm. at 850^{o}C, the protection due to pre-oxidation lasted up to 1500 h (Weber & Hocking 1985). FeCrAl with and without Mn have been examined in H_2-H_2O and H_2-H_2S atmospheres, and the formation of duplex and lamellar scale formation is illustrated. The effect of Mn is noteworthy (Colson & Larpin 1987).

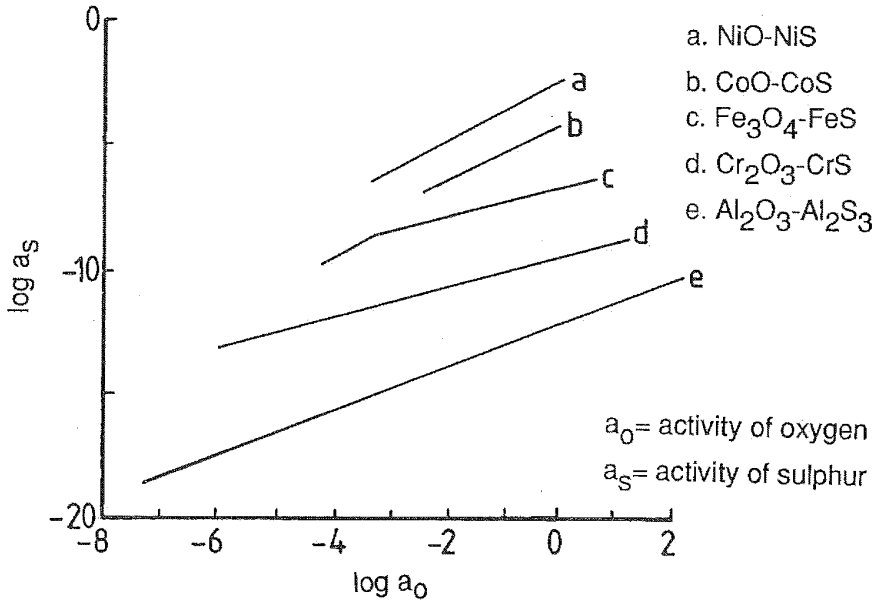

Fig.8-25: Oxidation-Sulphidation Equilibrium Boundaries for Al, Co, Cr, Fe & Ni at 900^{o}C.

The solubility of S in oxides is detectable (Strafford & Hunt 1983; Alcock et al 1969), but proposals for the mechanism of sulphur transport for the formation of internal sulphides are wide and varied. When the outer scale cracks or opens up fissures under stress generated by any means, it is pertinent to expect direct ingress of the reactant to near the metal/scale interface. Both solute diffusion and diffusion through physical defects as transport media are likely to operate in Cr_2O_3 scale (Perkins & Vonk 1979). The mechanism for the Ni-alloy systems has been explained by Hocking (1979) in studies in SO_2-SO_3 atmospheres and is also discussed in the context of coal gasifier corrosion in a review by Hsu (1987). The sulphur effect in non-oxygen atmospheres has been elucidated by Strafford and co-workers (1969, 1981, 1983), and many others (see reference list for Mrowec et al, Smeltzer et al, Narita et al, Jacob et al). Iron and Chromium sulphides are shown to have large mutual solubilities, and do not form liquid phases under intermediate sulphur potentials unlike Ni- and Co-base alloys.

Cr and $Cr_{23}C_6$ are shown to have similar sulphidation kinetics and scale structure at 800°C in the range of $pS_2 = 10^{-3.5}$ to 10^{-6}, except that the sulphidized carbide had an additional inner layer Cr_7C_3. Co, Fe- and Ni-Cr alloys show their sulphidation dependence on the Cr-content, but in Fe-Cr alloys suphidation is shown to be confined to grain boundaries as the chromium carbides sulphidize and not the Cr in the matrix (Narita & Ishikawa 1987). Addition of 10 wt.% Al to Fe-25Cr alloys showed two modes of early stage scale growth, viz. slow-growing alumina scales or faster growing sulphide scales depending on the pH_2O/pH_2S in the range 50 to 7. With time a shift in morphology was imminent (Yurek & Przybylski 1987). Corrosion with H_2/H_2S and H_2/H_2O mixtures with CO have been monitored over 100, 400 and 900 h at 600 and 800°C for a number of steels with 17-20% Cr, 8-26% Ni with major additives as Mn, Mo, Si and minor additives of Ti, Al, Ce etc., Ni-base alloys and ferritic stainless steels. Sulphur attack was observed in almost all of the alloys tested and the chromia stability depended on the sulphur potential and time. Grain boundary attack was evident (Debruyn et al 1987).

Porous sulphate deposits are more damaging in causing sulphidation than any assessment made on the sole basis of their composition because of the tendency to attain higher sulphur potentials at the deposit/oxide interface by creating possible entrapment channels. The deposition of $CaSO_4$ under fluidized-bed combustion conditions has been investigated with reference to the corrosion of heat exchanger alloys. The deposits appeared to contain 10-40% porosity, with the corrosion ascribable to the decomposition of the sulphate deposit, its porosity and the solid state reaction with the protective scale (Saunders & Spencer 1987).

Fig.8-26 and 8-27 show some representative line diagrams of sulphide corrosion product morphology (Hocking & Weber 1986; Hocking & Johnson 1988; Colson & Larpin 1987; Yurek & Przybylski 1987).

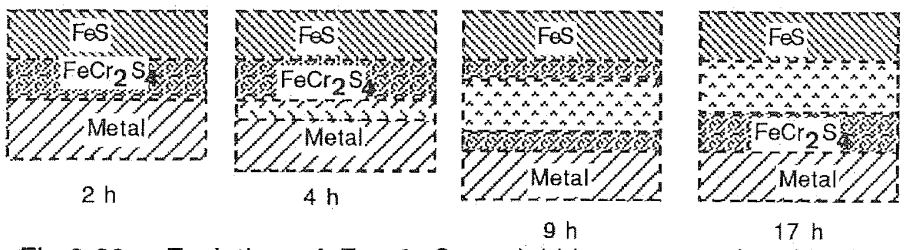

Fig.8-26a: Evolution of Fe- & Cr- sulphide compounds with time in Suphur Vapour in the 800 - 900 °C Range

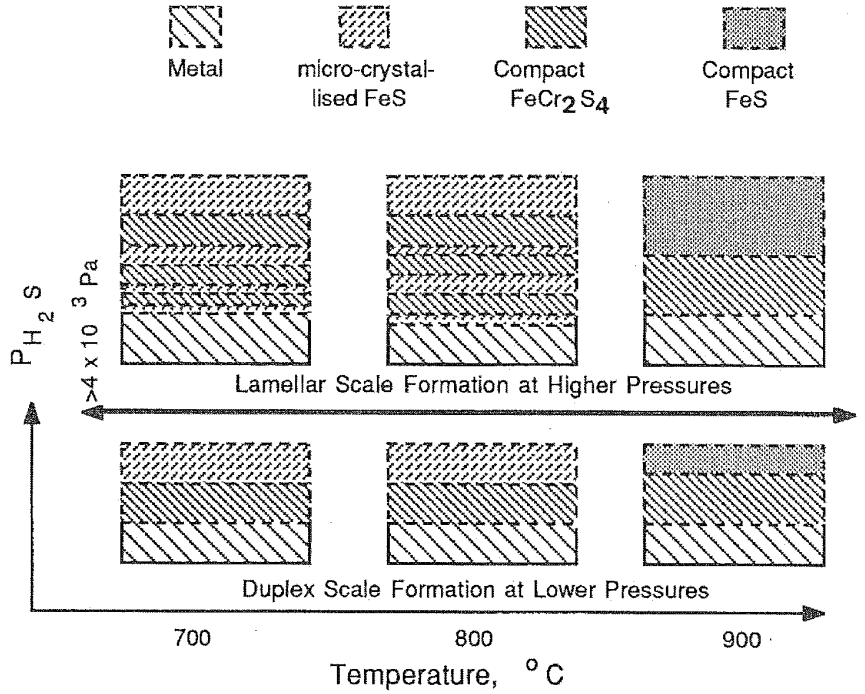

Fig.8-26b: Sulphidation in H_2 - H_2 S Gas Mixtures - Schematic Diagram of Scale Formation

439

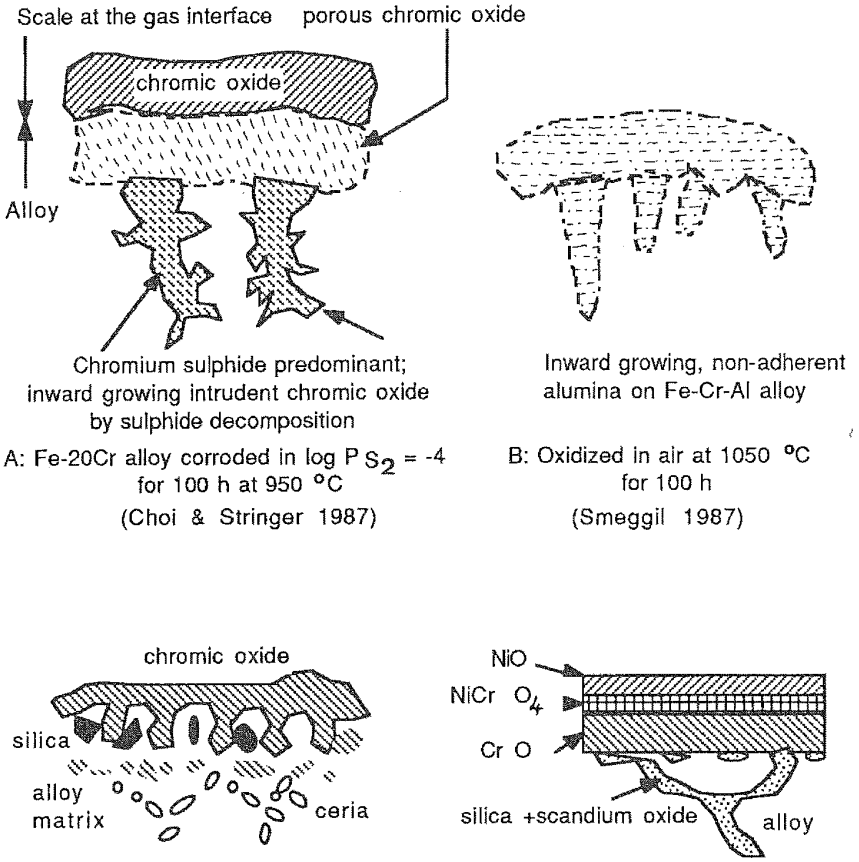

Chromium sulphide predominant; inward growing intrudent chromic oxide by sulphide decomposition

A: Fe-20Cr alloy corroded in log P_{S_2} = -4 for 100 h at 950 °C

(Choi & Stringer 1987)

Inward growing, non-adherent alumina on Fe-Cr-Al alloy

B: Oxidized in air at 1050 °C for 100 h

(Smeggil 1987)

C:Ni-20Cr-1Si-0.34 Ce
Oxidation at 1250 °C for 100 h

D. Ni-20Cr-1Si-0.34Sc
Oxidation at 1000 °C for 200 h

(Y, La and Er produce shallower scallops in chromia, some mixed oxide with Si and a compound MNi_Y ,with Ni, M=Y ,Er , y=17;M=La,y=5)

(Saito et al 1987)

Fig.8-27: Schematic of Oxide Scale Growth

8.10.2. S_2, SO_2 EFFECT IN GAS TURBINE CONDITIONS:

8.10.2.1. General:

SO_2 and SO_3 are the principal reactants in a predominantly oxidizing atmosphere. The sulphur potential as pS_2 is considered because of the equilibria involved where sulphides are the stable end corrosion products with oxides and sometimes with spinels, while the intermediate product reaction involves reactions to form sulphate and decompose it under certain temperature and activity conditions. Investigations to simulate corrosion under gas turbine conditions range from testing a candidate alloy or coating in gas environment with and without sulphate and chloride media, to electrochemical polarization in molten salt media, and crucible tests, thin melt film tests, exposure to molten sea salt and burner rig tests with and without salt injection at the air intake. Effects of mechanical and thermal factors have been followed up with applied stress effects, vibratory rigs and thermal cycling. Thermodynamic calculations have greatly assisted product assessment. The state-of-the-art survey (Rahmel et al 1985; Lacombe 1986) may be mentioned in this context.

Some of the laboratories which have contributed to gas turbine hot corrosion research in the last twenty years are listed here by quoting the group leaders and/or principal workers:-

Alcock, Armijo, Barrett, Bennett, Birks, Booth, Bornstein, Carew, Conde, Coutsouradis, Cutler, Davin, Decresente, Douglass, Duret, Elliot, Erdos, Fairbanks, Foster, Fryburg, Gadomski, Galsworthy, Giggins, Goebel, Goward, Grabke, Hancock, Hart, Hed, Hocking, Jacob, Jones, Kedward, Kofstad, Kohl, Kubaschewski, Lambertin, Luthra, Lloyd, McGill, McCreath, McKee, Meadowcroft, Mevrel, Misra, Mrowec, Natesan, Nicholls, Nicoll, Pettit, Pichoir, Rahmel, Ramanarayanan, Rapp, Restall, Rhys-Jones, Romeo, Taylor, Saunders, Shores, Sidky, Smeggil, Stearns, Stephenson, Stern, Stott, Strafford, Stringer, Swidzinski, Smeltzer, Vasantasree, Wallwork, Wagner, Whittle, Wood, Worrell, Wright.

Many of their publications are listed and can be used for further reference. Individual references are not quoted in this section. Several more investigators who may have published in this area have not been specifically mentioned in the above list; again, the list is not exhaustive.

8.10.2.2. Hot Corrosion Reactions:

Ni and Co are the main matrix metals, and it is their preferential formation that has to be prevented in order to arrest hot corrosion reactions. Ni forms NiO, while Co can oxidize to CoO and Co_3O_4 and unless sufficient Cr is in the alloy and the temperature is sufficiently high, e.g. 900°C, these oxides will form preferentially because of the faster cationic diffusion. The formation of Ni (or Co) and Cr sulphide products beneath these oxide scales, to be distributed in the scale in a multi-layered morphology, as well as form internal sulphides preferentially with Cr has led to controversial explanations for sulphur transport through the growing scale. Considering the corrosion in just gaseous reactants, simple reactions such as

$$7Ni + 2SO_2 = 4NiO + Ni_3S_2 \text{ and,}$$

$$9Ni + 2NiSO_4 = 8NiO + Ni_3S_2$$

may be expected, permitted by the stability of the possible products and available Ni (or Co) activity within the scale. A similar approach is written for Co, Cr and all other additives. The reaction becomes a hot corrosion reaction because of the eutectic reactions of $Ni+Ni_3S_2$ (645°C) and Co+CoS (879°C), the liquid phases of which de-stabilize solid state transport, assuming that the oxide scale is free of physical defects generated by factors such as strain and stress. Both the oxides grow at quite a rapid rate, to considerable thickness and are rarely coherent at temperatures below 850°C. Scale formations at high temperatures are non-coherent, and the thicker the scale the worse its coherence, because of volume expansion and stress generation. Once a liquid product is formed a rapid rate of attack is imminent. This is the baseline of gas turbine hot corrosion. For alloys with less than 18-25% Cr and 10-12%Al preferential Cr_2O_3 and Al_2O_3 can be manipulated and these reduce the sulphidation effect for long periods unlike Ni and Co. Thus if hot corrosion is viewed to occur in two stages, the initiation and the propagation, Cr and Al are able to prolong the initiation stage. The controversies are in agreeing to a mechanism by which the prolonging of the initiation stage occurs and what happens during that time to trigger the later higher corrosion rates.

Sections 8.6-8.9 discuss the various effects of the sulphate and chloride on hot corrosion. Much of the information has been the outcome of gas turbine alloy research and will not be re-elaborated here. It suffices to point out that two temperature regions are recognized in hot corrosion with a low temperature region from 600-850°C and the high temperature from 850°C and above. Cobalt alloys are attacked by the formation of $CoSO_4$ and its eutectic formation with the Na- (and K in some cases) sulphate and stability diagrams for this system have been given.

Gas turbine alloys are multi-component with additives such as Ti, Al, W, Mo, Zr, Hf, Nb, Ta and the coatings formulated follow the same pattern in composition. Co-alloys which are more resistant than Ni-alloys below 850°C in gaseous reactants, are more liable to hot corrode in sulphate and sulphate-associated media. The effect is not as drastic in Ni- or Fe-alloys, but in general all the three groups of alloys have shorter survival records at low temperature in the presence of molten salts. Coatings with multi-element NiCoCrAl- compositions are thus formulated to compensate for the individual vulnerabilities with additive 'reactive elements' such as Y, Ce, Hf etc. Hf showed a critical minimum corrosion effect at 0.85-1.2%, below and above which the corrosion rate was higher in Ni-30Cr alloys. At 700°C at $SO_2:O_2$=2:1, ternary alloys are rated in the order Ni-20Cr-3Al > Ni20Cr-0.3Si > Ni-20Cr-5V > Ni-22Cr with the aluminium alloy as the best in reducing corrosion rate. Pre-oxidation contributes to a retardation

in corrosion rate, or prolonging the initiation stage. Care has to be exercised in not depleting the metal content that is being preferentially oxidized, and to ensure that the scale developed is free of defects such as pores and fissures.

Breakaway corrosion is suggested to occur in Fe-Cr alloys in SO_2/O_2 atmospheres due to a critical microstructure development characterized by intrusions of relatively coarse chromia into the substrate matrix. The intrusions are reasoned to develop via the progressive oxidation of CrS which also causes the oxide intrusions to be porous and thus allowing access to gas to develop a reaction front close to the metal interface. Oxides of Ca, Ce, Y, La and Hf applied by conversion of nitrates on Co-15% and 25% Cr and Ni-25% Cr appeared to have considerable influence on the oxidizing properties of the nickel alloy but very little effect on the cobalt alloy.

Schematic diagrams given in Fig.8-28a,b,c, and Fig.8-29 elucidate scale formation typical of a number of alloy hot corrosion in $S_2/SO_2/SO_3$.

8.11. EROSION - CORROSION

The mixed-mode degradation of erosion-oxidation and erosion-hot corrosion is caused by deposition and impact of particles on the developed scale, resulting in scale damage under oxidation or hot corrosion conditions. The erosion aspect of the damage can set in by adhesion, surface-fatigue, delamination, fretting and gouging effects. Particle size, shape, velocity, rate of arrival, mass, physical state, chemical nature and retention control the extent of damage. Three velocity ranges are classified, viz. low impaction velocities <10m/s; medium range 10-100 m/s and the high velocity range >100 m/s. A uniform, smooth scale can be cracked or peppered on impact; the embedded particle may be non-reactive by itself but can change the local reactive conditions; or the particle can change its state from solid to liquid, or react to form a liquid. It also enables liquid retention as the surface is rendered rough. The resultant effect is that erosion reduces the useful lifetime of a coating by mechanical damage and more often by physical-chemical impairment of a protective scale. Any self-repair capacity of the coating attenuates as the constituent reserve depletes (Raask 1988; Santoro et al 1984).

Erosion-related problems in the field of coal-gasification have been well documented (Raask 1988). They may be identified as given in Table 8:9 and Fig.8-30 (Wright 1987).

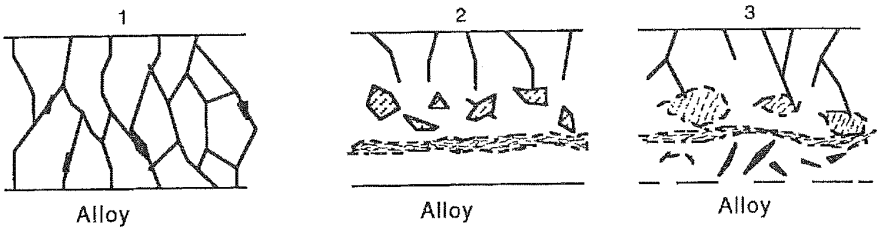

1.protective alumina scale with titanium oxide nucleating at the grain boundaries, partially blocking paths for oxygen.

2 & 3. Non-protective alumina with FeS islands above a vestigial alumina layer; $Fe(Fe,Cr)_2 S_4$ above alloy in 2, and in 3 an internal alumina nucleates along with internal oxidation.

FeCrAlTi-alloy in Coal Gasification atmosphere in protective & Non-protective Modes at (low and high P_{S_2})

Fig.8-28a

(Hocking & Weber 1987)

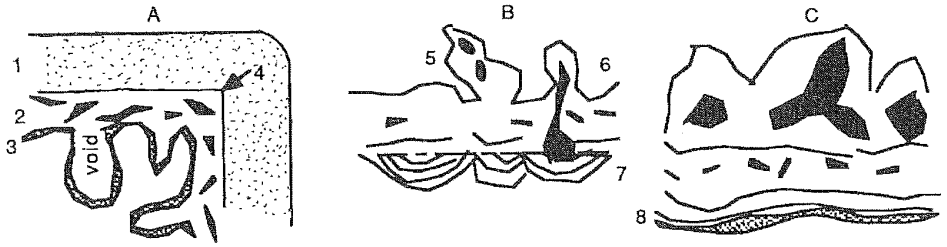

A: Ni-20Cr B: Ni-20Cr-3Al C: Ni-20Cr-4Ta

1. Compact NiO layer with $Ni_3 S_2$ islands; 2. Porous region with $NiO+Cr_2 O_3$ + $Ni_3 S_2$ islands; 3. CrS layer in contact with alloy; 4. Retained sharp corner of the original metal surface; 5. Multiple globule formation from $Ni_3 S_2$ reservoir and subsequent oxidation shell with remnant sulphide inside; 6. Globule development; 7. Sulphide striations; 8. Multiple layer formation in high pressure hot corrosion

(Hocking & Vasantasree 1971; Hocking & Sidky 1981; Ma, Baker, Hocking & Vasantasree 1984)

Fig.8-28b: Hot Corrosion of Binary & Ternary Ni-20Cr- Alloys in SO_2 /O_2 Gas Mixtures - 2:1; 1:4; 1:39 (air) at 20 atm. Respectively, at 700 ^{0}C

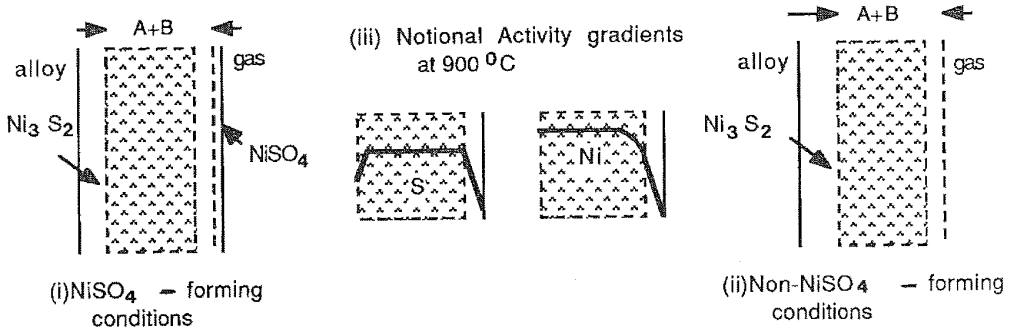

(i)$NiSO_4$ – forming conditions

(ii)Non-$NiSO_4$ – forming conditions

Schematic of Sulphate-Sulphide-Oxide Stability in SO_2 -O_2 -SO_3 Gas Mixtures

Fig.8-29

Table 8:9

Type of Boiler/Turbine	Erosion Area
Conventional coal -fired boilers:	Fireside
Pulverized coal -fired boilers	: Fly-ash erosion of pulverizers, coal feed pipes, burner nozzles, superheaters and economiser tube banks.
Steam Turbines	: Flue gas de-sulphurization equipment.
AFBC and PFBC	: Heat transfer tubes, side walls proximate to the turbulent top surface of the fluidized-bed; fouling of the expander turbine

Alloys which are weak but ductile at the erosion conditions, and form tenacious oxide scales exhibit very good resistance to erosion-oxidation (Wright et al 1986). Erosion rates of mild steel by sand was found not to be linear with time at ambient temperatures at low particle velocities; morphologies observed indicated ductile erosion (Lloyd et al 1987). Fig.8-31 shows the relative slurry-erosion rates for valve material candidate ceramics and cermets (Wright 1987).

Degradation in sulphur bearing environments is generally much more severe, as sulphide eutectics tend to form. A sulphur + oxygen environment to a gas turbine alloy is as damaging as sulphur, or hydrogen sulphide is to fluidized bed combustion materials. It is the threshold pS_2 at the attack interface or corrosion front that will decide the sulphide product formation and not the ambient sulphur pressure. The initiation and propogation mode of sulphide formation has been shown to be dependent on temperature and thermodynamic stability (Hocking 1979). Further arguments on direct transport of SO_2 and SO_3 through fissured oxide layers and molten subscales, the temperature effect, eutectic formations and the relative importance of SO_2, SO_3 and sulphates have been put forward (Vasantasree 1971; Vasantasree & Hocking 1976; Sidky & Hocking 1987; Wooton & Birks 1972). The mode of degradation of cobalt and its alloys has also been developed based on similar arguments (Luthra & Shores 1980; Luthra 1982).

Erosion-hot corrosion in gas turbine environments occur as a result of ingested particulates in the air intake. Pyrolytic carbon and NaCl deposition are two of them. Coatings enhance erosion resistance by developing thin and slow-growing films

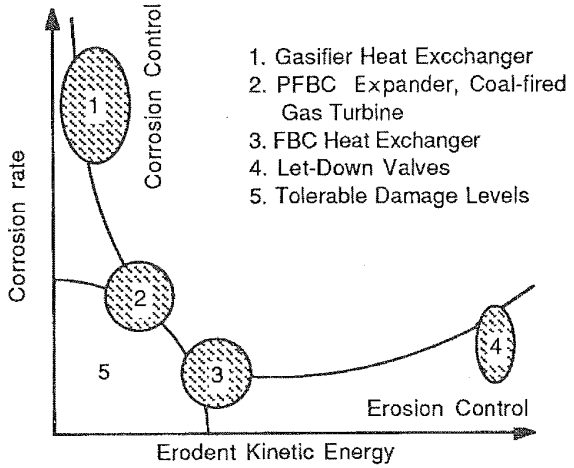

Fig.8-30: Schematic of Corrosion-Erosion Regime
(Wright 1987)

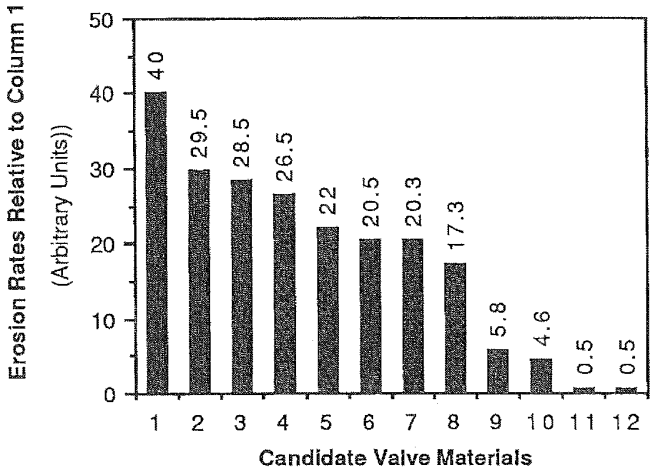

Fig.8-31: Erosion Tests with a Slurry of Coal Derived Solids+Anthracene Oil
(Wright 1987)

Column No.	Test Material	Column No.	Test Material
1	WC+Co+Cr(Std.)	7	B_4C
2	WC+Co	8	WC+Co+Cr(c)
3	B_4C+Co	9	CVD SiC
4	WC+Co+Cr(b)	10	Sintered alpha-SiC
5	WC+Co	11	CVD TiB_2
6	SiAlON	12	Diamond Compact

primarily based on SiO_2, Al_2O_3 and Cr_2O_3 or combinations of these. Erosion modes in superalloy aero-engine blades and helicopter blades by carbon and sand respectively have been presented (Restall 1976; Galsworthy et al 1982; Nicholls & Stephenson 1986). Erosion which is significant on thermal barrier coatings over 10000 h on surfaces parallel to flow may be seen within 3000 h on vane leading edges or wherever normal impingement may occur. For airfoil applications requiring smooth finishes and good erosion reistance PVD ceramics are thought to be suitable (Bennett et al 1987). A Monte Carlo model for erosion-corrosion as applied to a typical gas turbine environment is proposed taking into account, the particulates, protective oxide and the substrate alloy. The degree of damage is shown to depend on substrate temperature, scale composition and scale thickness. If a high velocity (150-300 m/s) is maintained the particle role is thought to be minor (Hancock et al 1987). Test conclusions were as follows:

1. Irrespective of the coatings beneath, top alumina scales formed on coated superalloys exhibit the same fracture behaviour under erosive conditions.

2. Quantitative predictions can be made on the influence of surface oxides on the stresses generated at the substrate/coating interface and the surface oxides show a considerable influence on the erosion response of the underlying coating.

3. High rates of strain of the order of 10^5 - 10^8 /s are created at high velocity particle impact (150-300 m/s), and at these high strain rates all types of particles can be viewed on par because divergence in their mechanical behaviour is very insignificant.

4. At high velocity, similar impact damage is caused by particles from 50 microns to 1 mm, and the hertzian stress theory can be used to predict damage caused by smaller particles.

5. Tests conducted with single-impact erosion in the range 700°-1000°C under low and high particle loading have yielded quantitative oxidation-erosion data agreeing satisfactorily with a Monte Carlo model of prediction.

The significance of the DBTT of a coating has been demonstrated by single impact tests on aluminized MAR-M002 and IN 738 with sea salt or pyrolytic carbon particles at impact angles 30° or 90°. Aluminide coatings provide the greatest deterrent to erosion at higher than 850°C, above the DBTT of Al_2O_3 in marine gas turbine applications. But for the coal-fired gas turbine, components such as nozzle guide vanes and turbine rotor blades, erosion prevention has to be via gas clean-up procedures rather than material improvements (Restall & Stephenson 1987). Fig.8-32 shows the magnitude of loss in coating lifetime under erosion-oxidation and erosion-hot corrosion of aluminided IN 738, a typical gas turbine alloy (Barkalow et al 1984; Wright 1987). Alumina used as an erodent indicated a particle effect where 0.3 micron reduced

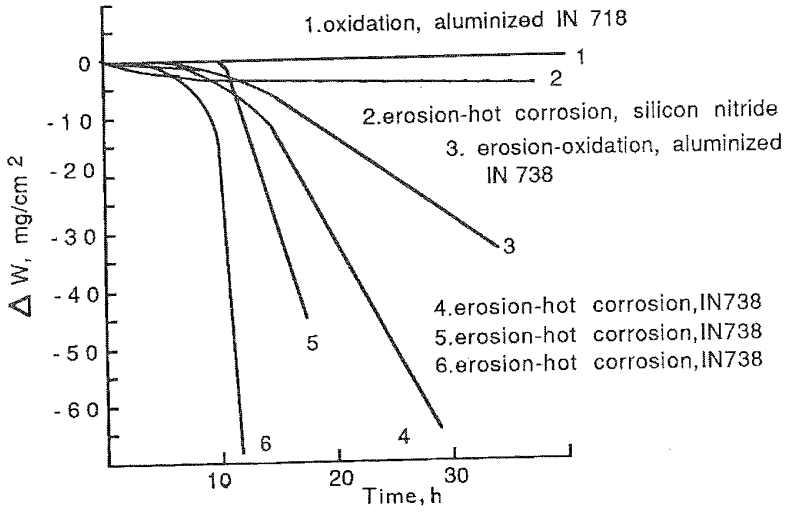

Fig. 8-32: Oxidation, Erosion & Hot Corrosion Interaction Effects on Superalloy IN 738 in Burner Rig Tests

(Barkalow, Goebel &Pettit, 1980)

sulphate hot corrosion and 2 micron enhanced it, although without sulphates it was non-erosive. Impacting at 245 m/s velocity, the corrosion rates at 871°C on gas turbine alloys was ranked at 0.05, 0.1, 3 and 7 mg/cm^2/h for oxidation, hot corrosion, erosion and erosion-hot corrosion respectively (Barkalow 1984). Ash impaction at 344 m/s gave the following ranking of erosion-hot corrosion in decreasing resistance to wastage (Spriggs & Brobst 1982; McCarron 1984):-

At 737°C: CoCrAlY > FeCrAlY > IN 671 > FSX 414> Pt-Cr-Al> IN 738
cladding cladding cladding alloy coating alloy

At 872°C: Pt-Cr-Al > CoCrAlY > FeCrAlY> IN 738 > IN 671 > FSX 414

Raask (1988) has compiled a comprehensive discussion on gas turbine erosion in coal-energy systems.

Effects of coating ductility, bond strength and microstructure on erosion -oxidation resistance have been evaluated for application in power recovery turbines and aircraft gas turbine compressor sections. On an IN 718 substrate, D-gun coatings of chromium carbide-nichrome and WC with pre-alloyed Ni and Co metal matrices were sprayed and tested at 760°C, with impact angles 30° and 90°; the erodent was 27-micron alumina in a heated gas stream. Smaller particles of coating powder gave better resistance. Chromium carbide-nichrome was better than the WC composite; microstructural differences and greater oxidation resistance are believed to be contributory (Sue & Tucker 1987). The erosion resistance

and hardness of sputtered $NiCr_3C_2$ increases with increasing deposition rate. The deposit is homogeneous at 25% bias above which microstructure is adversely affected and also reflects in poor erosion resistance. At 30^o impingement erosion results in a ductile forging-extrusion mechanism, and at normal impingement brittle chipping occurs. Coating defects greatly enhanced erosion rates with rapidly expanding pinhole formation, stressing the importance of microstructure effects (Wert et al 1987).

PVD arc evaporated TiN shows a similar crystallographic influence to erosion resistance (Sue & Troue 1987). Ion plated TiN-Cr on 12%Cr stainless steel substrate showed that good resistance to cavitation-erosion is achieved by strong adhesive force at the bonded substrate/coating interface, along with high compressive residual stress, small grain size and preferred orientation. Substrate bias voltage was once again shown to have a decisive effect. WC-Co and TiC were inferior to TiN-Cr in many respects. Cavitation-erosion resistance is enhanced with a metallic interlayer between the coating and substrate (Odohira et al 1987). Thick coatings of PVD-TiN were more resistant to angular particle erosion, and thin coatings to blunt impact. Stresses in coatings cause aggravation by spalling in both cases (Rickerby & Burnett 1987). Ductile IN 617 coatings magnetron-sputtered and nitrided onto Ti-6Al-4V substrates exhibited good resistance to normal impact erosion by 15 micron SiC particles (Emiliani et al 1987). Plasma sprayed porous ZrO_2 ceramic eroded at 1287^oC with 27 micron alumina at 244 m/s showed plowing, fracture and tunnelling at low, medium and high incidence impact angles. The strength of the ceramic, the porosity distribution between intersplat boundaries, and discrete pores at a given porosity level could be used to predict erosion rate (Eaton & Novak 1987).

Histograms in Fig. 8-33 to 8-35 (cf. Fig.7-14a and 14-b) indicate chromia-forming alloys to be inferior to alumina-forming alloys with both being inferior to coated alloys. Al-rich/Al-Fe coating on Hastelloy X ranks almost equal to Si_3N_4, the most resistant. Fig.8-36 and 8-37 show erosion reistance of coated stainless steels with chromite powder as erodent (Qureshi et al 1987). Data with erodents which occur in practice, such as sand, pyrolytic carbon and sea salt have to be assessed against test erodents to obtain more realistic ranking and extrapolations. Further work is clearly needed to clarify alloy performance under well planned erosion-corosion conditions.

Sections 8.12 to 8.15 consider individual coating systems in three groups viz. aluminides, silicides and thermal barrier coatings.

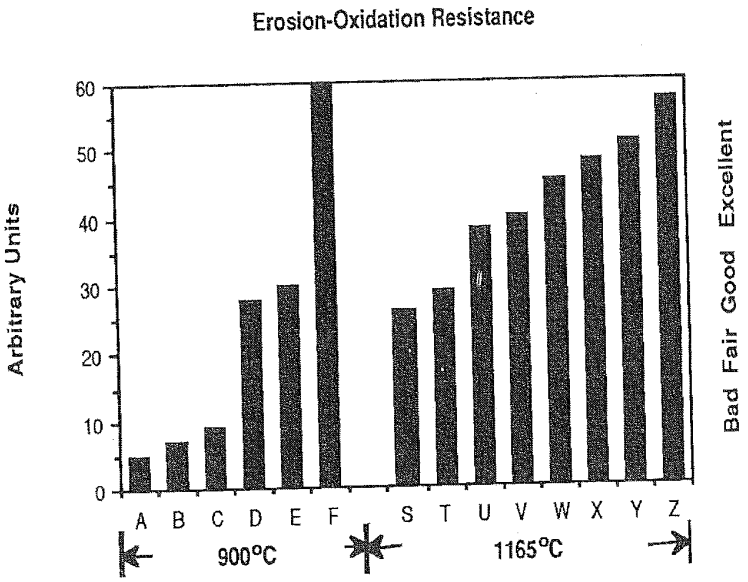

Fig. 8-33

Erodent:- Alumina particles; A-F: Tested at 900°C
S-Z: Tested at 1165°C

Legend	Substrate	Legend	Coating
A	IN738	U	Al
B	X40	V	Haynes C
C	MA754	W	CrAl
D	IN738 (with Al coating)	X	Al-Cr-Si
E	CoCrAlY	Y	Al-rich Al-Fe
F	Si_3N_4	Z	Al
S	Haynes C9		
T	Hastelloy X		

Where no coating is shown the material was tested alone for comparison.

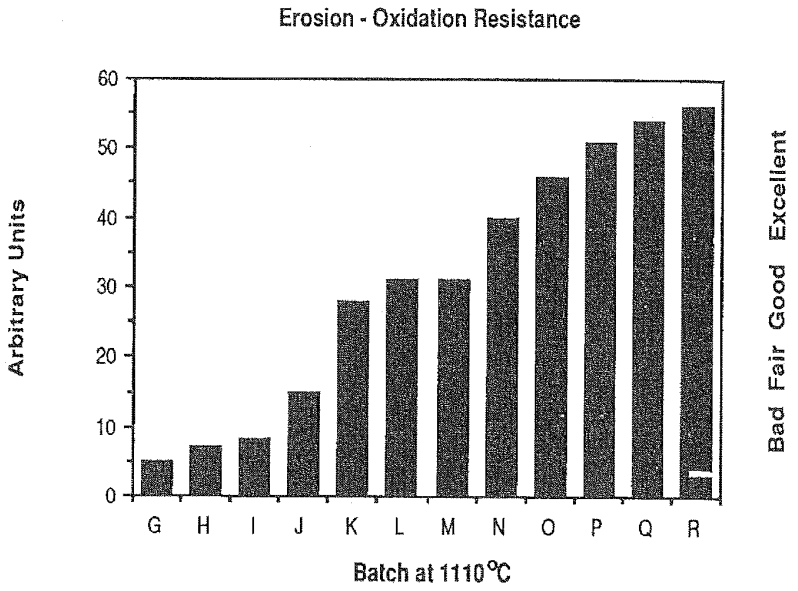

Fig.8-34

Erodent:- Alumina particles; G-R: Tested at 1110°C

Legend	Substrate	Coating
G	TRW1900	none
H	SM200	none
I	SM211	none
J	IN100	none
K	IN717	none
L	IN713LC	none
M	PDRL162	none
N	B1900	none
O	PDRL162	Al
P	IN100	Al
Q	B1900	Al
R	IN713LC	Al

where no coating is shown the material was tested alone for comparison.

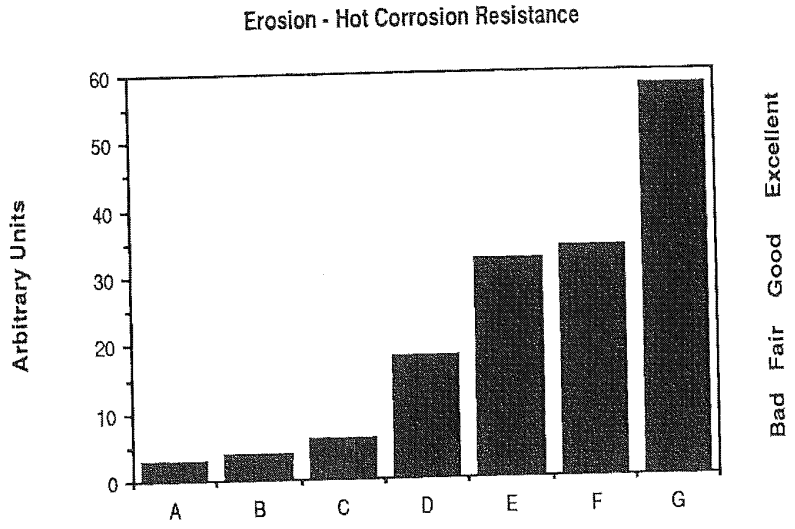

Fig.8-35

Legend	Substrate	Coating/Conditions
A	HA188	none
B	IN738	none
C	X40	none
D	MA754	none
E	IN738	NiAl
F	IN738	CoCrAlY
G	Si_3N_4	none

The erodent was alumina (particulate) at 871°C and the hot corrodent was a Na_2SO_4 .25K_2SO_4 melt. Where only one material is shown, it was tested alone.

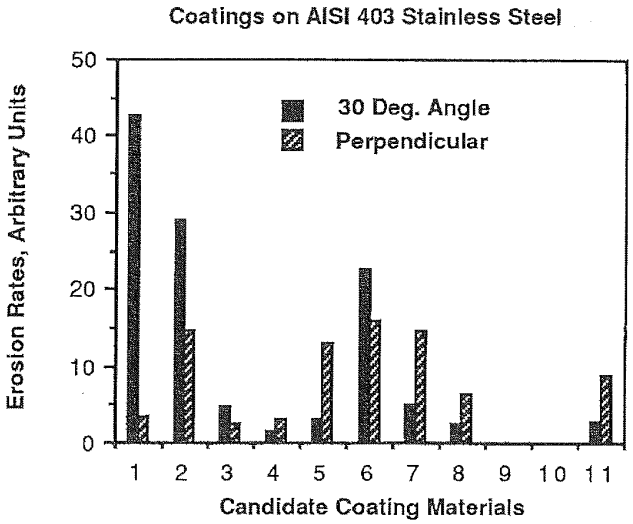

Fig.8-36: Erosion Rates of Coatings on AISI 403 Stainless Steel

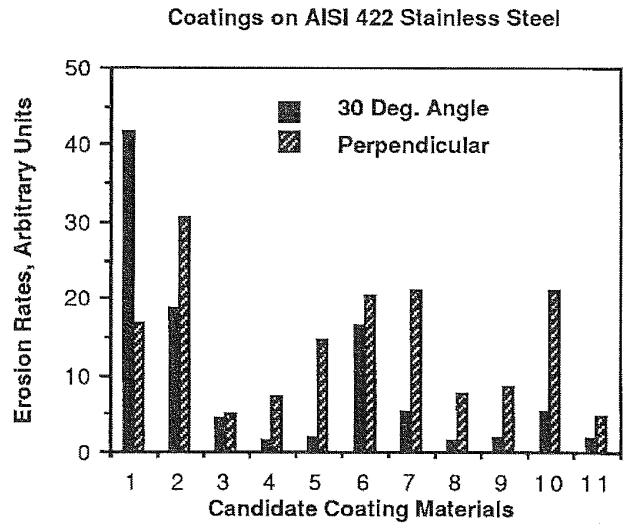

Fig.8-37: Erosion Rates of Coatings on AISI 422 Stainless Steel

Column No.	Test Material	Column No.	Test Material
1	Substrate Steel	7	WC+Co; High velocity Plasma Spray
2	Nitrided Case; Diffusion Process	8	XC+NiCrB; Clad Overlay
3	CrB+FeB(a); Diffusion Process	9	WC; CVD
4	Cr_3C_2; D-Gun	10	Co-Mo-Cr; Electrospark Dep.
5	TiN; PVD	11	CrB+FeB(b); Diffusion Process
6	NICrBC; Plasma Spray		

8.12. DEGRADATION OF ALUMINIDE COATINGS

In this and the next two sections chemical degradation of specific coating systems is reviewed. All of them have been extensively investigated in all high temperature applications. A few new methods developed and applied in recent years are also examined in the context of their efficacy over conventional methods of coating application in improving the performance of the coating and the component.

A broad grouping can be made under three categories of coating:

Group 1 : Aluminides; chrome-aluminides; and Pt-aluminides; the MCrAlX systems, M = Ni, Co, and/or Fe; X = Y, Hf, Ce, Ta, Zr etc.

Group 2 : Silicides (single or in combination)

Group 3 : Thermal barrier ceramics with overlays

This section deals with coatings in Group 1. Sections 8.13 and 8.14 consider silicides and thermal barrier coatings respectively.

8.12.1. GROUP 1. ALUMINIDES

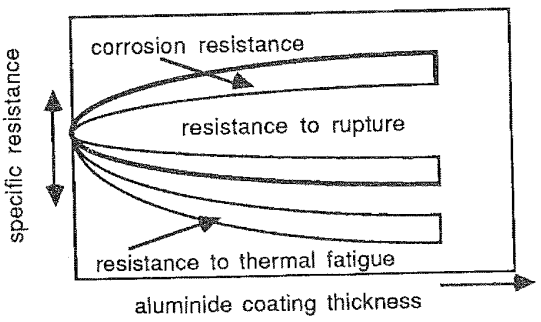

Fig.8-38: Aluminide Coatings - Thickness Related to Corrosion Resistance.

The overall durability of any coating can be assessed as its specific resistance to degradation by corrosion, rupture and thermal fatigue. Fig.8-38 shows a schematic diagram of the resistance of aluminide coatings to thermal fatigue and hot corrosion. Fig.8-39 shows the compositional changes occurring in NiAl on Ni. Morphological changes in CoAl on Co and NiAl on Ni are shown schematically in Fig.8-40 (Fontana & Staehle 1976; Nicoll 1984). Degradation of aluminide coatings is largely dependent on the coherence and structure of the Al_2O_3 layer which is largely influenced by the available Al-activity from the substrate, and the transition metal it is alloyed with in the diffusion band.

Diffusion processes from the substrate always happen in conjunction with those occurring in the coating itself. At an early stage Al in the aluminide coating is expected to diffuse into the substrate. But as degradation proceeds the diffusion direction reverses with Ni from the substrate entering the coating that is being consumed. This situation is ideal for Kirkendall void formation and causes physical dislodgement of coating if the

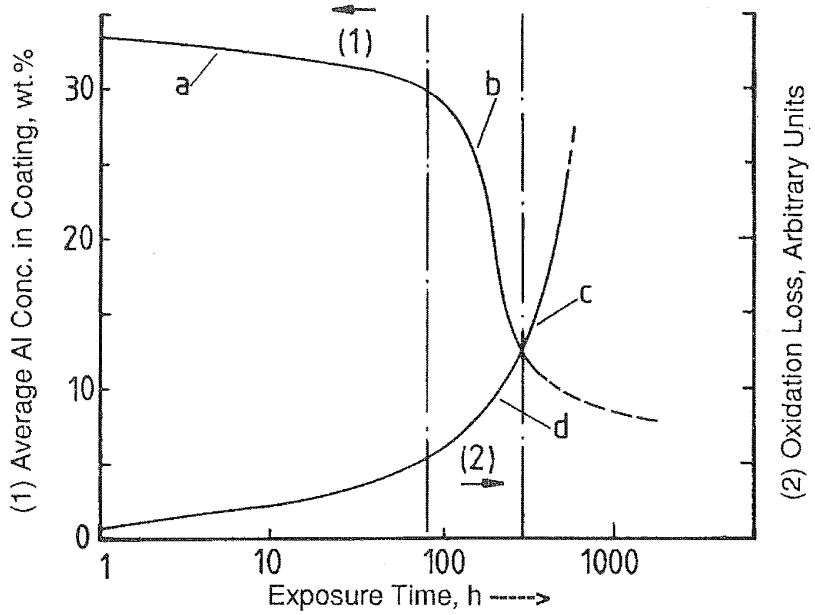

a. spallation induced loss
b. enhanced loss due to martensitic transformation
c. rapid oxidation of γ
d. rapid oxidation of γ

Fig.8-39: Oxidation Kinetics of Ni Coated with NiAl.
- Schematic of Variation in Al Level & Loss due to Oxide Penetration.

voids coalesce at the substrate/coating interface. Although Al_2O_3 is generally considered as an n-type oxide, it is argued that it is so only at low pO_2. Thus at 600°C, crystalline alpha Al_2O_3 grows beneath an amorphous film of gamma Al_2O_3 by inward diffusion of O_2. At 1300° - 1750°C, Al_2O_3 is n-type up to $pO_2 = 10^{-5}$ and becomes p-type at higher oxygen pressures (Natl.Acad. Sci.1970).

Nickel aluminide is still the best aluminide system in the gas turbine field although aluminiding was first used to benefit steels. At the commencement of oxidation the non-protective gamma alumina forms and spalls easily. A more dense and adherent alpha alumina then forms and as long as this remains undamaged it confers protective kinetics on the substrate. However, a damage and repair cycle soon causes Al depletion which affects the diffusion mode and composition of the NiAl below the scale. Below the critical Al concentration the single phase NiAl now rendered Ni-rich tends to precipitate the gamma prime Ni_3Al phase which causes NiO to react with Al_2O_3 to form spinels and also NiO on its own develops porosity during growth, thus increasing mass transport. Appearance of the gamma prime phase thus marks the onset of the rapid oxidation stage. In a mixed gamma and gamma prime the gamma phase is more readily oxidisable and forms a voluminous, porous multi-phased non-protective scale.

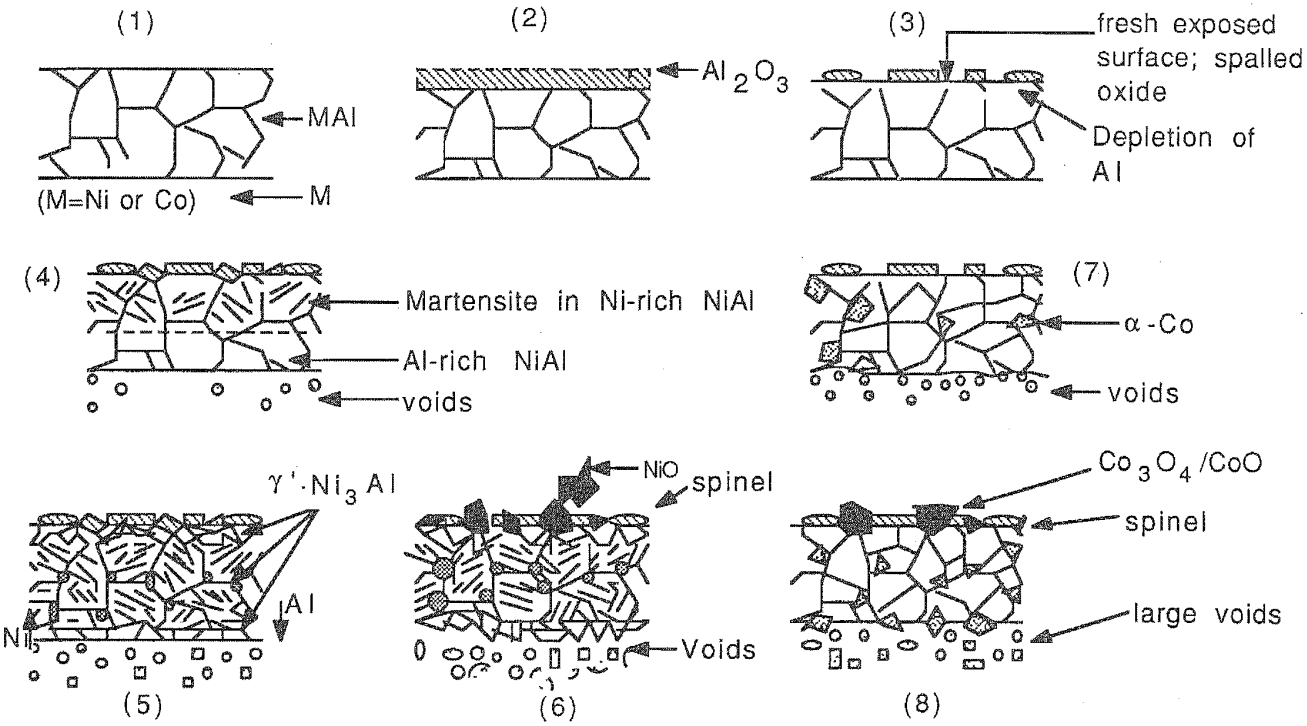

Stages (1)-(3): Common features to both NiAl & CoAl;
Stages (4)-(6): NiAl Coating on Ni Substrate;
Stages (7) &(8): CoAl Coating on Co Substrate

Morphological Changes in NiAl & CoAl Alloy Coatings on Ni & Co Substrates respectively

Fig.8-40

8.12.2. ALUMINIDE CASE HISTORY: SELECTED WORK

Carbon steels with varying Cr-content are being employed over a wide range of applications, and aluminide is an important surface coating. A high bulk Al is necessary for most carbon steels as diffusion levels the Al concentrations in the surface aluminide layer. A level of 18% Cr in the substrate leads to a lower level of Al on the surface for protection (Kindlimann & Greeven 1983). At 750-900^{o}C although there may be some spalling of the outer layer the inner layer is more compact and offers protection.

Low carbon steels used in higher mass production than the more expensive structural steels resort to a logically cheaper method of aluminizing by a hot dip process. A Ti- modified low carbon steel, ALUMA-Ti, with aluminide coatings of 75 - 120 g/m^{2} shifted breakaway behaviour beyond 2000 hours at 704^{o}C, a far greater period than the projected useful life. Its cyclic behaviour is yet to be tested (Denner & Kim 1983). Pack aluminizing done on low carbon steels is yet to be optimized as diffusion of iron outwards is still a predominant feature of aluminide degradation. Application in the petrochemical industry is linked to the development of aluminided low grade steel to substitute for 18-8 stainless steels. A promising oxidation rate at 900^{o}C has been achieved within an order of magnitude with uncoated low carbon steel and aluminided low carbon steel (rates of 3.0 x 10^{-2} and 3.6 x 10^{-3} mg/cm^{2}/sec at 900^{o}C) and at 700^{o}C with low carbon steel and 18-8 stainless steel (rates of 0.14 and 6.1 X 10^{-14} mg/cm^{2}/sec at 700^{o}C) (Mitani 1983). Simultaneous aluminizing and chromizing has also been done on austenitic stainless steels and their degradation investigated (Miller et al 1988).

At 850 and 900^{o}C aluminide layers less than 50 microns thick on EN-3 plain carbon steel oxidized in the first 24 hours at a slower rate than thicker coatings but over a 72 hours period the overall weight gains of coatings thicker than 50 microns were still low while the thinner coatings oxidized completly progressing deep into the substrate. A 75 micron thick coated EN-3 is more oxidation resistant than 304 stainless steel at 900^{o}C (Kindlimann & Greeven 1983). Fe-17Cr alloys pack aluminized and oxidized at 800^{o}-1000^{o}C form quite thick alpha-alumina scales unlike Fe-Cr-Al alloys. Although the oxidation is diffusion controlled, the rate constant varies due to scale sintering (Majid & Lambertin 1987). Al as an alloy additive to Fe-Cr-alloys is found to be more beneficial, and with Ti the improvement even allows economy in the more expensive addition of Cr (Becquerelle et al 1987).

Molten $NaNO_3$ - KNO_3 is considered as an energy transfer and storage medium for solar central receiver applications. Molybdenum steels with 2-9Cr and 1-2Mo, and 316 stainless steel were aluminided by pack cementation. The coatings were found to survive 6000 hours at 600^{o}C with a slow degradation occurring over the period. $NaAlO_2$ and $NaFeO_2$ were found to be the corrosion products (Carling et al 1983).

60 micron beta NiAl coatings on INI00, IN738LC and IN939 yielded a different morphology of the substrate coating complex as processed by Cr or Al pack, or Cr or Al vapour phase, wherein the latter samples were coated with 1 mg cm^{-2} Na_2SO_4 every 100 hours and hot corroded in oxidising conditions in air at 1 atm with hourly thermal cycling between 850°C and room temperature. Hot corrosion under reducing conditions was carried out at pO_2 = 10^{-15} in a N_2 - CO - CO_2 mixture; a small amount of H_2O is suspected. Air exposure cycled with a 2 hour exposure to the above mixture followed by nitrogen purging was adopted for any "redose hot corrosion".

Under oxidizing hot corrosion conditions the pack and vapour phase aluminides on IN738 recorded lifetimes of 1500 and 1300 hours as against 300 and 100 hour on IN100, and 400 hour each on IN939. Substrate influence is again evident. In hot corrosion under reducing conditions in Na_2S, $NaCrS_2$ and $NaCrO_2$ were observed as reaction products within an hour of reaction with the melt, while $NaAlO_2$ appeared after 70 hours. Eutectic Na_2S-Na_2O (m.p 682°C) is also formed as Na_2S reacts with traces of H_2O.

$$Na_2SO_4 + 4CO = Na_2S + 4CO_2$$

$$Na_2S + H_2O = Na_2O + H_2S$$

$$Na_2O + H_2O = 2NaOH$$

are the reactions proposed for Na_2SO_4 reduction. Al_2O_3 is more stable in molten Na_2S than Cr_2O_3 is, and in reducing conditions gets undermined by the molten reaction products (Steinmatz et al 1983; Sivakumar 1982). Aluminiding was first done on steels, but optimization has continued as its application has spanned over several grades in various environments and higher temperatures. In sulphidizing atmospheres at pS_2 of about 10^{-5} the alpha alumina scale thickness is grown over by sulphide scales in pure sulphur while in 10%H_2S-H_2 mixtures the sulphide is found nucleated under the alpha-alumina layer (Mari et al 1982).

Improved oxidation characteristics at 900-1000°C under both isothermal and cyclic conditions were achieved for an aluminided Ni-Al-Cr_3C_2 directionally solidified alloy by applying an intermediate layer of a Ni-20Co-10Cr- 4Al coat. A 10 micron Pt was more successful and alpha Al_2O_3 was formed and maintained; at 1100°C under thermal cycling it broke down but was capable of self-healing (Wood et al 1980).

Substrate influence on aluminides can be considerable. Ni-base alloy of composition Ni10Cr5Co12Ta4W1.5Ti withstood cyclic hot corrosion, the longest clocking 144 and 168 hours at 7 cycles. Mo, Re, Hf in the alloy were not beneficial to either or both low and high activity pack coated aluminides, while V strongly decreased the oxidation resistance (Smeggil & Bornstein 1983). This is shown in Table 8:10. Morphology and RBS studies on the Hf-effect on NiAl coatings on IN 738 and Rene 80 show that oxide

intrusions ('pegs') into the substrate increased with the Hf content 1-2 wt.% with scale adhesion for Rene 80 alloy increasing as follows:

Alloy added with 3.5Ti, 2Ti+1.5Hf and 3.5Ti+1.5Hf in high activity aluminide registered adhesion coefficients of 55, 82 and 95%;

Alloy added with 5Ti, 2Ti+1.5Hf, 3.5Ti+1.5Hf and 5Ti+1.2Hf in low activity aluminide had adhesion coefficients of 70, 69, 50 and 100 respectively.

Hf diffusion through the aluminide coating of low or high activity was a function of time. RBS data IN 738 with 1Hf analysed only Al and Ni initially and after 100 h at 1000°C Mo, Hf+W were identified (Muamba et al 1987). Titanium alone has been aluminided and oxidized at 850-1000°C with thermal cycling in static air. Interdiffusion effects have to be considered (Subrahmanyam & Annapurna 1986).

Low activity aluminide on IN738 and MAR-M002 was resistant to both O_2 and O_2-SO_2 environment at 700 and 830°C but in the presence of Na_2SO_4 (8 micro-gm/cm^2) in the latter gas mixture produced catastrophic corrsion discussed in sections 8.8-8.10 (Rhys-Jones & Swindels 1987). Substrate influence and diffusion effects

TABLE 8:10

HOT CORROSION TEST RESULTS

	High Temperature / Low Activity Coating		Low Temperature / High Activity Coating	
Alloy	Cycles to Failure	Time to Coating Failure (hrs)	Cycles to Failure	Time to Coating Failure (hrs)
MAR-M200	3	59	4	72
MAR-M200+Hf	3	72	1	0.08
Alloy 454	6	144*	7	168*
Alloy 231	7	144	3	53
Alloy 245	4	72	3	60
Alloy 250	7	168	3	66

* Failure determined by visual inspection of test specimen, not thermogravimetric results.

are further confirmed in the studies on aluminided gamma-phase Ni-base alloys in air at 1100°C. Ni-7Al, Ni-12Cr, Ni-23Cr and Ni-12Cr-7Al alloys used to monitor the additive flux at the substrate/coating interface indicated that ternary "cross-term" effects could be often large and determine the direction and magnitude of both Cr and Al fluxes. Oxide spalling was a common feature, with the 12Cr binary proving the best resitant to spalling. Inter-diffusion coefficients are derived (Fink & Heckel 1987). Mechanically alloyed and oxide dispersed Ni-base alloys (ODS MA-alloys) exhibit acute porosity effects. Diffusion aluminide coatings on all ODS MA-alloys showed porosity after 146 h at 1100°C. Higher Al levels in the substrate alloy reduced the porosity. The combined effect of Cr+Ta was also found beneficial (Benn et al 1987).

Beta NiAl implanted with Y in doses of $2x10^{14}$, $x10^{15}$ and $x10^{16}$ ions/cm^2 with penetration to about 300 angstroms showed that scale growth on the implanted specimen was only by the outward diffusion of Al and did not have the inward diffusion of oxygen in addition as in the non-implanted sample. Scale adherence and reduced growth rate was attributed to the growth mechanism influenced by Y (Jedlinski & Mrowec 1987). Incorporation of Y into an aluminide by pack cementation did not result in the beneficial effect normally associated to Y addition to that alloy. It is not clear how sustaining implantation of Y is and how it compares with Y as a substrate alloy additive. Pack yttriumizing with or without pack aluminiding IN 738 resulted in an adverse effect on cyclic oxidation (Tu et al 1987).

The mechanisms which govern aluminiding impose particular limitations in composition and microstructure. Incorporation of a second and third element either as a pre-deposit/treatment or together with Al, combining the advantages of it being a simple process, unrestricted to line-of-sight offers scope for further exploration of aluminide coating formulae (Mevrel & Pichoir 1987).

8.12.3. CHROME - ALUMINIDE COATING DEGRADATION

Chromium is the principal metal linked with aluminiding, and most high temperature alloys rely on the oxides of Cr and Al for a consolidated resistance to degradation. The effect of many of the substrate components on the aluminide layer has been given in Chapter 5. The following solubilities in NiAl have been reported: Pt - up to 30% (Betz et al 1976), which with Fe and Co forms the first group with highest solubility. An average solubility of about 4 wt% is observed for Ti, Cr, Ta and W at 1000°C. Nb and Mo at 1 wt% in NiAl exhibit the lowest solubility. Thus:

Increasing solubility in Ni-rich NiAl

<---

Fe, Co, Pt Ti, Cr, Ta, W Nb, Mo

--->

Increasing tendency to form diffusion barriers

The total element content in the substrate and in Ni_3Al and NiAl and the thickness of the solid solution barrier layer after 50h at 1000°C as Al diffuses inwards and the substrate elements dissolve in the Ni-Al complex, is reported (Fleetwood 1970). A barrier layer for resistance to degradation is found effective when Al diffusion towards the substrate is arrested and this is achieved when the cumulative content of Cr, W, Ti, Ta, Nb and Mo is more than 20 wt%. It is evident that in most alloys a high level of Cr is necessary to compensate for the absence of a low level of the other elements listed above. The chrome level can be increased by Cr in the substrate, a better degradation resistance by chromization before or during aluminization.

The degradation in a chrome - aluminide layer is influenced closely by the major element diffusion and degradation mode and the temperature effect on them. In general nickel-base alloys form Cr-rich intermediate layers during aluminizing unlike Fe-base alloys (Fitzer & Maurer 1979). Fe-25Cr were found to be the most resistant to sulphide-forming and sulphur containing environments at temperatures less than 800°C where Ni-and Co- base alloys fail, the latter especially in Na_2SO_4 deposition conditions (Upadhya & Strafford 1983). Oxidation with thermal cycling and isothermal oxidation in exposure to fused Na_2SO_4 showed that the beneficial effect of Cr was to arrest spallation, and change in the coating microstructure was considered instrumental in restricting pitting of the chrome-aluminide diffusion coating. It is postulated that the Cr-enriched zone acts as a barrier to refractory metal diffusion, e.g. Mo, W, V, from the substrate and their subsequent oxidation (Godlewski & Godlewska 1987, 1986). An internal sulphidation zone where the spinel $(Cr,Al)_3S_4$ can exist with a broad range of Cr/Al ratio has been characterized (Erdos & Rahmel 1986).

A mathematical model has been developed to explore carbon diffusion through aluminided layers to form Cr_7C_3 (Marijnissen & Klostermann 1980).

8.13. DEGRADATION OF MCrAl-SYSTEMS

The extension of aluminided coating life for degradation is rarely achieved by Al alone. At its simplest, it is a dual metal system like Ni-Al, Co-Al, Cr-Al or Pt-Al and at its most complex a minimum of 4 and a maximum of 6 elements are formulated, usually of the general form MCrAl-X1 or MCrAlY-X2. These formulae are the most investigated; M = Ni, Co, Fe; X1 and X2 = Ce, Hf, Pt-group, Si, Ta, Ti, Y, Zr etc.; unusual additives like Mn, Zn and Cu have also been investigated. Schematic representations of degradation morphology of CoAlX and NiAlX are shown in Fig.8-41 and 8-42 respectively. Investigations on gas turbine coating systems have mostly concerned NiCrAlX1-X2 and CoCrAlX1-X2 compositions while the coal gas conversion systems have concentrated on FeCrAlX1-X2 systems. Fig.8-43 a,b show the oxide regions of

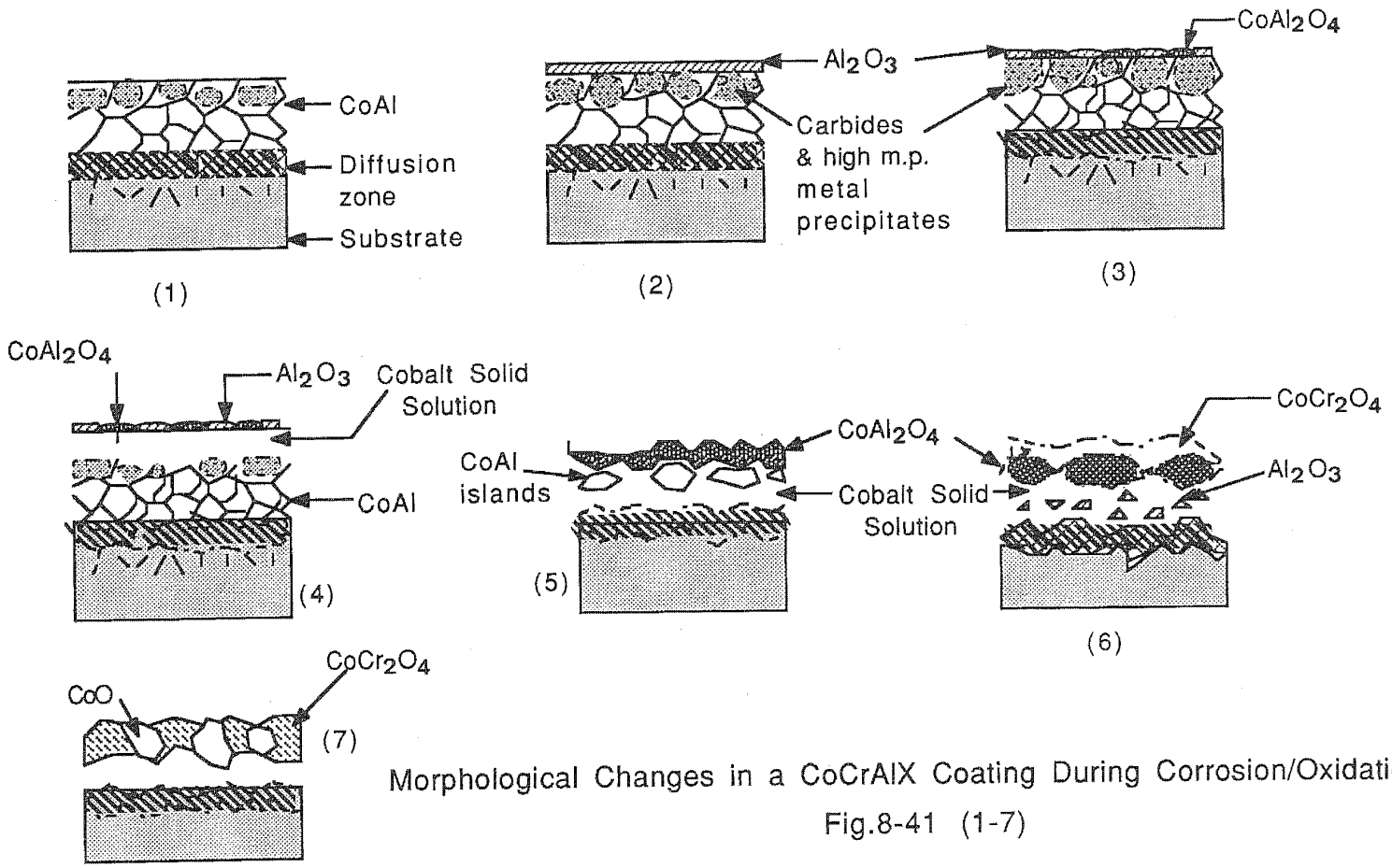

Morphological Changes in a CoCrAlX Coating During Corrosion/Oxidation

Fig.8-41 (1-7)

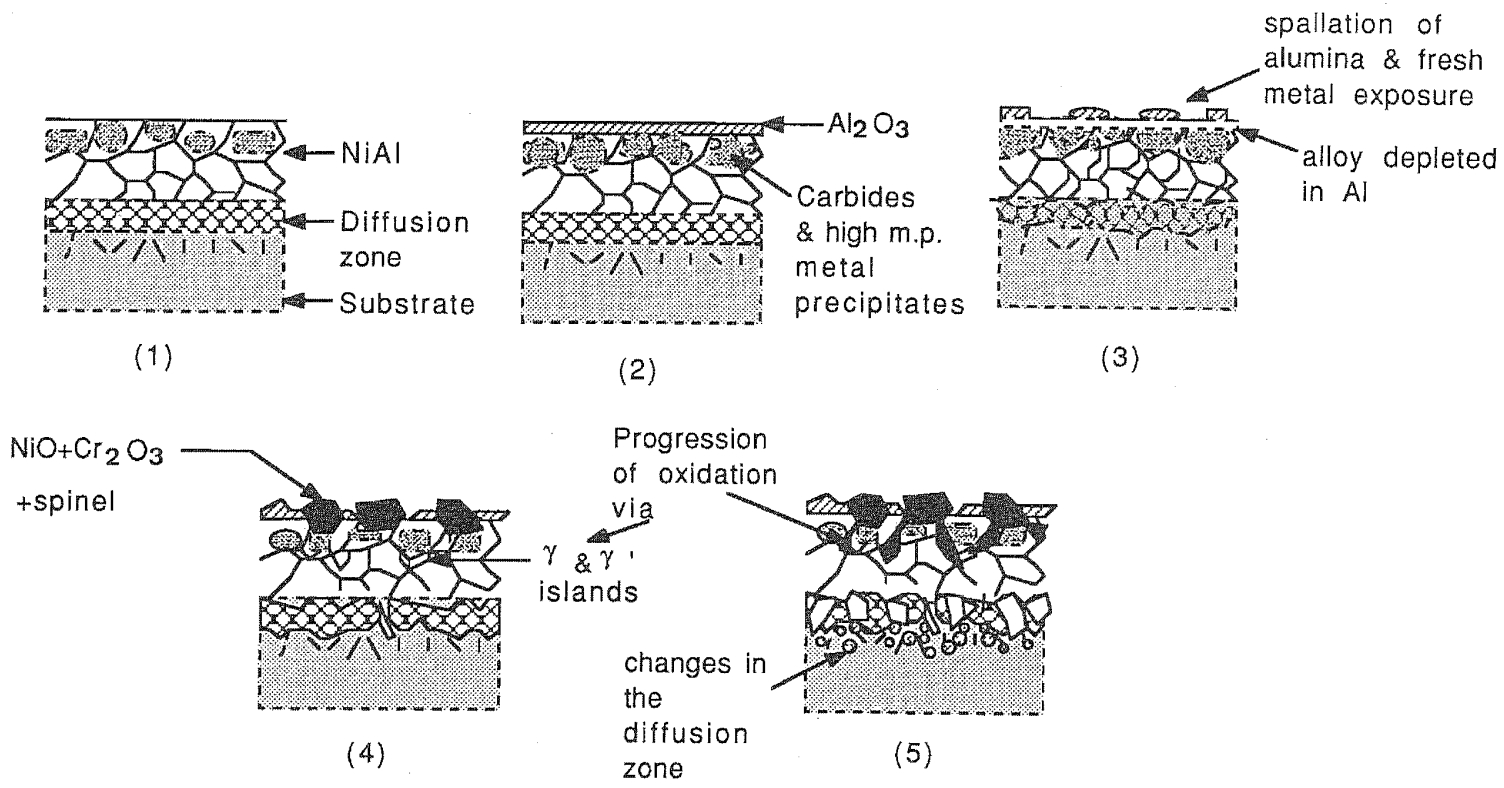

Fig.8-42: Morphological Changes in a NiCrAlX Coating During Corrosion/Oxidation

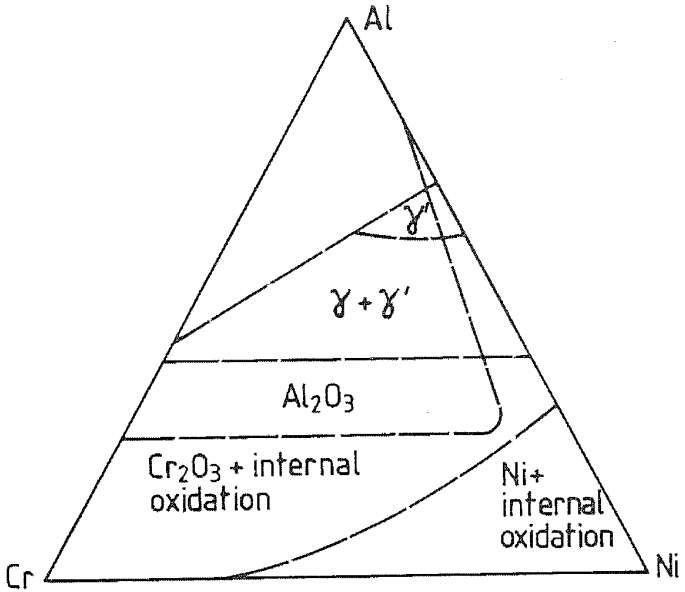

Fig.8-43a: NiCrAl-Oxide System at 1000°C

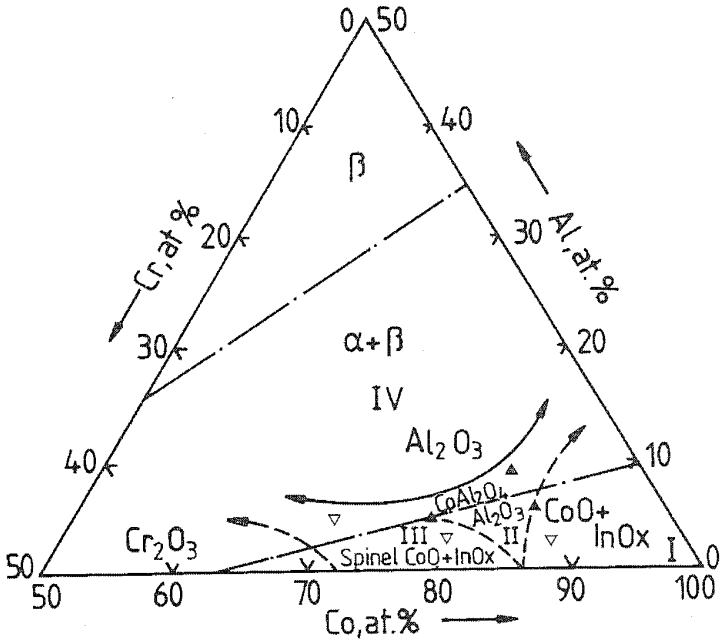

Fig.8-43b: CoCrAl-Oxide System at 1000°C

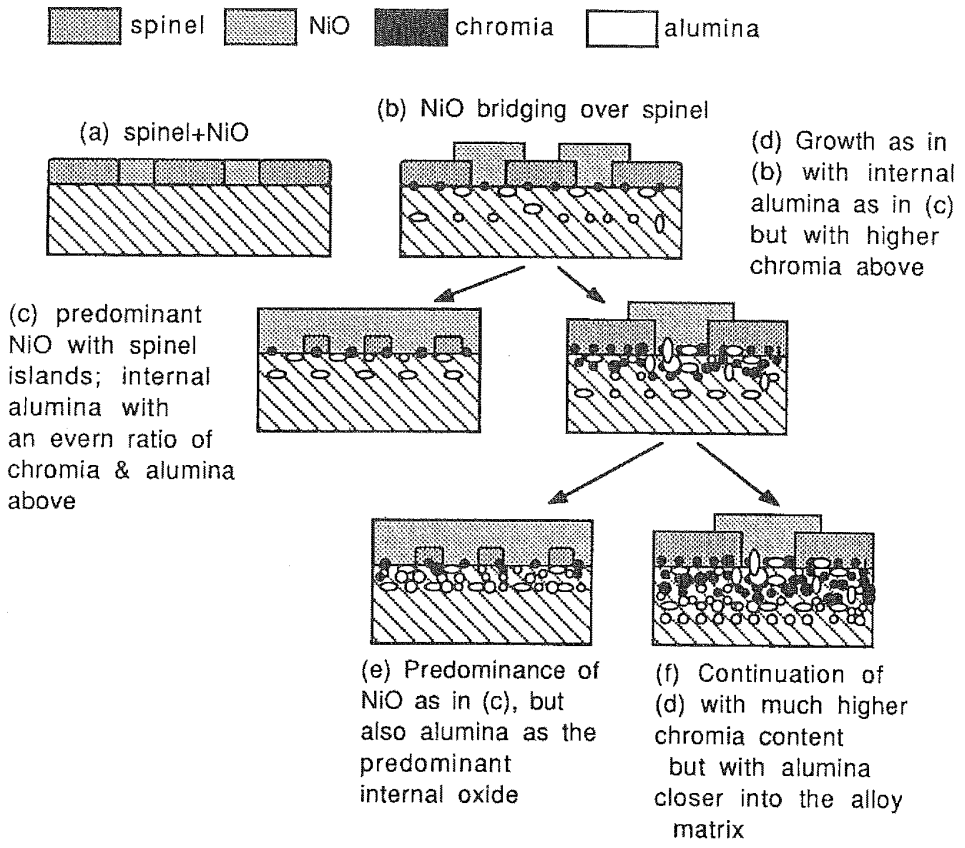

Schematic Representation of Oxides and Spinel Formation in NiCrAl Alloys

Fig.8-44

ternary NiCrAl and CoCrAl systems. Fig.8-44 and 8-45 give an idea on oxide and spinel formation across the substrate/coating/environment and the distribution modes of internal oxides/sulphides in MCrAl systems, M= Ni, Co or Fe. In sulphur-predominant environment sulphide products take a major spectrum in distribution (Nicoll 1984; Wallwork & Hed 1971).

Chromium is an essential additive in all aluminide systems as it influences the stability, coherence and continuity of the alpha-alumina layer sometimes as a top-scale and often as the scale immediately beneath the chromia layer. There have been several investigation groups working on optimization of the additive elements to MCrAl-systems. A full discussion of these results for even the last few years is beyond the scope of this chapter. MCrAl coatings mainly rely on their ability to form barrier layers of alpha alumina and chromia. Degradation of these coatings therefore means a breakdown in the scale coherence and in the ability to repair and sustain the barrier layer. The actual mechanism by which a breakdown in the scale occurs depends on the

Corrosion Mode, Group 1: Low Temperature

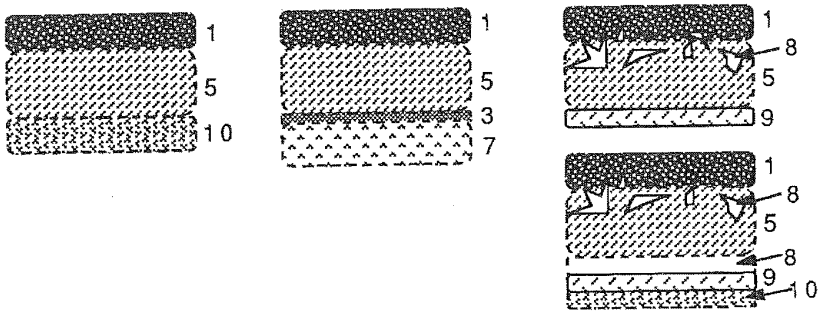

Corrosion Mode, Group 2: Intermediate Temperature

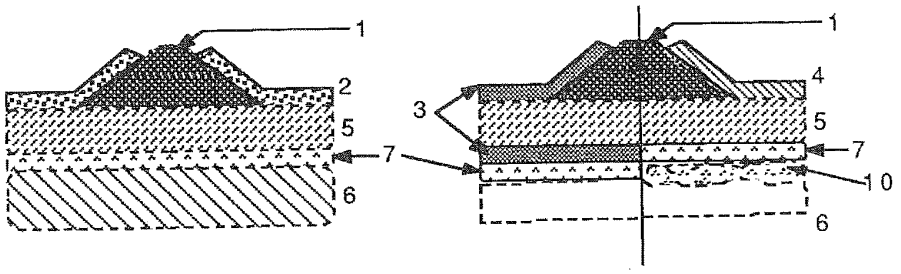

Corrosion Mode, Group 3: High Temperature

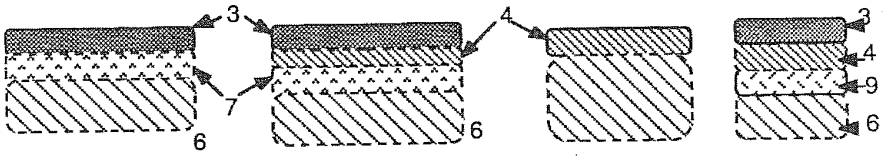

Schematic Representation of Scale Formation, Breakdown, Reformation and Compositional Changes Which Occur in NiCrAl, FeCrAl & CoCrAl Coatings.

Fig.8-45

1 MO/MxOy 2 broken MO 3 chromic oxide 4 alumina

5 complex (M+Cr+Al) oxides 6 oxidising alloy 7 internal oxide -alumina

8 M-sulphides 9 Cr-sulphides 10 internal oxide of alumina & chromia

interaction of the several parameters involved: the environment composition, particulate effect/velocity and temperature. It would be futile to ascribe any one mechanism as a rule of thumb to even one of the M-Cr-Al systems. The majority of MCrAlY applications has been as overlay coatings with ceramic barrier coatings in the field of gas turbines. A broad picture of degradation is provided with reference sources.

The behaviour of some MCrAlX alloys with Cr levels of 20-35% and Al contents of 2-5% has been studied (Strafford et al 1981), where M is Ni, Fe, Co, Fe+Ni or Fe+Co; X is Zr or Hf , with 1.5%Si , 1-4%Ti and 3-4%Ti or 11%Ta. A main aim was to find a composition range with improved resistance to low temperature sulphur-induced hot corrosion while maintaining adequate performance at high temperature (900°C). Specimens coated with $NaCl+Na_2SO_4$ and in SO_2+O_2 mixtures showed the detrimental effects of high Ni contents at 700°C. Additions of 0.5-2% Si and of Zr and Hf delayed the onset of accelerated attack. In contrast, (FeCo)CrAlX alloys had low corrosion rates at 700°; negligible sulphidation occurred. Good scale adherence was found for alloys with both Ti and Si additions. Ta was very effective in reducing the sulphide content in the scale while enhancing chromia formation. At 900° corrosion was much less for all the alloys studied, due to decreased sulphide stability and formation. Additions of Ni and Co (reducing the Fe content) were beneficial at 900°. It should be possible to develop coatings with adequate performance at both 700 and 900°C (Upadhya & Straford 1983; Conde & Booth 1972; Hocking & Vasantasree 1978,1984; Conde et al 1984).

It is common knowledge that an Fe-18Cr-8Ni is a chromia former at room temperature. The situation for oxide formation is more complex at higher temperatures. The entire oxidation phenomenon is temperature dependent and easily responsive to additional reactants in apparently low levels of concentration. Oxide predominance of any one species, either Cr , or the main matrix metals will not occur. Mixed oxides, and multi-layer scales are more common as Fig.41-45 indicate. Fe-base alloys can accept up to 4 to 5 wt% aluminium in alloying before fabrication difficulties arise; the Fe-15-25Cr-4Al series is principally an alpha-alumina former (Bennett et al 1980). Unlike Fe- base alloys the Ni-and Co-base superalloy compositions form chromia only when not superseded by the faster-growing Ni- and Co- oxides respectively. The aluminium levels here have to be high to influence an alumina-forming capacity, although chromium helps considerably in lowering the critical Al level needed. The systems NiCrAl and Co-Cr-Al have been extensively studied and reviewed (Wright 1972; Wallwork & Hed 1971). The Ni-Al system requires 15 wt % Al to form Al_2O_3 while a Ni-10Cr alloy requires only 5 wt% Al. Co-30Cr and Co-25Cr-2Al are both mainly Cr_2O_3-formers while Co-15 to 21Cr-10 to 12Al form alumina preferentially at 1000°C (Irving et al 1977). Preferential alumina formation is, again, temperature dependent requiring temperatures above 900°C and more commonly manifested in the Co-Cr-Al compositions rather than the NiCrAl based coatings, the latter being more often chromia formers above 800°C.

The degradation patterns of the Ni-Cr-Al and Co-Cr-Al systems change drastically when the corroding environment changes from O_2 to SO_2/Na_2SO_4-NaCl environment, although the severity may be more curtailed unlike in the binary alloys. The mechanism has been discussed in the previous sections, viz. 8.6-8.10 (Bornstein et al 1973; DeCrescente & Bornstein 1968; Giggins & Pettit 1980; Hart & Cutler 1973; Hocking et al 1977; Johnson et al 1975; Lewis & Smith 1962; McKee et al 1978; Reising 1977; Sequeira & Hocking 1978; Strafford & Hampton 1978). Sea salt and sulphur seriously affect scale coherence and subscale composition (Conde & McCreath 1980; Hossain et al 1978) but in pure O_2 NiCrAl alloys develop more protective and adherent scales than CoCrAl alloys (Barrett & Lowell 1978; Stott et al 1971).

8.13.1. MULTIPLE ADDITIVE EFFECT ON MCrAl-DEGRADATION:

Yttrium is the only additive which has been very widely investigated in all the three systems, viz. FeCrAl, NiCrAl and CoCrAl, in both laboratory and rig - evaluation tests. Other additives have been tested in addition or as an alternative. Degradation of M-Cr-Al-X systems is mostly the degradation of the M-Cr-Al scale. The mechanisms for the remarkable beneficial effect yttrium has on scale retention especially under thermal cycling conditions, have been reviewed (Lacombe 1987; Stringer 1985).

The directions investigations need to take would be to see how metal-oxide bonds are established, how stress generation modes change, how scale plasticity gets affected at the metal/scale interface both for the substrate metal and the growing scale, how vacancy and void formations are affected, how preferential growth in directions towards and inwards into the substrate occur, and how do cracks propagate (Stringer 1985).

Additives such as Y, (and Ce, Hf, Zr etc.) are referred to as active additions. The observed effects as summarized from various investigations are (Lacombe 1987):

(i) Y influences the scale plasticity due to the alteration in scale microstructure,

(ii) Oxide pegs are grown which anchor scale to substrate,

(iii) Mechanical property differences are graded between the scale and the substrate,

(iv) Scale growth mechanisms are influenced by influencing the diffusion parameters, thus reflecting on the transport and growth of the barrier layer

(v) Pore formations are eliminated by vacancy coalescence effects, and,

(vi) Chemical links between the scale and substrate are improved.

(Whittle & Stringer 1980; Stringer et al 1972; Douglass 1970; Cathcart 1975; Tien & Pettit 1972; Giggins & Pettit 1975; Stringer et al 1977; Allam et al 1978).

Transport properties and microstructure studies made on doped alumina show that results from these cannot be interpreted for thermally grown alumina. The yttrium effect is likely to be several phenomena acting simultaneously, so that, although the pegging mechanism cannot be ruled out, the more prominent effect is felt to be in microstructural modifications which result by a decrease in either anionic or cationic diffusion and in the scale stresses caused by oxidation (Huntz 1987). Porosity at the metal/scale interface is found to be present irrespective of Y as an additive; excellent adherence occurred in both NiCrAlY and FeCrAlY with small pegs; FeCrAl and NiCrAlHf with well-developed Al_2O_3 pegs had poor scale adherence, and it seems that adherence is not necessarily due to 'pegging'. While elemental Y is adherence promoting, Y added as sulphide is not; the adherence effect of Y added to a sulphur-containing alloy at levels adequate to getter the sulphur in alloy as well as any sulphur produced by the decomposition equilibrium of Y_2S_3, has been examined (Smeggil 1987). It appears that the nature and geometrical features of pegs are important from a scan of all the micrographs presented in literature. The mystery of Y still is to be solved acceptably!

The beneficial effect by Y is not realized unless its levels are kept low as an additive. Y is shown to produce a series of oxides, viz. $Y_3Al_5O_{12}$, $YAlO_3$, $Y_4Al_2O_9$ apart from two spinels - $Ni(Cr_{0.7}Al_{0.3})_2O_4$, $Ni(Cr_{0.45}Al_{0.55})_2O_4$, and oxides of Y, Al and Ni when its concentration is varied over 0-5.5 wt.% in triode sputtered NiCrAlY coatings on NiCrAl substrates, when oxidised in 1 h cycles in air at 1100°C. Convoluted surface oxides, with fractures, voids entrapped in the mid-layers and internal yttrium oxides, were identified (Choquet et al 1987).

Yttrium is added at a level not more than 1%, more usually in the range 0.3-0.8%. It forms intermetallic compounds YNi_9 and YNi_5 with Ni. A Ni9CrAl formed NiO as the main product at 800° and Al_2O_3 at 1000°C and 1200°C in O_2. Variation of Y over 0.005 to 0.7 wt% showed that 0.1-0.2 wt% was optimum for NiCrAl. CoCrAlY alloys consist of the dark beta-CoAl phase in a light matrix of the Co-rich alpha phase. The intermetallic Co_3Y localized the grain boundaries. Below 0.1 wt% this phase disappears suggesting a solubility limit below 0.1 wt%. One view is that Y provides enhanced diffusion of Al to the surface and increases the number of oxidation sites. An Al-Y double oxide forms giving a key-on effect and thus an increased oxide adherence (Kvernes 1973). In Ni10Cr5Al0.5Y, spallation was evident over long periods. It was postulated that $Y_3Al_5O_{12}$ forms at grain boundaries, Y_2O_3 releases Ni to form NiO or $NiAl_2O_4$ and yttrium annihilates voids leading to improved scale adherence (Kuenzly & Douglass 1974).

Alloy structures have an important influence on the degradation modes of multi-component alloys (and also for binary and ternary alloys), which becomes evident in systems such as NiCoCrAlYTa with 22-24 Co, 18-21 Cr, 7.5-9.5 Al, 0.7-0.8 Y and 3.5-4.5 Ta wt.%. Both the cast alloy and the LPPS-sprayed alloy had gamma, gamma-prime, and beta-aluminides, and sigma and M_5Y phases. The cast alloy also had Y_2O_3. Isothermal and cyclic oxidation in air at 850°C showed that the cast alloy with its large grain size of gamma and beta phases promoted scale heterogeity with chromia mainly in the gamma phase and alumina in the beta phase. In contrast, the LPPS alloy favoured a compact, homogeneous alumina partially modified by chromia (Frances et al 1987).

Y and Hf decrease the corosion rate of NiCrAl-, NiCrAlTi- and NiCrAlZr- alloys but this beneficial effect does not extend in full over the hot corrosion environment in the range 600-800°C because of liquid product or liquid product-deposit formations. The medium is particularly damaging to CoCrAlY coatings (Smeggil & Bornstein 1978; Jones & Gadomski 1977). Earlier theories postulated appear to be on lines similar to those discussed above (Bolshokov & Fedorov 1956). Co22Cr11Al0.3Y deposited on IN 738 superalloy by EBPVD and implanted Y and Hf on Co22Cr11Al were both found to degrade badly at 700°C under hot corrosion conditions (Provenzano & Cocking 1987).

Using CoCrAlY or NiCrAlY as the main coating system, many permutations and combinations have been studied; Hf has been a prime additive element (Hocking & Vasantasree 1986; Swidzinski 1980); Zr, and Si follow close and several others have been tested; e.g. W, Mo, Mn, Ce, Zn and Cu. Overlay and underlay coating systems are well known. The degradation in all these involve interlayer - adhesion - compatibility to thermal cycling and stress, and of corrosion interdiffusion effects during hot corrosion, and high temperature oxidation/carburization, nitridation, etc. Some of the candidate coating systems and their corrosion performance may be cited here (Atkinson & Gardner 1981). The data in Tables 8:11 to 8:13 and Fig.8-46 to 8-48 were generated on a directionally solidified Ni-Nb-Cr-Al eutectic superalloy (Strangman et al 1977). At high temperature the substrate influence especially on interdiffusion is considerable. The hot corrosion test was with coated Na_2SO_4 for 20 hour intervals at 870°C; the chloride effect is not registered. It must be re-emphasised here that degradation patterns are specific to the substrate/multilayer-coating/temperature/corroding environment system. Assessment can be broadly generalized. In the above study NiCrAlY / Pt and NiCrAlY physical vapour deposition coating systems exhibited the best combination of properties.

It was discussed in Section 8.8 that pure Na_2SO_4 melts at 884°C, NaCl-Na_2SO_4 is solid-liquid at 620°C, and a $CoSO_4$-Na_2SO_4 eutectic forms at 565°C from Co_3O_4, it being the stable oxide below 947°C. CoCrAlY degradation occurs in the form of pits or what is called a discontinuous precipitation effect in the coating adjacent to the hot corrosion pits. Beta-CoAl is found to dissolve locally in

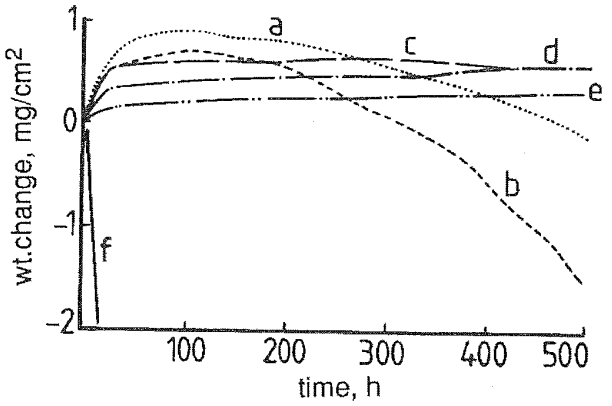

a. NiCrAlSiY
b. CoCrAlTaY
c. NiCrAlY+Al
d. NiCrAlY+Pt
e. CoNiCrAlY
f. Uncoated

Effect of Coatings on Cyclic Oxidation at 1093°C. Substrate: $\gamma/\gamma'\ \delta$ eutectic alloys
Fig.8-46

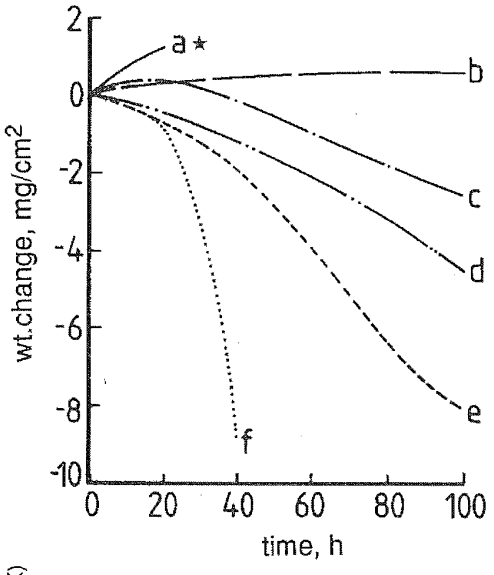

a. CoNiCrAlY
b. NiCrAlY+Pt
c. NiCrAlY+Al
d. NiCrAlY
e. NiCrAlSiY
f. CoCrAlTaY
*incipient melting observed

Oxidation at 1205°C. Substrate: $\gamma/\gamma'\ \delta$ eutectic alloys
Fig.8-47

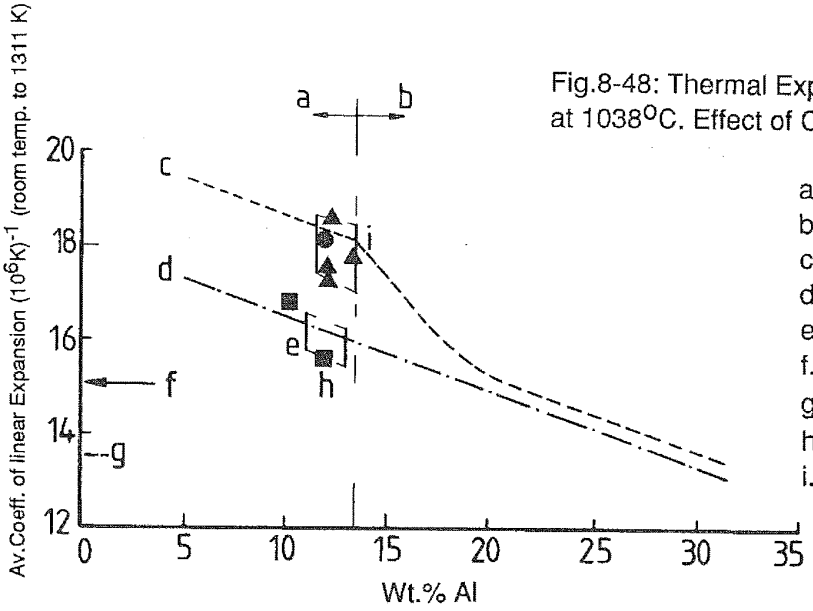

Fig.8-48: Thermal Expansion of NiCrAl at 1038°C. Effect of Co & Pt addition.

a. Ductile coatings
b. Brittle coatings
c. NiCrAl maximum
d. NiCrAl minimum
e. typical NiCrAlPt
f. Mar M200 Hf
g. $\gamma\gamma\ \delta$
h. 5Pt, 10Pt
i. typical NiCoCrAl (21.9Co)

the alpha-Co (Cr, Al) matrix immediately adjacent to such pits. On re-precipitation, the fine beta-CoAl lamellae are dissolved in the alpha-Co matrix all the way to the oxide pit (Smeggil & Bornstein 1981).

TABLE 8:11

A SELECTION OF COATINGS TESTED IN HOT CORROSION TRIALS

A. Overlay Coatings

Coating	Process	Thick-ness,μm	Coating	Process	Thick-ness,μm	Notation
Ni	E-pl	25	Co-a	EBVD	127	Ni+CoCrAlY
W	Sp.Dep.	13	Co-a	- " -	127	W +CoCrAlY
			Co-b	EBVD	127	CoNiCrAlY
			Ni-a	EBVD	63, 127	NiCoCrAlY
Ni-a	EBVD	63	Pt	Sp.Dep.	6	NiCoCrAlY-Pt
			Ni-b	EBVD	127	NiCrAlY
Ni-b	EBVD	63,127	Pt	Sp.Dep.	6	NiCrAlY-Pt
W	Sp.Dep.	13	Ni-b	EBVD	127	W+NiCrAlY
Ni-b	EBVD	127	Al	Pack		NiCrAlY-Al
			Co-c	Pl.Spry.	127	CoCrAlTaY
			Ni-c	Pl.Spry.	127	NiCrAlSiY

B. Aluminide Coatings

			Cr+Al	Pack	51-76	Cr-Al
Ni	E-pl	76	Cr+Al	Pack	51-76	Ni-Cr-Al

Note: E-pl: Electroplating; EBVD: Electron beam vapour deposition; Sp.Dep.: Sputter Deposition; Pl.Spry: Plasma Spraying; Pack: Diffusion coating by Pack Cementation.
Co-a: Co 18Cr 11Al 0.6Y; Co-b: Co 33Ni 18Cr 15Al 0.6Y;
Co-c: Co 18Cr 11Al 5Ta 0.3Y
Ni-a: Ni 23Co 18Cr 12.5Al 0.3Y; Ni-b: Ni 18Cr 12Al 0.3Y;
Ni-c: Ni 18Cr 12Al 2Si 0.3Y

The initiation of hot corrosion attack on Na_2SO_4-coated CoCrAlY at 700°C in SO_3-O_2 mixtures was observed to be due to hole formation in the oxide scale. It was thought to occur due to a reaction between yttrium oxide and Na_2SO_4, but this is not supported as holes develop in oxide scales formed on alloys not containing yttrium (Hwang et al 1983) A similar scale porosity was observed in NiO scale on a Ni- Mo-W-Al after 25 hours at 800°C in air (Smeggil & Bornstein 1981). It seems hole formation is a scale oriented phenomena and not concerned directly with any one base metal alloy Co- or Ni-. Some of the main differences in the hot corrosion of NiCrAlX and CoCrAlX alloys at 600-800°C and above 800°C may be summarised here. Given the same composition, in an

SO_2-O_2-SO_3 atmosphere, with a salt deposit of Na_2SO_4, NiCrAlX is attacked to a high degree only when the Ni- Ni_3S_2 eutectic is allowed to form, which will be when Cr_2O_3 and Al_2O_3 layers break down either to allow Na_2SO_4 and gas in or promote NiO growth outwards which leads to Ni_3S_2 nucleation within it (Hocking & Vasantasree 1981).

TABLE 8:12

CYCLIC HOT CORROSION TESTS ON COATED ALLOYS

Test Conditions: Substrate (Eutectic Alloys);
Coatings listed in Table below;
Duplicate test samples were salt-coated with 0.5 mg/cm^2 Na_2SO_4 every 20 h and oxidised for 13 cycles of 20-h at 871°C

Coating	Total Weight Change, mg/cm^2	Alloy Performance
Ni+CoCrAlY	0.06, 0.04	Very low-degree attack
W+NiCrAlY	0.10, 0.60	Excessive attack at coating repair sites
NiCrAlY	0.17, 0.12	Post-test state of samples excellent
NiCrAlY-Pt	0.11, 0.03	As above; excellent resistance
NiCrAlY-Al	0.36, 0.43	Localized failures at coating defects
CoNiCrAlY	0.06, 0.02	Low-degree attack
CoCrAlTaY	0.64, 0.15	Samples covered with a bluish spinel oxide; reproducibility only fair
NiCrAlSiY	0.02, 0.01	Loss due to spalling and Cr-removal as soluble Na_2CrO_4
Cr-Al	1.47, 1.57	Selective attack at corners
Ni-Cr-Al	0.37 0.38	Localized failures at coating defects
Uncoated Alloy	4.90	Accelerated attack

TABLE 8:13

HIGH TEMPERATURE STRESS RUPTURE TESTS ON COATED & UNCOATED ALLOYS

Test Conditions: 1038°C; 151.7 MN/m^2, in air. Where 'Y', samples were furnace aged in argon at 1093°C for 500 h (except no.5 which was aged in air instead of argon)

A. NiCrAlY-Pt Coated Alloys:

Coating thickness, um	Aged, Y/N	Time to rupture, h	Affected thickness, Coating +/- oxidation affected substrate, um	Recalculated Stress level MN/m^2
107	N	206.2	27.9	160.0
107	N	206.1	25.4	158.6
39	Y	213.4	42.2	162.8
46	Y	287.3	47.0	164.1
95	Y	328.8	42.7	163.4

B. Uncoated Alloy

	N	106.2	67	169.7
	N	122.9	76	171.7
	Y	114.7	67.3	169.0
	Y	166.4	80.0	173.1

Note: Original stress level was calculated on the basis of gauge cross-section area of the uncoated alloy sample. The new stress level was then calculated on the cross section unaffected by either oxidation or diffusion with coating.

Unlike NiCrAlY, in CoCrAlY, breakdown in Al_2O_3 and Cr_2O_3 leads to Co_3O_4 formation which forms a $CoSO_4$ as a secondary product, and forms a eutectic with Na_2SO_4. It is this reaction that results in a major degradation of CoCrAlY and most other Co-base systems. At 1100°C CoCrAlY coatings showed very good corrosion resistance to V_2O_5-Na_2SO_4 and NaCl-Na_2SO_4 synthetic corrosion ash (Nakamori et al 1983). Ni-base alloys are not suitable , since they undergo catastrophic attack. Creep rupture and alternate load tests have shown that a high Co content is desirable for scale retention of aluminides, chromide-aluminides and MCrAlY-X coatings on IN100 as substrate (Schmit-Thomas & Johner 1983). Other additives like Hf, Ce, Zr and W, reduce the corrosion rate in general. Hf has been very rarely identified as a part of the scale product, but the other elements have been found as oxides incorporated in the Cr_2O_3 matrix or presenting an internal oxide precipitate band at the coating/scale interface.

MCrAlY coatings 100-150 microns thick, applied by LPPS onto superalloy substrates, heat treated for 4 h at 1115°C in vacuum were tested in O_2 potentials from 10^{-24} to 10^{-25} with pS_2 potentials ranging from 10^{-10} to 10^{-8} and carbon activities of 0.65-1.00 at 650 and 871°C. The degradation was on the lines discussed above; high aluminium NiCrAlY and CoCrAlY gave the best resistance over a wide range of pS_2 at both temperatures. NiCrAlLaY, CoNoCrAlY and NiFeCrSiBC were promising in the low to intermediate pS_2 (Natesan 1987).

The beneficial effect of yttrium on the scale adherence of Fe-Cr-Al alloys is similar to its role in Ni- and Co-base alloys except that more than one iron oxide and sulphide is involved in the diffusion process and in the oxide / sulphide scale degradation. The aluminium content has to be increased as the chrominum content rises and on addition of Ni more Al is needed. Thus a 20 wt% Cr requires 2-3% Al while with 20% Ni, 12-14% Al is required (Tomaszewicz & Wallwork 1978) and and it will be at the cost of the mechanical properties, viz low creep strength from 650-900°C (Wilhemson 1983). At $pS_2 = 10^{-4} - 10^{-6}$ in H_2S/H_2 over 700-900°C a 26.6 atom% Cr-Fe alloy developed a rapid growing (Fe,Cr) S and a slower growing $(Cr,Fe)_3S_4$ scale; at $pS_2 = 10^{-2}$ three layers are formed, a duplex scale at 10^{-5} and a single scale at 10^{-5} (Narita & Smeltzer 1984).

8.14. DEGRADATION OF SILICIDE COATINGS

Silicon is the third element chosen in hot corrosion systems for its ability to form a barrier layer to resist degradation, the protectivity relying on the formation of SiO_2. It offers the best melt fluxing resistance in hot corrosion environments at high pSO_3. The pattern of growth and retention of SiO_2 alone or as an oxide associate is influenced by the manner in which Si is introduced into the system, as an element additive to form an alloy by slurry or CVD methods, or by deposition or controlled oxidation to form SiO_2 or deposition as ceramics such as SiO_xN_y or Si_3N_4 or SiAlON. Although normally very stable, the degradation of SiO_2 can occur through cracking, peeling or spallation or vaporization loss as SiO (Pettit & Goward 1983; Goebel & Pettit 1975; Caillet et al 1979).

8.14.1. SILICIDE ON STEELS:

A pre-annealed thermal silica on steel shows a reduced reactivity in steam by a factor of x20 (Rigo et al 1982). In steam over 950-1100°C SiO_2 > 8000 angstroms was rated as a zero oxidation barrier. The thickness corresponding to stabilized reproductive index was taken as a measure of the unoxidized ceramic applied as SiO_xN_y or Si_3N_4 (Gaird & Hearn 1978). A layer of $MoSi_2$ on steel was found to give an oxidation resistance time increasing linearly with the increasing thickness with no cracks or peeling

developed up to 10 microns thickness (Motojima & Fujimoto 1982).

A $MoSi_2$ layer of high stability could be achieved at low siliconizing (CVD) temperatures when $SiCl_4$ was maintained at greater than 10 vol %. The reduced oxidation resistance at $SiCl_4$ < 5 vol% was probably due to the formation of Mo_3Si (Motojima et al 1982). A similar thickness-related oxidation resistance has been observed on a CVD-SiO_2 on 20/25/Nb stainless steel for over 5975 hours in CO_2 at 825°C. A layer > 2 microns reduced cation diffusion and decreased oxide spalling and attack by a factor of 5 with a chromium content of 15-16% complementing this prevention of spalling. Provided an adherent, non-spalling silica scale was maintained, pitting attack was also prevented (Bennett et al 1982).

The efficacy of silica layers on Fe-base alloys has been ascribed to a barrier effect, the diffusion of iron (Fe^{3+}) being 10^5 times slower in amorphous silica than in Fe_3O_4. The diffusion coefficient in silica is also lower than that of Cr in Cr_2O_3 and of the same order as that of Fe in Fe_2O_3 at 1100°C, and SiO_2 films slow down formation of sesquioxides on high Cr-steels (Atkinson & Gardner 1981). This has been amply proved in the use of SiO_2-coated structural steels in the nuclear industry. Vapour deposited silica coatings give extented life to 20/25/Nb stainless steels with protection against both oxidation and carbonaceous deposition (see Fig.8.49, 8.50) (Bennett et al 1984). Plasma sprayed WSi_2 coatings proved satisfactory in mechanical testing but failed in corrosion and scaling tests because of porosity (Knotek et al 1987).

8.14.2. SILICIDE ON REFRACTORY METALS

Si deposited on titanium substrates via silane (SiH_4) formed Ti_5Si_3 which was found to decrease the oxidation rate over the temperature range 700-1020°C in O_2. Scale formation was found to be a mixed oxide (TiO_2 + SiO_2) layer at temperatures below 875°, while above 900°C, an outer TiO_2 and an inner, inward growing TiO_2SiO_2 developed (Abba etal 1982). A similar mixed oxide of NiO + SiO_2 is reported on silicided Ni at 950-1000°C (Subrahmanyam 1982). Silicides have also afforded over 600 hours protection at 870° and 1315°C on Ta-9.6W-2.4Hf-0.01C and a 1064 hours survival at 1315°C on 35Mo-35W-15Ti-15V alloys (Wimber & Stetson 1968). The coating lives of complex silicides were found to be shorter under reduced pressure (0.01-0.1 torr) than at higher (50 torr) and ambient pressures. Coatings 0.003 inches thick were applied by the slurry technique : Si20Ti10Mo on Ta alloys, Si20Cr0.5B_4 on Mo alloys and Si20Cr20Fe on Nb alloys. The coatings survived 553 pressure cycles at about 290°C and were ductile and at 1425°C survived in excess of 100 hour cycles (Priceman & Sama 1968).

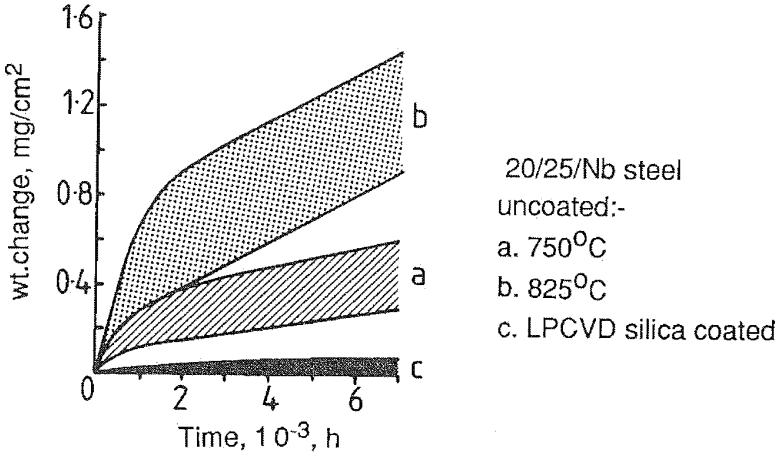

Fig.8-49: Effect of LPCVD Silica Coating on the Oxidation of 20/25/Nb Steel in 2%CO+300 ppm CH_4+200 ppm H_2O+CO_2.
(scatter bands shown)

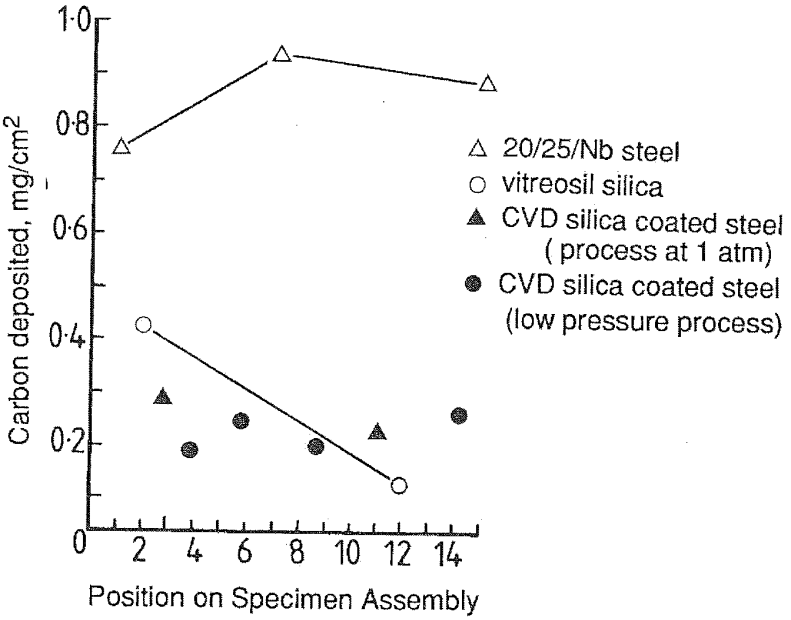

Fig.8-50: Carbonaceous Deposition Inhibition by LPCVD silica Coating. Substrate - 20/25/Nb Steel.

8.14.3. SILICIDE DEGRADATION IN GAS TURBINE ALLOYS:

Silicon-containing protective scales can be formed by Ni-5Si, Ni-11.5Si; a chromia-silica scale on Ni-40Cr-5Si and Ni-40Cr-11.5Si; and an alumina-silica scale on CoCrAlY-5Si and CoCrAlY-12.5Si. Co-silicides melt above 1200°C and no liquid silicates form below 1380°C. But a solid state reaction between CoO and SiO_2 is said to occur by an unusual surface diffusion process; Fig.8-51 (Schmalzreid 1974). None of the refractory Cr-silicides melt below 1300°C but a Ni-50Cr with a protective Cr_2O_3 scale is pitted extensively when pressed in contact with a Si/SiC composite for 120 hours at 1150°C in air. A Ni-Cr silicide underlayer in the molten state at 1150°C is envisaged (Ni-5wt%Si solid solution and silicides Ni_3Si and Ni_5Si_2) (Mehan & McKee 1976).

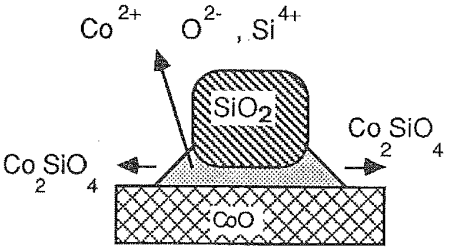

Cobalt oxide - Silica Interaction

Fig.8-51

An Al-11.7w%Si alloy forms a eutectic at 577°C and an Al_2O_3-SiO_2 reaction yields mullite at very high temperatures. Except at very low pO_2 a reduction reaction between Al and SiO_2 is unlikely. A Ni-30Al alloy (NiAl) showed Al_2O_3-scale fracture at 1150°C on 120 hours contact with Si/SiC, with a Si-rich phase penetrating the alloy. Contact reaction between IN718, a Ni-base superalloy, and Si/SiC showed severe pitting at 1150°C, and 1050°C, which was largely reduced at 1000°C and absent at 950°C. In all cases there was surface depletion of Si and the alloy matrix was seen to have complex mixed silicides some with Nb and Ti. A similar behaviour was observed for IN 738. Silicide phases $Ni_{16}Cr_6Si_7$, Co_2Si and Ni_2Si were identified along with Ti- and Nb- silicides. Degradation of Incoloy 800H was reduced by more than 50-80% by PAVD SiO_2 at 700-900°C in oxidation, carburization, and sulphidation. Laser fused SiO_2 have shown similar arrests, the coating having interacted with the substrate on application to result in a Cr:Si at 66:25 (Ansari et al 1987).

Silicide degradation in hot corrosion conditions must be viewed in the context of the above data. It is clear that Si diffuses inwards into the alloy substrate, with the diffusion penetration more marked at low pO_2. SiO_2 can be reduced by outward diffusing species like titanium which will then need a barrier layer to prevent this. Silicon gives a slight improvement in oxidation in air in the presence of NaCl in Ni and CoCrAlY systems but hot corrosion tests conducted in our laboratory showed scale spalling at both 700° and 900°C (Sidky & Hocking 1979, 1987a,b; Hocking & Sidky 1987a; Marriott et al 1980; Vasantasree & Hocking 1984). $MoSi_2$ is unsuitable for the protection of Ni-base alloys because of its low thermal expansion and also its high reactivity with

the substrate, while it is so successful on Nb- and Ta- based substrates. A Ni-Cr-Si with about 8-10 at % Si and a low Cr content, about 10% in gamma-solid solution is found very beneficial (Fitzer et al 1979).

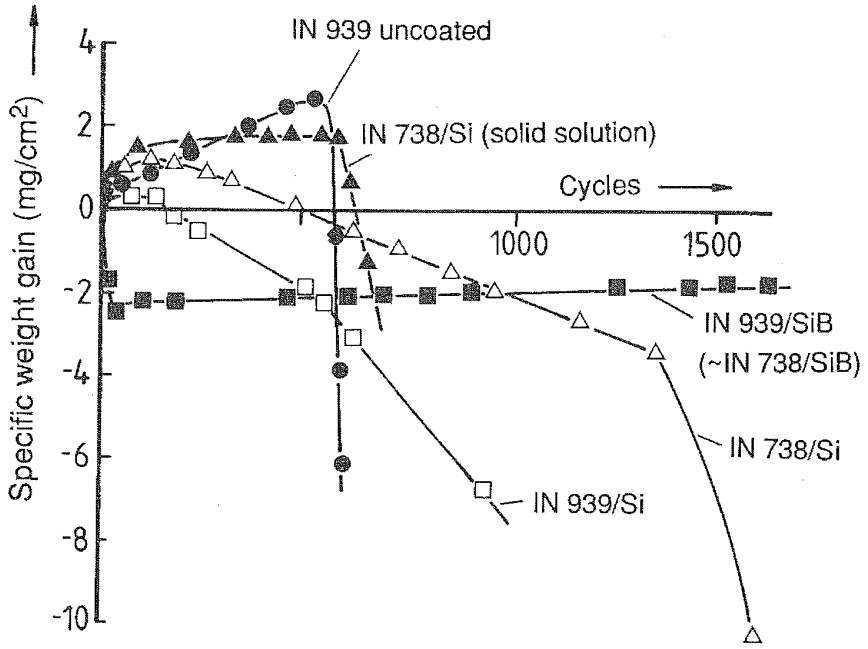

Fig.8-52: Effect of CVD Silicide Coatings on Cyclic oxidation. (Superalloy Substrates)

The phase stability of a vapour deposited silicide (Si on Ni) with a plasma sprayed chromium boride and their hot corrosion characteristics have been investigated. Siliconizing IN738 sprayed with Ni results in a gamma-Ni zone enriched with Co, Cr and Al, upon which develop the Ni_3Si and Ni_5Si_2 phases. Exposure to air at 1000^{o} for 300 hours resulted in a breakaway of the coating which was clearly associated with the separation of the Ni-Si eutectic structure. A brittle Si-rich Ni_5Si_2 below which is Ni_3Si followed by a heterogenous gamma-Ni layer with voids and inclusions leads to the degradation; Fig.8-52. Degradation of the better substrate-coating configuration of C73-Ni-silicide followed a similar pattern but with improved performance. The directionally solidified eutectic superalloy consists of Cr_7C_3 fibres in a CoCr matrix. After 1000 hours exposure at $1000^{o}C$ the Ni content in the coating dropped from 90% to 50%; Cr and Co of about 10% were present in the porous zone; the carbide from the substrate yielded a lamellar carbide layer of the type $Cr_{23}C_6$ with large amounts of Co, Ni and Si; no Ni_3Si_2 was formed but a Co-rich (up to 20 at%) Ni_5Si_2 compound was formed. It is the lattermost layer which would determine the corrosion resistance over long periods (Hildebrandt et al 1979).

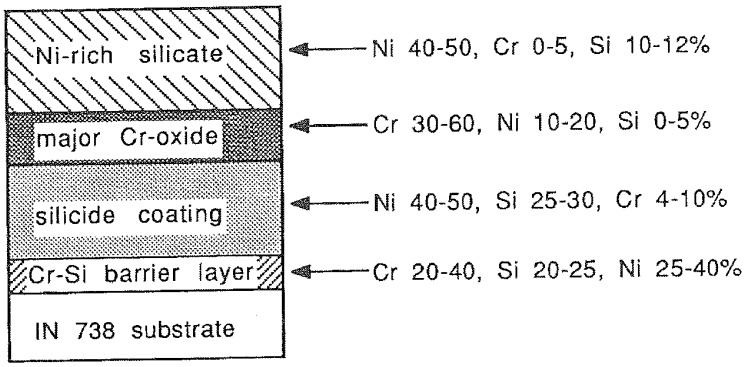

Fig.8-53: A Typical Morphology of Corrosion Product Formation of a Silicided Superalloy

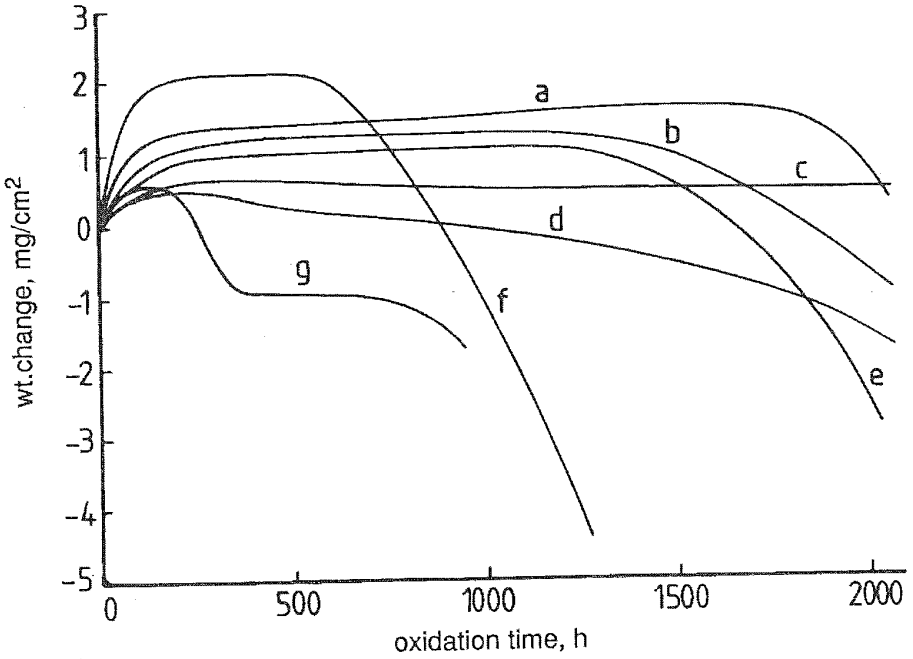

a. IN738 aluminised
b. ATS 340 aluminised
c. IN738 chromised
d. ATS340 chromised
e. IN100 chromised
f. IN100 aluminised
g. -SS on Nimonic 90

Fig.8-54: Silicide Coating 50Si-26Ni-24Cr wt.% on ATS 340 (equivalent to Nim 90). Oxidation effect over long exposure times in natural gas with excess air at 1000°C.

Much improved resistance based on the theory of providing a Cr-reservoir is achieved in a NiCrSiB coating on IN738LC. At 900°, during a 1000 hour exposure, the Cr-boride zone decreased as the oxide layer thickened, with the volume fraction dropping from 65-45% in 50 h reaching a stable condition after undergoing an Ostwald ripening process up to about 500 hours (Hildebrandt et al 1979). No data has been recorded on these coatings in sulphur-containing environments, but good oxidation resistance of 26Ni24-Cr50Si wt% coating in natural gas with excess air has been reported; Fig.8-53, 8-54 (Fitzer et al 1979).

Very good resistance to vanadic attack has been reported for silicon coated Ni-20Cr alloys at 900°C with a reduction of as much as 80% in the corrosion rate. No breakaway effects were observed for more than 600 h at 900°C in $80V_2O_5$-$20Na_2SO_4$ melts. The increased protection appears to be due to the development and retention of a Cr-rich barrier layer beneath a Si-rich surface with the slag showing little reaction with Si. Although Si coated by pack, vapour deposition, plasma spraying or ion plating methods was uniformly effective, ion plated coatings were found to be the most reliable with good adhesion, uniform composition and even thickness (Elliott & Taylor 1979). Fig.8-23 (p.434) shows the effect of a Si coat (Holmes & Rahmel 1979). The combined effect of molten sodium sulphate and vanadate is catastrophic in most cases as shown in studies on binary and ternary Ni-Cr(10-30 wt.%)-X alloys (X=Al, Si, V) and IN 738 (Sidky & Hocking 1987b).

A superior performance of ion plating as a coating method has been recorded for duplex coatings containing Si which have shown excellent resistance to attack by melts of $80V_2O_5$-$20Na_2SO_4$ at 850°C and 10% NaCl-90%Na_2SO_4 at 850 and 950°C. The tests were cyclic with 24 hr residence and recoating steps. A Ni-base alloy (Udimet 500) showed a 50% reduction in weight loss while the coatings were more effective on the Co-based alloy X-45 with a reduction by a factor of 24 (Nakamori et al 1983). The effect of fusing conditions of a Si-15Cr-10Ti-10Zr coating on C-103 niobium alloy was investigated. 1300°C for 30 minutes gave the best high temperature oxidation resistance (Kun et al 1982).

8.15. DEGRADATION OF THERMAL BARRIER COATINGS

Failure of thermal barrier coatings could be initiated by poor bonding to the substrate matrix, or the coating parameters such as porosity, microstructure-microcrack distribution, thickness, phase distribution and cohesive strength, or the relative thermal expansion mismatch and residual stress of the substrate-coating system. Ceramic sintering and bond coat inelasticity could also contribute to TBC degradation. Bond coat pre-oxidation causes degradation by adhesion failure. The actual failure generally occurs within the ceramic layer near the bond coat, and is believed to be due to slow crack growth and microcrack link-up with the ceramic. Table 8:14 (and Tables 8:12 and 8:13) give a

qualitative comparison of cyclic oxidation resistance. (Lowell et al 1976; Miller 1987; Kvernes & Forsyth 1987; Chang et al 1987; Strangman et al 1977).

TABLE 8:14

EFECTS OF THERMAL CYCLING ON NiCrAlY & NiCrAlZr ALLOYS COATED WITH ZrO_2-Y_2O_3

A. NiCrAlY/ZrO_2-Y_{23}

Heating Cycle Duration, h	1		7		20	
	Calc.	Exp.	Calc.	Exp.	Calc.	Exp.
No. of Cycles to failure	148	150	48	50	16	16
	110	120	35	35	15	15
	75	74	28	18	12	14
Time, h, to failure	148	150	300	300	320	320
	120	110	75	200	240	240
	70	75	160	115	220	280

B. NiCrAlZr/ZrO_2-Y_2O_3

Heating Cycle Duration, h	1		7		20	
	Calc.	Exp.	Calc.	Exp.	Calc.	Exp.
No. of Cycles to failure	49	50	13	17	6	8
	38	38	13	13	5	5
	-	30	15	9	5	5
Time, h, to failure	50	52	70	100	150	160
	40	40	75	75	90	90
	-	30	52	70	90	90

Note: the coating performance is superior on the NiCrAlY.

With the failure criterion defined as surface cracking visible under X10 magnification, an oxidation based model has been developed for predicting ceramic barrier coating life. The model is based on the cumulative effect of oxidation and thermal cycling on strains which promote crack growth. A fair agreement appears to have been achieved but the model fails where more complicated reactions are involved, and is also vulnerable to variations in coating characteristics during coating production. Table 8:14 indicates ceramic coated NiCrAlY to be superior to NiCrAlZr in thermal cycling tests (Miller 1984). Thermal fatigue failure is common in ceramic coats. The first order rule-of-thumb may be

postulated to be that a coating should have 1-2% ductility at the temperature of occurence of maximum strain and should have enhanced thermal fatigue resistance compared to elastically brittle coatings (Pettit & Goward 1983). For Ti-Si coats on superalloys by CVD the DBTT and the minimum strain to spalling or cracking were a function of both the coating composition and thickness. CVD-Ti added to CVD-Si increases the DBTT from 450-700^{o}C to 850-1000^{o}C. Decreasing the thickness from 180 to 50 microns for Si-B increased the minimum strain at 600^{o}C from 1% to 6% (Wahl et al 1981).

Ceramic coatings degrade by spallation due to transient thermal stresses aggravated by salts which induce hot corrosion. For non-oxide based ceramics such as silicon carbide and nitride, resistance depends strictly on the nature of secondary phases at grain boundaries due to the densificaton of additives, e.g. MgO, Y_2O_3, Al_2O_3 etc. (Billy 1987). Reaction-bonded Si_3N_4 and self-bonded SiC coatings were severely attacked in vanadic-sulphate melts at 820^{o}-1100^{o}C when exposed to a residual oil-fired environment in burner rigs (Brooks et al 1979). Tested in both crucible and burner rigs with melt compositions based on Na_2SO_4 with additions of NaCl, NaCl+V_2O_5 and NaCl+Li_2O (950^{o}, 200 h) reaction-bonded Si_3N_4 was found to be highly dependent on the overall environmental conditions for its corrosion. Excellent resistance was observed in oxidising and acidic media but very poor resistance in reducing and mildly alkaline environments. Several crystalline phases also occur on the ceramic surface during the corrosion reactions (Erdos & Altorfer 1979). Sintered SiC also suffered a similar attack in sulphate melts at 900^{o}C, less in oxidising conditions but more in basic melts or slags especially with carbonaceous material. However SiC was inert in pure N_2, H_2 or H_2-H_2S mixtures at 900^{o}C. Fig.8-55 shows the possible modes.

Pressure sintered Si_3N_4 exposed to air with Na_2SO_4 at 1000^{o}C showed extensive oxidative corrosion and the Na_2O-SiO_2-Y_2O_3 phase equilibrium and is examined in relation to it since the nitride ceramic contained traces of $Y_2Si_2O_7$, YSi and $SiYNO_2$. The silica film formed during oxidation dissolved and reacted with basic fluxing to form sodium silicate (Riley et al 1987). Degradation by pS_2-environment at 900-1300^{o}C with pS_2 at 10^{-6} and pO_2 at 10^{-15} show attack increasing via suphide products and volatile SiO (Datta et al 1987). Migrations of cations Mg^{+2} and Y^{+3} from the secondary phase material at silicon nitride grain boundaries are considered to contribute and interfere in the protective SiO_2 film growth (Riley & Andrews 1987).

Coatings of Si_3N_4, TiB_2 and Al_2O_3 proved to be effective barriers when free of fissures and pinholes (Hintermann 1981). Self-fluxing alloys of Ni-Cr-Si-B have great oxidation resistance. These are arc-sprayed from wire or powder stock and surface oxidation of the particles (which would prevent coalescence) is removed by the B and Si to give a fully dense fused deposit, also cleaning the base metal. If the substrate is Cr-rich, its oxidation occurs however, unless spraying and fusing are simultaneous.

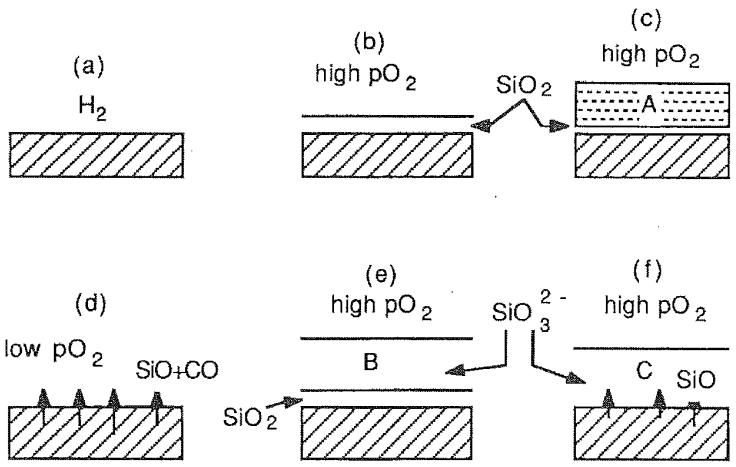

(a) Reduction environment; SiC is inert and suffers no material loss.
(b) A protective scale of silicon dioxide forms; could be termed as passivation.
(c) As long as the oxygen partial pressure is high, a passive layer of silica forms in the presence of an acidic or neutral melt.
(d) At oxygen pressures less than 10^{-16} SiC undergoes material loss via the formation of gaseous monoxides of silicon and carbon.
(e) Accelerated corrosion of SiC occurs in basic salt melts with soluble ionic silicates; a high oxygen partial pressure induces a layer of silica on the substrate.
(f) The highest degree of attack occurs in spite of a high oxygen pressure if an oxygen-depleted salt melt confronts SiC. Loss occurs through gaseous products as well as soluble silicates..

Fig.8-55: Effect of Gas &/or Molten Salt Environment on the Stability of SiC

Failure of SiC, Si_3N_4 (and also WC and Ni-Cr-B) by brittle fracture on erosion has been recorded on components used in fossil fuel energy proceses. The brittle fracture showed no relationship to hardness, the erodent being SiC particles (200 microns) at a velocity of 300 m/sec. The test conducted was at room temperature for 8-15 min with an erodent impingement of 5 gm/sec. Fine-grain structured, low porosity ceramic surfaces had the lowest erosion rates (Levy et al 1983). Attack on SiC under thin films of molten sodium carbonate and sulphate at 1000°C was found to occur at structural discontinuities with a crater-like material loss. The latter was correlated to bubble formation during the oxidation of SiC which created unprotected regions subsequently to be exposed to enhanced attack leading to pit formation. The simple oxidation reactions were (Jacobson & Smialek 1986):

$$SiC + 3/2\ O_2 = SiO_2 + CO$$

$$Si_3N_4 + 3O_2 = 3SiO_2 + 2N_2$$

Alloy compositions which have themselves been used to retard hot corrosion have been used as interlayers. A plasma-sprayed calcium silicate ceramic layer with a CoCrAlY or NiCrAlY interlayer was applied on to B 1900 and Mar M-509 and corroded at 1030°, 1100° and 1160°C under hourly cyclic conditions in air. The specimen life was a strong function of the temperature although the weight gain at the time of specimen failure was temperature-insensitive; Fig. 8-56 a,b (Miller 1983). Immersion in synthetic slag melts is used to rank on an accelerated test basis. Fig.8-57a shows tests on IN 738 coated with various bond coat materials (Bauer et al 1979). Creep rupture life of diffusion, overlay and thermal barrier coatings on IN 900 show the degradation of the uncoated IN 100 and the improvement gained by the bond coats and TBC (Fig.8-57b).

A good bonding interlayer betwen the ceramic coating and the substrate superalloys is vital for TBC survival. Titanium carbide and nitride are well-bonded to superalloys if the Ni_3Ti intermetallic phase is controlled. An excess produces a rough deposit and thus a poor bonding. A marginal carburization is also a requirement for good bonding (Bertinger & Zeilinger 1981). Without an interlayer, ceramic-substrate interactions are inevitable. MgO, Al_2O_3, S_iO_2 (as fused quartz), SiC and Si_3N_4 were all found to react with a Ni-based superalloy substrate, with the most severe being Si-SiC over 700°- 1150°C, with conditions at the interface held at minimized pO_2. Si and C diffused inwards forming silicides and carbides with the degree of reaction on the ceramic side being similar to that of the substrate below 900°C, and less above 900°C (Mehan & Bolon 1979).

Chemical and thermal-mechanical interactions are cited for the failure of porous, plasma-sprayed ZrO_2-Y_2O_3 (8,15,20 wt%), ZrO_2-MgO (24.65 wt%) and Ca_2SiO_4 with NiCrAlY as a bond coat on U-720 and ECY 768 alloy samples. Fuels ranged from pure diesel GT no.2 to doped 1-100 ppm Na, 2-180 ppm V, 2-18 ppm P, 0.25-2.25 wt% S impurities. Partially stabilized ZrO_2 containing small fractions of monoclinic ZrO_2 out-performed fully stabilized ZrO_2. The 2-phase ZrO_2 could develop micro-fissures to relieve thermal stresses. In contaminated fuels graded coatings of NiCrAlY bond coat/ NiCrAlY-oxide graded zone/oxide overcoat were better than a duplex NiCrAlY bond coat/oxide overcoat. Higher impurity content, higher mass flow rate or gas velocity and thermal stress conditions were detrimental, especially in vanadium 180 ppm and sea salt 100ppm (Lau & Bratton 1983). Plasma sprayed magnesia-stabilized zirconia (MSZ) thermal barrier coating over a mixed MSZ+NiAl coating over a thin NiAl bond coat has been used in gas turbine combustion chambers but oxidation of the NiAl occurs. Better bond coats are NiCrAlY and CoCrAlY which resisted hot corrosion. The best ceramic overcoat was 8% yttria-stabilized zirconia, which did not peel or spall (199) in molten salt tests at 800°C in 11 ks or in 1000 cycle 400°C to 900°C burner rig tests. The substrate was Hastelloy X or Haynes 188 (Akikawa & Uenuna 1982).

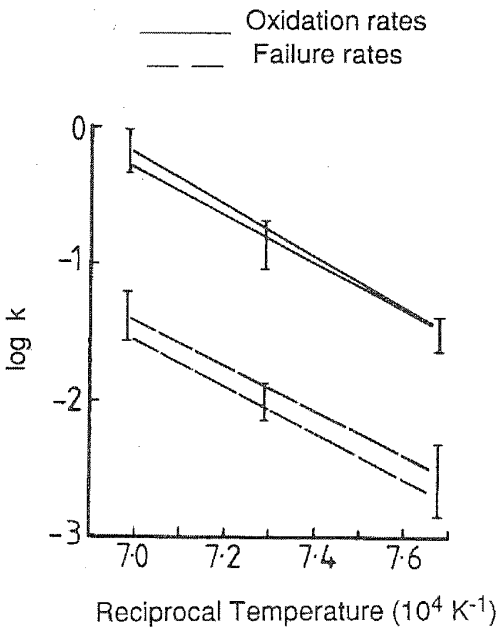

Fig.8-56a: Bond Coat Effects on Oxidation & Failure Rates. Arrhenius plots for Ca_2SiO_4/MCrAlY/MAR M509; (M=Ni or Co)

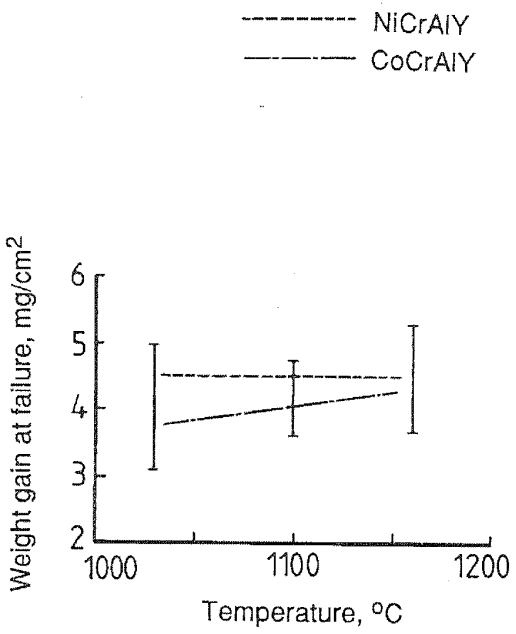

Fig.8-56b: Bond Coat Effects on Weight Gain at Failure for Ca_2SiO_4/MCrAlY/MAR M509; (M=Ni or Co)

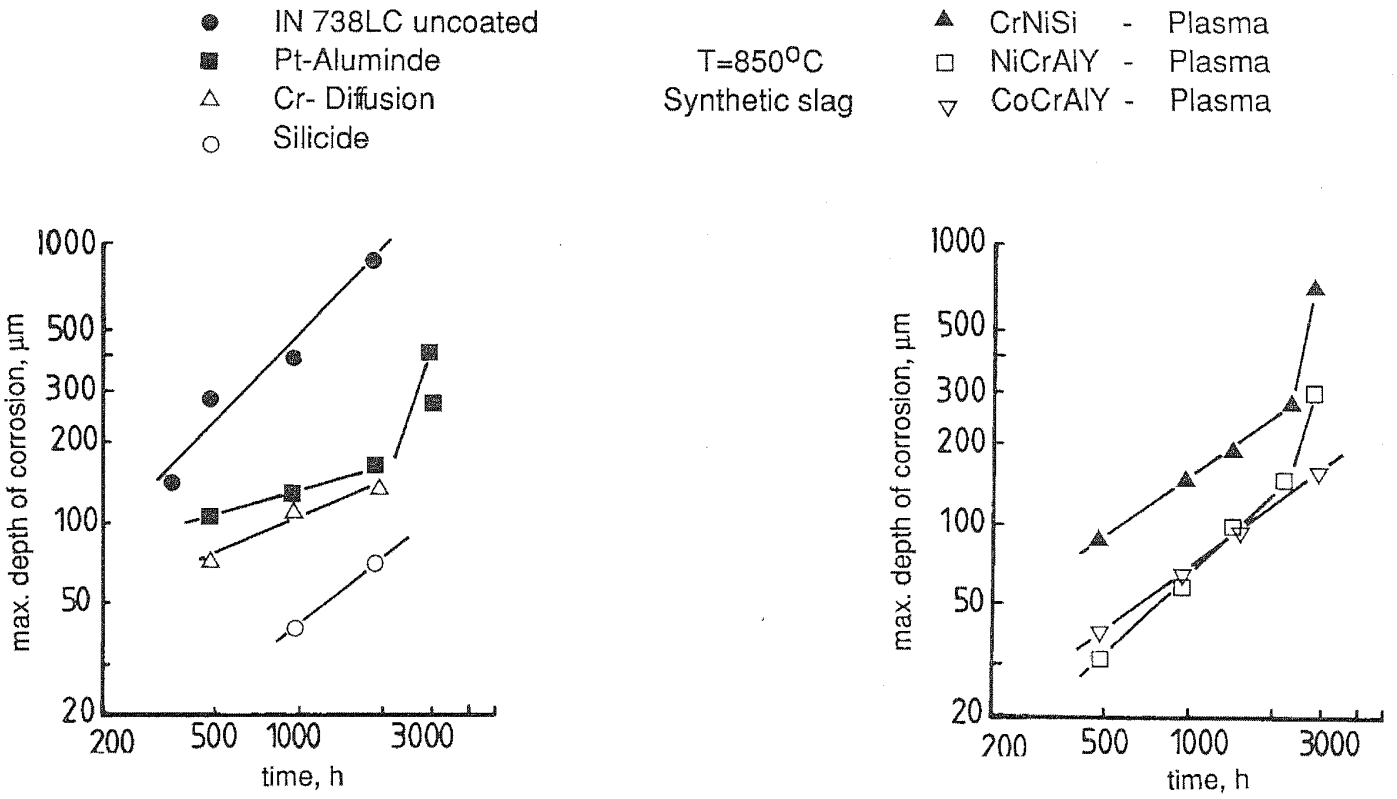

Fig.8-57a: Resistance of Coated IN 738LC to Hot Corrosion in Synthetic Slag Immersion Tests (Bauer et al)

Single crystal ZrO_2 ceramic with CeO_2 and yttria as stabilizers degraded less than the sintered variety in sodium vanadate melts. Although ceria and yttria did not react with the vanadate in the solid state, the melt leached out ceria (Jones & Williams 1987). Improved yttria-stabilized zirconia ceramics were found to adapt very well to thermal cycling with sealing coats inserted into the columnar ceramic, but molten sodium sulphate was found to penetrate the ceramic. The bond coat/sealing coat resistance was thus proved to be a key factor in determining coating life (Prater & Courtright 1987). Pt-ZrO_2 and Pt-Y_2O_3 have been tested in methane at 500°C, hydrazine at 800°C and in CO_2, H_2, NH_3, N_2, and steam at 1200°C for 2000 h as potential space station resistojet materials (Whalen 1988).

Unlike in the oxidation-hot corrosion area, the failure mode of ceramic coats used for wear resistance is via micro-chipping. The combined effect of wear and hot corrosion conditions would be such as to allow access to the bond layers. Cemented carbides such as TiC, TiC_xN_y and TiN degenerate with abrasive excursions and impact. The ceramics fail by transverse crack development, TiC being superior to TiN (Venkatesh et al 1981; Cho & Chun 1981). The CVD temperature has to considered relative to the tempering treatments required for the steel substrate so that the projected hardness can be achieved in use (Ruppert 1981). Boron-based ceramic coats offer good wear resistance, the process being boriding succeeded by metalliding (electrodeposition from molten salts). B-Cr, B-V, B-Si and B-Cr-Ti have been used with B-V giving excellent wear (Chatterjee-Fischer 1981).

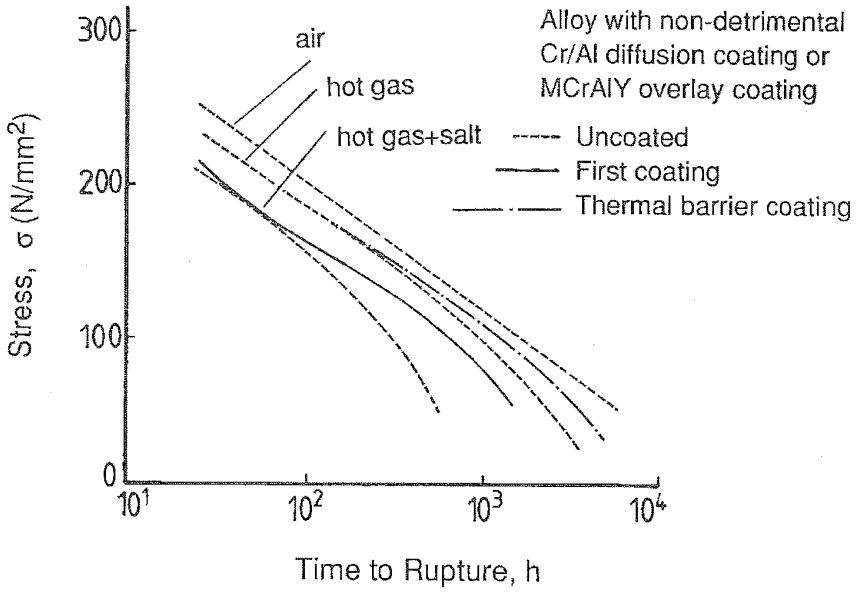

Fig.8-57b: IN 100 at 950°C. Creep Rupture Life under Imposed Hot Corrosion Conditions.
(Scweitzer & Track)

8.16. BURNER RIG DEGRADATION DATA

Service-like tests carried out in burner-rigs have been helpful in ranking the performance of various types of coatings in a variety of environmental conditions. Table 8:15 gives a number of groups of coatings evaluated in this manner, the burner rig design is not necessarily identical. Specimens tested appear to vary from a simple form of cylindrical pin or are more specifically close to the component design. Fig.8-58a shows the schematic of a burner rig. Specimens are evaluated in several combinations, broadly along the following lines:

1. Coated and uncoated; coatings from various processes, variations in coating thickness, variations in substrate shapes, preparation and heat treatment,

2. Isothermal and cyclic temperatures,

3. Hot gas - in varied velocities with various potentials of pO_2, pS_2, SO_2, pSO_3, pH_2, pH_2O, pCO, pCO_2, pCH_4 etc.,

4. Air intake injected with combinations of sulphates, chlorides, vanadates, etc.,

5. Erodent additions in the gas stream, the particles being carbon, sand, salt (e.g. sulphate, chloride) etc.,

6. Hot gas spinning tests,

7. Creep and fatigue tests, and,

8. Temperature and load cycling conditions.

Conclusions drawn on coating performance on IN 100 from one such series of tests summarize as follows (Schweitzer & Johner 1985):

Diffusion Aluminides: High temperature/low activity (HTLA) aluminides show adequate hot corrosion resistance at <950°C for lifetimes <1200 h; High temperature/high activity (HTHA) aluminides tend to reduce creep life of the substrate alloy and is unsuitable for use on components likely to be subject high mechanical stresses. Cooling passages are protected by HTHA coatings. Re-aluminiding is possible with a small loss in the substrate alloy.

MCrAlY Overlay Coatings: LPPS or PVD coatings allow longer lifetimes of x3-x4 over the aluminides up to about 1050°C with tolerance to higher corrosion. Coatings, however, need to be on parts directly visible, but can be renewed without loss of substrate alloy.

Modified Aluminides: Coatings in this class such as Pt-aluminides - LDC 2, RT 22 etc., are preferable to MCrAlY on complex shaped components like nozzle guide vane segments.

9.11. FUNCTIONS OF HIGH TEMPERATURE COATINGS

High temperature coatings are required to provide resistance to the following effects:

- abrasion
- corrosion in aggressive media
- cyclic operating conditions (thermal and stress)
- erosion
- excessive heat flow
- friction
- interdiffusion
- oxidation
- wear

Coatings are also used as catalysts in high temperature processes.

Tables of coatings and their functions are given in Tables 9:7 to 9:9.

Key:				
	ER	Erosion	DB	Diffusion Barrier
	FR/WR	Friction & Wear	HC	Hot Corrosion
	OX	Oxidation	NI	Nuclear Industry
	TB	Thermal Barrier		

Note:- No individual references are indicated; several sources have been cited from literature; list may not be exhaustive.

CHAPTER 10

Strategic metal conservation, coatings achievements, and future

10.1. INTRODUCTION

The following two sections of this last chapter survey the role of high temperature coatings in conserving strategic metals, and the extension of working life achieved by reclamation, replacement and re-coating procedures. The present achievements of coatings are also assessed in these two sections and the last section sums up the current status and future efforts required to provide the much needed fundamental data together with research and development work necessary for further improvement in coating life and increasing efficiency.

10.2. COATINGS TO CONSERVE STRATEGIC METALS

Eight metals which are vital to the European and World economy are classed as strategic metals, viz. Cr, Co, W, Mn, V, Mo, Nb and the Pt group (Anon., Inst.Mech.Eng. 1981). The definition of strategic materials, which includes non-military uses, has been discussed (Archer 1980). Listings of strategic minerals have been compiled (Hargreaves and Fromson 1983). Table 10:1 shows prices and reserves available. Summarised information is provided below on strategic metals, their uses and sources (Anon., Inst. Mech. Eng. 1981).

Cr: This is one of the main alloying elements added for corrosion resistance and application of coatings can be expected to reduce the percentage required in substrates. The main sources of this

metal are S.Africa, Zimbabwe and a small amount for Scandinavia (ferrochrome). USSR reserves are falling and USSR import from Africa may soon be necessary.

Co: This is also a vital anti-corrosion alloying element and coatings can be expected to reduce requirements in substrates. Zaire and Zambia are the main suppliers. Belgium is the main European importer and distributor. The main uses are in magnets, superalloys and cemented carbides.

W: This is used in high speed W-Mn steel and for WC tipped tools. It is imported mainly from Portugal, Thailand and East European countries, although the main reserves are in China, Canada, USSR an USA. There are W reserves in Austria and Turkey, and also in the UK, sufficient to allow exports, but these are presently undeveloped.

Mn: This is used in most steels and would be very difficult to substitute for. The main reserves are in S.Africa, USSR and Australia. Coatings applications cannot alleviate shortages of Mn or W.

V: This is used in alloy steels, high temperature alloys and catalysts. The main sources are USSR and S. Africa. Precipitates of vanadium carbide in steels confers hot strength and creep resistance and coatings cannot alleviate shortages of V.

Mo: This is mainly used in alloy steels and the major reserves are in N. and S. America. As its main use is to improve the mechanical properties of steels, coatings cannot alleviate Mo shortages. It would be very difficult to substitute for Mo in Nimonic alloys where it is also an important constituent.

Nb: This is an alloying element in steels and superalloys, added for grain refining in steels and for creep resistance. In its acid corrosion-resistance aspect its use could be reduced by applying protective coatings. The main reserves are in Brazil, USSR and Canada.

Pt, Pd, Rh, Ir, Ru and Os: The concentration of these rarely exceeds 10 parts per million even in the richest deposits. Chemical inertness, catalytic activity and high melting points are their important properties. None of these materials is likely to be reduced in quantity required, by the application of coatings.

Much of the literature on strategic materials is of limited availability. The survey published by Strang et al (1984) is a useful source of accessible references. Table 10:2 shows strategic materials imports. The USA, EEC and Japan depend greatly on imports but the COMECON countries are self-sufficient except for Co. Stockpiling of strategic metals in the USA is mainly intended for military use and not available for general use.

Substitution technology has been discussed but little specific attention has been given to using coatings technology for saving strategic metals. It is felt that industry has little incentive to invest in research and development just to find solutions which would only be used in an emergency. Table 10:3 gives various approaches to the strategic materials problem (Strang et al 1984). Use of all coating methods could be quickly increased in the event of a severe Cr shortage, but advances in coating processing methods should be pursued to develop the technology into a usable option for any emergency. The lead-time is very short in an emergency and so an information stockpile on substitution and conservation technology is also a stockpile of time and is of low cost.

Non-coatings approaches, such as joining very different materials can produce items with strategic metals only in the places where they are really needed. Machining losses can be reduced by contour forging, flow turning and powder metallurgy. Some parts can be made re-usable if only the coating needs to be replaced.

Cladding with stainless steel allows Cr reduction (where the Cr is used for corrosion or wear resistance. Electroless Ni plate and nitriding can be similarly used. Pack chromising on steel can replace ferritic stainless steels and pack aluminizing of steel gives oxidation resistance similar to Cr-steels.

Coating efforts to reduce the content of the strategic element Co in the hot section of gas turbines involves replacing Ni for Co in substrates and reducing the Co content of coatings. The coating developments which allow this are (Hecht & Halfpap 1984):-

1. Development of MCrAlY overlay coatings.
2. Pt-modified diffusion aluminide coatings.
3. Thermal barrier coatings.
4. Development of multiple layer coatings.
5. Wear resistant coatings.

CoCrAlY coatings with 67%Co gave a 3-fold increase in corrosion life of first stage blades and allowed higher strength Ni-base superalloy vanes to replace the Co-base aluminide-coated vanes; this reduced Co requirements by 36Kg per engine.

NiCoCrAlY coatings were developed for higher temperature use, giving higher ductility. They have the same hot corrosion resistance as CoCrAlY but contain 45% less Co. NiCoCrAlY coatings on new Ni superalloys containing no Co and Cr give corrosion resistance similar to conventional coated conventinal Ni superalloys (Strang et al 1984).

Pt aluminides do not give the corrosion protection of CoCrAlY but have contributed to Co saving. Pt is strategic but only $0.01 g/cm^2$ is used in coatings (1/60 of the Co used in CoCrAlY) (Hecht & Halfpap 1984).

Co-base sheet metal alloys are preferred over Ni-alloys for their better creep/rupture strength and fatigue properties. To substitute Ni alloys for Co alloys, thermal barrier $MgO.ZrO_2$ coatings were developed to get about 60 C degrees substrate temperature reduction. There is a 7-fold reduction in Co usage for these alloys.

Use of thermal barrier coatings on turbine airfoils has developed considerably to enter the field of practical application, but the system requires further investigation for a fool-proof consolidation.

The best area for reducing strategic metals, apart from redesign, is component life extension.

TABLE 10:1

STRATEGICALLY SENSITIVE MATERIALS

ELEMENT	PRICE*		RESEERVE INDEX*** years
Chromium	£4400/tonne, lump (UK) $3.750/lb, electrolytic (US)	£3650**	340
Cobalt	$7.20/lb (Europe) $6.65/lb (US) $11.30/lb as shots	£25000**	49
Tungsten	£13.50/kg metal powder	$6700**	47
Manganese	$1920/tonne, electrolytic $1810/tonne, flake	£780**	190
Vanadium (as V_2O_5)	$2.65/lb	£3700**	340
Molybdenum	$3.20/lb Mo (canned molybdic oxide)	£20000**	83
Niobium	$2.90/lb (ore with Ta-oxide)	£30000**	950

* Millbank (1987) (metal prices are not quoted where ore prices are indicated)
** Solid, pure, basic forms, London, January 1982
*** Reserve Index = Known World Reserves/Current Prodn. Rate (this figure does not take into account any future increase in the production rate).

TABLE 10:2

NET IMPORTS AS A PERCENT OF CONSUMPTION

MATERIALS	U.S	E.E.C	JAPAN	COMECON
Manganese	98	100	99	3
Cobalt	97	100	100	68
Bauxite	91	97	100	28
Chromium	91	100	98	2
Asbestos	85	90	98	1
Nickel	70	100	100	13
Zinc	57	91	74	9
Iron Ore	48	82	100	5
Silver	36	93	71	10
Copper	13	100	97	4
Lead	13	76	78	3
Phosphate	Export	99	100	23

Source: Bureau of Mines data (1977)

TABLE 10:3

WORLD PRODUCTION & CONSUMPTION*

MATERIAL	YEAR	PRODUCTION	CONSUMPTION
Al	1986	11938000	6585100
	1985	15428700	16138200
Ni	1986	446800	341000
	1985	762700	786800
W	1985	43382	46629
(ore & concentrate)	1984	43699	48490

* Tonnes; figures do not include data from communist countries (Millbank 1987).

TABLE 10:4

DISTRIBUTION OF R&D FUNDING FOR CRITICAL MATERIALS BY TECHNOLOGY GOAL

TECHNOLOGY GOAL	FUNDING IN $1000		
	DIRECT	RELATED	TOTAL
Substitution	9,648	13,960	23,608
New Sources	10,258	2,523	12,781
Reclamation	560	1,850	2,410
Life Extension	28,010	3,060	31,070
Conservation	1,585	2,400	3,985
Total, all technology	50,061	23,793	73,854

TABLE 10:5

WEIGHT % OF STRATEGIC ELEMENTS USED IN THE MANUFACTURE OF AN F100 GAS TURBINE ENGINE

ALLOY	Cr	Ni	Al	Ti	Ta	Cb	Co
Cobalt base:							
MAR-M 509	23.4	10	-	0.2	3.5	-	55
MAR-M 302	21.5	-	-	-	9	-	58
WI-52	21	-	-	-	-	-	64
Nickel base:							
B1900	8	65	6	1	4.3	-	10
IN100	9.5	61	5.5	4.7	-	-	15
MAR-M-200	9	61	5	2	-	1	10

TABLE 10:6

STRATEGIC ELEMENTS IN COBALT- & NICKEL-BASE SUPERALLOYS USED FOR CAST TURBINE VANES & BLADES
(Composition given in weight percent)

ALLOY	Ni	Cr	W	Nb+Ta	Co
Cobalt base:					
L605	10	20	15	--	53.5
Ha 188	22	22	14.5	--	41.4
Nickel base:					
Hast X	Bal	22	0.6	--	1.5
IN 625	Bal	21.5	21.5	3.65	0

TABLE 10:7

STRATEGIC ELEMENTS IN Co- & Ni-BASE SHEET ALLOY USED IN COMBUSTOR, AUGMENTOR & TURBINE NOZZLES (wt%)

Alloy	**Ni**	**Cr**	**W**	**Nb+Ta**	**Co**
Co-base:					
L605	10	20	15	-	53.5
Ha 188	22	22	14.5	-	41.4
Ni-base:					
Hast.X	Bal.	22	0.6	-	1.5
IN625	Bal.	21.5	21.5	3.65	0

10.3. PRESENT ACHIEVEMENTS & FUTURE REQUIREMENTS OF COATINGS

Chapters 1 and 2 gave a broad outline of the high temperature areas and systems which required coating applications. Further requirements and present achievements of coating applications in the following areas are indicated in this section:

- Aerospace
- Combustion engines
- Energy conversion (MHD, solar, H.T. fuel cells, coal gasifiers)
- Industrial (e.g. petrochemical, glassmaking, machine tools)

Further development work is needed for coatings forming dense glasses, complex oxides or spinels, and self-healing coatings for longevity (Kear & Giessen 1984; Das & Davis 1988).

10.3.1 AEROSPACE:

Engines operating at 1000°C and rocket nozzles at higher temperatures need refractory and oxidation resistant coatings. A several hundred degree temperature reduction is achieved by applying ceramic thermal barrier coatings. Thermal barrier coatings are an important area needing further research. Abradable coatings are needed to restrict gas escape around turbine blading and through labyrinth seals, at 700 to 1000°C, e.g. Ni-Cr-Fe-Al and aluminium bronze, containing BN (Sickinger & Wilms 1980).

Improved coatings are needed for Nb alloys for use above 1500°C, for Mo and Ta alloys 1650°C and for W alloys above 1820°C. Creep occurs in Si20Cr20Fe coatings on Nb alloys at 1465°C, although scratches are self-healing by slow oxidation and cycling does not affect ductility. $MoSi_2$ on Nb forms a protective SiO_2 layer and is a successful coating because it has the same thermal expansion as the substrate. $MoSi_2$ on Mo is good up to 1760°C. V-(80Cr20Ti)-Si coating on Nb alloys reduces the tensile strength of 20 mil sheet by 25% at 25°C and 1205°C and fatigue 50% at 25°C, embrittling the substrate, but the bcc coating is ductile and resists air oxidation at 1260°C. CrSiTi coatings on Nb alloys resist 150 oxidation cycles at 1444°C, better than VSi_2 coatings. W barrier layers between Ni30Cr and Ni30Cr20W + 3 to 5% Al coatings on Cr5W0.1Y prevented interdiffusion with resistance to cyclic oxidation over 600 hours at 1150°C. ThO_2 and HfO_2 with a W diffusion barrier layer on Ta10W resist air oxidation up to 2482°C. Cr_5Al_8 and $(FeCr)_xAl_y$ coatings on Cr5W0.1Y were also satisfactory (Allen 1968). Claddings of Hf-24Ta-2Cr-1Si on Nb alloys and Hf-24Ta-1.2Cr-0.7B-0.12Al cladding on Ta-10W extends oxidation life 25 hours at 1482°C; minor elements decrease oxygen diffusion by occupying octahedral sites in HfO_2.

$SrZrO_3$, $Nd_2Zr_2O_7$ and $Yb_2Zr_2O_7$ are structurally stable coatings on W, good in vacuum, with no vaporization or reaction of the coating with substrate or O_2. On Ta10W, $MoSi_2/ZrO_2$ and WSi_2/ZrO_2 showed good spalling resistance to cylic oxidation and lasted longer than 23Sn5Al or 7Mo coatings (Allen 1968c). 20Cr20Fe60Si

and CrTiSi coatings on Nb alloys are good in subsonic air at low presssure at 1538°C (Allen 1968a,c). Bend tests showed Ir on Nb is ductile but on W and Mo is brittle (Allen 1968a). SiO_2 coatings on refractory metals have limited self-healing at low temperatures due to cracking of the glass formed. Otherwise, glassy oxides flow and accommodate mechanical strain. But SiO is evolved at low pressure. Pt- Ir coatings on aerospace alloys form volatile oxides but are useful due to boundary layer effects retarding the loss. Ir is satisfactory on graphite. Modified silicides performed better than FeCrAlY, Pt, Pd and Al on Cr-5W-0.1Y and were the best coatings in a series tested on Ta and W alloys. Large and complex Mo shapes can be silicided but joining problems and a tendency for brittle fracture and dependence of strength and ductility on a strain hardened state limits use (Nat.Acad. Sci.1970).

Good erosion and fatigue resistance is shown by 35W35Mo15Ti15V and CrTiSi coatings on Nb alloys at 1205°C. High fatigue strength plus oxidation resistance is achieved by CrFeSi coatings on XB88 (Allen 1968a). V-(80Cr20Ti)-Si coatings on Nb alloys resist oxidation at 2300°F but the ductile bcc coating reduced the tensile and fatigue strength of the substrate by embrittlement (Allen 1968c). Cr ion implanted steel bearings are used in U.S. aircraft to increase corrosion resistance (Anon. 1984)

10.3.2. COMBUSTION ENGINES:

10.3.2.1. Gas Turbines:

Requirements include overlay coatings processes for low cost quality coatings, coatings for erosion protection which are compatible with overlay coatings and coatings processes for internal blade passages. Requirements for both alloys and coatings are reviewed (Kear & Thompson 1980; Foroulis & Petit 1976; Perkins 1982; Goward 1986; Stringer 1987; Rahmel et al 1985; Lacombe 1987; Miller 1987; Lewis 1987; Gurland 1988; Wadsworth et al 1988).

Thermal efficiency improvement and corrosion resistance requires coatings for gas turbine components. Metallic coatings reduce corrosion and ceramic types act as thermal barriers to reduce static component temperatures. Problems in adherence and thermal shock resistance of ceramic coatings prevents their use on rotating blades (Herman & Shankar 1987).

Alumina coatings on aluminised superalloys are successful due to the thin and thus adherent film with good mechanical properties. Failure is due to Al diffusion into the substrate reduced by using an Sn-Al coating in which Sn flow fills defects. But vaporization can cause breakdown. Oxides and carbides reduce high temperature creep of Nb alloys, but Ti regresses this by reducing these oxides (Nat.Acad.Sci. 1970). Aluminided Ni and Co alloys

(Anon. 1984) and Al-Pt, Cr-Al, Si-Al, Cr-Al/Pt and NiCoCrAlY on IN738LC and FX414 Ni and Co alloys have increased oxidation life. Some deleterious sigma phase formed in the Ni alloy, but no coating/substrate interaction occurred for the Co alloy. 25Cr3Al-10Ni5Ta0.2Y57Co coated IN738 showed no penetration in 13000 hours with 225 engine startups but uncoated IN738 showed 180 microns intergranular penetration . Pack aluminised and chromised IN100 developed stress due to the coatings (Betz 1979). Pack aluminised CrAl, SiAl, PtCrAl, and NiCoCrAlY coatings on IN738LC and FX414 were unaffected in their tensile, rupture and fatigue properties if the normal heat treatment was done after coating (Strang 1979). Good thermal stress resistance was achieved on aerofoils by ZrO_2-MgO and ZrO_2-Y_2O_3 coatings on superalloys and directionally solidified alloys (Pettit & Goward 1983). An inner NiAl or NiCr layer improved fracture properties in 7000 hours tests at 900°C (Mozar et al 1973). Otherwise, thermal cycling de-bonds such coatings. The presence of salt melts however prevents use of coatings such as ZrO_2-12%Y_2O_3 on Ni-16Cr-6Al-0.6Y intermediate layer on superalloys, due to absorbtion of salt in the porosity and subsequent thermal shock failure. Better resistance is obtained with glassy coatings like $2CaO.SiO_2$ or with a MgO- NiCrAlY cermet, on superalloys (McClanahan et al 1974). Pt in coatings for gas turbines has recently been reviewed (Anon. 1983).

NaCl vapour spalls the protective alumina layer on CoCrAlY coated superalloys (Jones et al 1975), although adherent, and crack-free fine grain structures are achieved (McClanahan et al 1974). NiCrAlY with a Pt top coat on a Ni-Nb-Cr-Al directionally solidified alloy gave protection for 1000 hours at 1366°K in a rig test, with very good interdiffusion resistance to 1478°C. Electron beam coating gave the best oxidation resistance and a long stress-rupture life and thermal fatigue resistance were achieved (Goward 1970).

Six and seven element MCrAlY-type coatings containing elements with widely varying vapour pressures can be produced, e.g.NiCoCr-AlYHfSi by EB-PVD. With a multi-source evaporation unit, coatings with composition graded from substrate to surface have been produced, as well as multiphase structures containing oxide dispersion. Zirconia coatings are important in the combustion zones of aero gas turbine engines. There is a need to develop thicker coatings or monolithic materials. Further work is needed on production of strain-tolerant ceramic thermal barrier coatings for combustion zones.

Good mechanical properties are reported for some coatings in the series Ni/Al, Ni/C, Co/WC, NiCr/diatomite, Ni/$WTiC_2$, NiCr/Cr_3C_2, Ni/CaF_2 and NiO/CaF_2, on superalloys (Clegg et al 1973). The corrosion resistance of Cr-Al and Al on Fe and Ni base alloys improves with thickness but the rupture and fatigue strength falls (Fitzer & Maurer 1979). Other studies on aluminide coatings on Ni and Co superalloys (Pichoir 1979; Duret & Pichoir 1987; Martinengo et al 1979) recommend the presence of Y. A Ta barrier layer under Al-Cr coatings prevents interdiffusion from degrading

the coatings, but these coatings are damaged by carbide intrusions from unburnt fuel. Al-Pt on Ni alloys gives increased oxidation life (3 times better than NiAl) but some substrate interaction forms sigma phase (Ubank 1977; Grunling et al 1987).

10.3.2.2. Diesel Engines:

Reducing heat losses increases efficiency but raises temperatures. Thus thermal barrier coatings are needed on valves, piston crowns and cylinder heads. To improve efficiency the engine can be operated uncooled, viz. the adiabatic engine (Fairbanks & Hecht 1987), requiring thermal barrier coatings such as zirconia. At least 3.5mm is needed to obtain an 80% heat loss reduction. This is beyond plasma spraying capabilities and thinner zirconia on a metal fibre layer has been suggested (Kamo et al 1979; Kvernes & Forseth 1987).

If cylinder liners are made from a solid ceramic, the piston rings need a wear resistant coating with compatible thermal expansion. Multicomponent plasma coatings can be self-lubricating up to 870°C (Sliney 1979), e.g. 30% nichrome, 30% Ag, 25% CaF_2, 15% glass (to prevent nichrome oxidation). Ag improves wear properties at lower temperatures (start-up). Stabilized ZrO_2 on a NiAl or NiCrAlY bond coating, graded and up to 0.8mm thick have perfomed well on piston crowns of marine diesels using normal fuel. Low quality fuel contains V which reacts with the Y_2O_3 or CaO stabilizers in the ZrO_2 and causes disintegration. MgO stabilizer is more resistant (Kvernes 1979). Large diesel engine piston heads plasma spray coated with self-sealing ceramic resisted sulphurous combustion gas attack up to 1500°C under severe thermal shock and fatigue stress (Perugini 1976).

Braze/cermet/ceramic coatings on steel (AISI-4320) gave very good corrosion resistance with hot wear and thermal shock resistance and good tensile and shear resistance (Houben & Zaat 1973). Pt, Ir and Pd are recommended for engine exhausts. W, Mo and piano wire coatings by wire explosion on mild steel and Al gave 5 times better adhesion than flame sprayed coatings (Kirner 1973). Cr_3C_2/Mo and Ti-Ni alloy with 3% free C as coatings on piston rings on marine diesel engines showed improved wear resistance compared with grey cast iron (Solomir 1973). Stabilized ZrO_2 coatings on steel components had big tensile strength differences (Kvernes 1983). Kvernes has recently discussed coatings for diesel engines (Lang 1983).

WC-12Co, 75CrC-25(80Ni20Cr), Mo and 80Ni-20Cr coatings on steel and Al-alloys are used for abradable seals in compressors, turbines and bores of hydraulic cylinders; plasma sprayed coatings are better than hard Cr. Sandwich coats perform better under thermal cycling (Malik 1973).

10.3.3. ENERGY CONVERSION:

10.3.3.1. Coal Gasifiers:

Fire-side corrosion of power station boiler tubes, especially with high Cl content coal, is a problem around 640°C. Higher Ni and Cr content claddings on stainless steel tubes reduce this corrosion. Flame sprayed coatings have not yet been very successful. Plasma sprayed coatings are difficult to apply in-situ. The shut-down cost of a power station plant is up to 50000 pounds per day (Flatley et al 1980); coating development, therefore, is certainly justified (Meadowcroft 1987; Colson & Larpin 1987; Debruyn et al 1987; Restall & Stephenson 1987).

The low oxygen (10^{-15}) atm and high S (10^{-8}) activity in coal and oil gasifier and coal fluidised bed combustors will cause sulphidation of Ni based alloys (forming low m.p. eutectics) and Fe alloys like FeCrAlloy are preferred. High pressure hoppers and valves are used for discharging hot char and ash at 1100°C (but metal temperature probably about 550°C) and valve seat inserts of stellite, silicon nitride or boron nitride are used. Need exists for other materials and coatings. Electrodeposited TiB_2, CVD SiC and B diffused into Mo or WC/Co are very erosion resistant and thermal cycling resistant up to 700°C (Hansen 1979)if at least 60 microns thick.

Heat exchangers are needed for waste heat recovery if SO_2 removal is done by cooling the gases. Coatings could protect heat exchangers. Plasma sprayed and then laser fused CoCrAlHf coatings (Packer & Perkins 1980) and slurry fused CoAl and CrAlHf (Dapkunas 1980) have good corrosion resistance but would be very difficult to apply to large heat exchangers. Claddings of FeCrAlMoHf (Perkins & Packer 1979; Lathem 1980), FeCrAlloy A and Super-FeCralloy , are probably the most suitable protection. Wrought MCrAlY and MCrAlHf on gasifier alloys, are better than cast versions (Packer & Perkins 1980).

Si on Ni20Cr alloy at 900°C in oxygen plus 80%$V_2O_5$20%Na_2SO_4 for 600 h, gave an 80% reduction in corrosion (Elliott & Taylor 1979; Wahl & Furst 1979). Cr on Nim 80H and IN738LC improved corrosion resistance in engine and crucible tests (Bauer et al 1979). On the more suitable Fe-based coal gasifier alloys, MCrAlY and MCrAlHf (M=Co, Fe or Ni), alumina-forming coatings were best (with 8-10% Al); mechanical properties were better with wrought alloys than cast (Packer & Perkins 1979). Laser surface fusion improved uniformity.

Some problems are reviewed (Robinson 1981; Southwell et al 1987; Meadowcroft 1987). A maximum corrosion rate of 50 nm/h is needed for 100000 hours tube life. Reduction of furnace wall corrosion by using finer coal particles, better distribution to each burner and increased secondary air to raise pO_2, have only given marginal corrosion reduction. Materials improvement is thus necessary and coextruded tubes have been evaluated. 18% Cr austenitic

steel suffers from stress corrosion cracking on the water-side, so coextrusion is used to prevent its waterside exposure and present a ferritic carbon steel core to the waterside. 30000 hours satisfactory service is reported (Hara et al 1978). Further work is needed on coatings (cladding) for coal gasifier environments.

Aluminide coatings on steel resist hydrocarbon and sulphide atmosphere corrosion and increase oxidation resistance. They are expected to have wide applications in coal gasification and liquefaction plants. Aluminized steel is better than stainless steel where oxidation-carburization is the main surface degradation.

10.3.3.2. Nuclear Reactors:

Advanced gas-cooled reactor (AGR): UO_2 pellets in 20Cr/25Ni/Nb stainless steel tubing are cooled by CO_2 at 40 atm., reaching 750 to 850°C. CVD SiO_2 on pre-oxidised 20Cr/25Ni/Nb stainless steel inhibits carbon deposition and spalling at 825°C, in 6000 hour tests (Bennett et al 1981).

Fast breeder reactor (FBR): Moving fuel handling components need protection only against wear and fretting corrosion in liquid Na. These components normally contact the Na only when it is cooled to about 250°C (from the 600°C operating temperature). Ferritic and austenitic steels are not significantly attacked by liquid Na at 600°C.

High temperature gas-cooled reactor (HTR): The He reactor atmosphere restricts oxide formation, so sliding movements (due to differential thermal expansion) cause galling or adhesive wear due to self-welding. Coatings are needed to stop this up to 950°C and for the reactor life duration. Plasma sprayed, D-gun and CVD ceramic and cermet coatings have been tested (Engel & Klenmann 1981); ZrO_2 and TiC performed well in wear tests up to 950°C but ZrO_2 disintegrated at long times due to phase destabilization. Further research is needed.

Sliding wear and corrosion resistance are areas where ion implantation has contributed but the very small penetration depth is a limitation and time dependence of corrosion protection needs study (Gebhardt et al 1978). The beneficial effects achieved by ion implantation has been updated (Bennett 1983; Bennett & Tuson 1988/89). HTRs also have the problem of radioactive tritium diffusing out through the heat exchanger tube walls (Van der Biest 1979). Oxide films on superalloys are good tritium diffusion barriers. Studies are in progress on the use of Al_2O_3 and SiO_2 coatings.

Fusion Reactors: Inner walls of the stainless steel or Cu plasma vessel receive high energy particle bombardment and high thermal

loading. Material thus eroded contaminates the plasma and cools it, more effectively for high atomic mass contaminants. Low atomic mass coatings are under study: TiC, TiB_2, B_4C and B (by CVD); TiB_2, Be and VBe_{12} (by plasma spraying); SiC (by sputtering); C and Be (by vacuum evaporation). The hottest parts are water cooled and are typically Cu-Cr alloy explosively clad with Ni-Cr alloy; surface temperatures are about 500°C.

General: The corrosion problems encountered in general are summarized by Quadakkers 1987. Ti, Mo, Zr, Nb and Ti-6Al-14V coatings on structural steel gave improved hardness with good adhesion (Muller 1973). TiC, VC, NbC and Cr_7C_3 coatings give good wear resistance (Child 1983). Sn on Zircalloy-4 prolongs the time taken for mechanical breakdown which occurs due to insufficient plasticity of the ZrO_2 layer (Hauffe et al 1975). Other successful coatings include SiO_2, CeO_2 and ZrSi (Bennett 1983; Niklasson & Granqvist 1982).

10.3.3.3. Magneto Hydrodynamic Converters:

A very hot fast gas jet is directed between the poles of an electromagnet. Presence of some alkali metal ions makes the gas conductive and electrodes collect the electric current thus induced. Co, CO_2, H_2O and N_2 from burnt coal, plus some K_2CO_3 at 2500°C produce problems in the ducting similar to those in slagging gasifiers. Refractory linings, or water cooling, may protect metalwork, but electrodes (water cooled Cu covered with stainless steel and an electrically conductive ceramic thermal barrier) have corrosion problems. Stabilised ZrO_2 is conductive above 1100°C but near the metal ZrO_2-Inconel cermet is needed to increase conductivity. Plasma spraying a graded composition minimises thermal mismatch effects but is slow to give the required 4mm thickness.

10.3.3.4. Solar Energy Converters:

Photovoltaic, photochemical or photothermal effects may be used. Solar heat collectors focus energy on a coated tube having a high absorption in the solar spectrum and low infrared emissivity. Coatings are oxides or semiconductors of controlled thickness, morphology and composition. Coatings are needed with long term thermal degradation resistance and good adherence under thermal cycling. The theories required for the optical properties of cermet coatings for selective absorption of solar energy have been outlined (Niklasson & Granqvist 1982). The theories are then used to interpret the evaluated complex dielectric function of coevaporated Co-Al_2O_3 cermet films. Finally these data are used to modify surface coatings with optimised spectral selectivity.

Radiative cooling was demonstrated for practical use with Si_3N_4 coatings on a reflective substrate. The dielectric function of evaporated Si_3N_4 is reported and employed to evaluate the obtainable cooling power and temperature difference (Eriksson et al 1982). Reactive ion plating is used to deposit InN for high efficiency solar cells (1.8 eV energy gap) (Takai et al 1982a,b). For effective collection and retention a solar collector must absorb at wavelengths below 2 microns and not radiate above 2 microns. Such selective absorption is obtainable by several methods: Mattox & Sowell 1974; Koltun 1971; Drummeter & Haas 1964. Suitable coatings include Si, Ge and PbS. Thickness control gives destructive interference at the wavelength of the solar maximum; energy reflectance is also reduced by anti- reflection coatings or by porous coatings. Cu can be blackened by a $NaOH + NaClO_2$ mixture and steels can be blackened by other treatments (Mattox & Sowell 1974). Dendritic surfaces have been developed for high temperature solar collectors (Pellegrini et al 1979).

10.3.4. INDUSTRIAL (Petrochemical, glassmaking, machine tools):

Coatings achievements cover a wide industrial range. Ceramic coatings protect graphite crucibles from corrosion by liquid Al; metal casting mold life is doubled by self-sealing ceramic coatings which decrease carburizaion. But for the present discussion, the petrochemical, machine tool and glassmaking industries have been selected.

10.3.4.1. Petrochemical Industry:

Most problems occur in oil and gas fired tube furnaces (Swales 1979; Edeleanu 1980). Fireside temperatures are about 1150°C. For strength, high alloy cast austenitic steels are used, giving adequate corrosion resistance. Carburization occurs in ethylene production. Carbon (coke) deposits thicken and tube temperatures need raising to maintain heat transfer. On reaching 1100°C cleaning is essential. Progressive carburization, called 'metal dusting' in extreme cases, occurs. Plasma spraying inside straight tubes with Cr, using a tubular plasma head in Ar, improves carburization resistance (Arcolin et all980). Subsequent saturation with ceramic paint fills pores. Sulphidation occurs in processes using CS_2 and H_2S.

Fuel ash (from residual oil) fireside corrosion is prevented by duplex centrifugally cast tubes, with an outer wall of 50%Ni50%Cr. Refinery furnace tubes are used at 550°C in desulphurization plant with Al diffusion coatings, but if too large it requires coating to be done in sections which gives a welding problem of how to protect the welded zones (McGill & Weinbaum 1979; Meadowcroft 1987).

Burner plates at 10^6 kcal/dm^2 at 1700°C in oxidising and carburizing conditions are protected by ceramic coatings. Combustors of hydrocarbon crackers have been protected from overheating and corrosion by 3 mm thick self-sealing ceramic coatings and soot scrapers in hydrocarbon crackers were found to withstand the hottest flame areas (Perugini 1976; Herman & Shankar 1987; Miller 1987).

Most petrochemical processes can work below 600°C and there is little interest in coatings designed for higher temperatures.

10.3.4.2. Glass Manufacturing:

Pt alloys containing 5% Au, are not wetted by molten glass but have insufficient hot strength. Adding Rh for strengthening lowers chemical resistance and causes embrittlement. A dispersion of 0.1% ZrO_2 in 5% Au Pt avoids these problems (Heywood & Benedeck 1982). Contamination of glass melts gives (unwanted) coloured glass and Pt coatings are widely used in the glass industry. Alternative cheaper coatings are being sought. Linings of mullite, Ca and Mg zirconates and silicides have been tried and plasma sprayed NiAl with some success (Nat.Acad.Sci. 1970).

For spinning of glass fibres for thermal insulation purposes, molten glass is passed downwards through a Pt sieve to spread out the stream and then into a fast rotating Rh-Cr-based spinner about 30 cm diameter and 10 cm deep. This cylindrical spinner has about 20000 small holes in its edge and strong external vertically-downwards directed flames force the emerging glass fibres downwards. (Centrifugal force forces the molten glass through the holes in the spinner). The spinner lasts only about ten days and coatings may offer an extended life and be of great production benefit in reducing the 'down time' of the plant. So far no coatings have been developed for this purpose.

Inclusion of Pt particles in glass laser rods degrades performance and is due to PtO_2 formation (as Pt solubility is very low). This precipitates and decomposes to Pt on cooling. Removal of oxygen from the glass furnace atmosphere should solve this problem (Kubaschewski 1971).

10.3.4.3. Machine Tools Industry:

When tools are reground, the coating left on the unground face (cutting face, for drills; flank for millers) continues to give a significant impovement over the uncoated tool (longer life between regrinds and faster cutting). Tool costs can be reduced by a factor of 10, biggest improvements being in tough materials (reinforced plastics, abrasive composites, high strength alloy steels). Better finish is reported, often removing the need for reaming and deburring. Cutting speeds are increased between about 20% and 400% and feed rates between 10 and 100% (Boston 1983;

Hansen et al 1979). Chapter 7 gives an updated outline on wear in hard coatings.

10.4. HIGH TEMPERATURE COATINGS: PRESENT & FUTURE APPLICATIONS

Salient points which emerge from the preceding chapters and sections are summed up in this and the last section.

Coatings have to withstand complex conditions; it is essential that research programmes in different laboratories should be coordinated on a well-phased programme to test different properties of the same coating on a stand alone and in a coating/substrate configuration and that the same type of test should be agreed for each property. It is lack of compliance with these which has made it very difficult to present coherent histograms and comparison tables which are outlined in the present survey. Normalization of units in assessing and expressing physical properties, and degradation data is essential on both sides of the Atlantic and would greatly help inter-laboratory data output. In 1985 an international workshop was held to assess the field of high temperature corrosion. An international code and standardization must now emerge for future work to avoid ambiguity and uncertainty of grading coating performance. High temperature coatings technology has developed adequately to allow a standardization of test procedures, a number of which have been evolved during the course of research in the last 30 years.

It is clear that no one coating can offer all aspects of resistance. Also, coatings must be developed for specific substrates as integrated systems and cannot be adequately developed in isolation. Duplex and multilayer coatings must be studied in a graded programme to enable assesment of the influence of each of the coating layers.

Further clarifications in fundamental studies such as thermodynamic data, phase diagrams, diffusion - its thermodynamics and kinetics, corrosion kinetics, heat and mass transfer, and modeling are needed. Mechanical property measurements require to be standardized, viz. hardness, adhesion, creep, stress and fatigue. The effects of thermal treatment of coatings on the mechanical properties of substrates is a field yet to be quantified meaningfully. Thermal and mechanical fatigue is an area that needs clarification. Cyclic tests devised for each application and environment have to be formulated and standard test procedures agreed upon on an international level.

Coatings and substrates systems should be developed as substitutes for those containing strategically sensitive materials. Directionally solidified and mechanically alloyed substrates, and rapidly solidified systems have yet to be much investigated.

Several new analytical tools are now available in the fields of microscopy and spectroscopy, but with very restricted and limited

availability and are expensive for access. Research, while staying competitive should also aim to be collaborative in order to optimise time, money and team efforts, if the end result is to be the development of efficient coating systems over wide fields of application and a maximisation of its users.

10.4.1. GENERAL PROPERTIES ASSESSMENT:

A coating system has to have/be,

- High resistance to oxidation and/or hot corrosion.
- Ability to form alumina, chromia or other protective oxides.
- Resistance to embrittlement, e.g. from carburization.
- Resistance to forming low melting eutectics.
- Resistance to forming vaporizing products.
- Adherence.
- Ductility.
- Resistance to mechanical and thermal shocks and fatigue.
- Compatibility with base alloy in composition, thermal expansion and DBTT.
- Low porosity.
- Low coating/substrate interdiffusion.
- No detrimental element transfer or phase formation.
- Self healing if damaged.
- No degrading effect on substrate mechanical properties.
- Possibility of repairing damaged coatings and of welding.
- Multiple sources of coating materials and alternates if strategic.
- Overall cost-effectiveness.

(Note that each application has its own list of priorities)

10.4.2.. FUTURE WORK IN COATINGS FOR GAS TURBINES:

Corrosion and degradation are affected by several factors. The following aspects appear to need further investigation:

- effects of elements like Ta, Ti, Nb, Si, Mn, Zr, B, Cu, P, Zn and Pb. Effects of these must be linked to specific failure modes.
- beneficial effects of Si and Ta not yet clear; siliconising embrittles coatings; electron beam evaporation of Si on CoCrAlY appears promising.
- re-coating processes without much loss of substrate.
- effect of corrosive salts on thermal barrier coatings, e.g. ZrO_2 and additive oxides added to it for structure stabilization, e.g. CaO, MgO, Y_2O_3. Other oxide additives must be sought as alternatives, if possible, and tests conducted to observe melt fluxing effects over the turbine operating and cycling temperatures.
- development of better spalling-resistant thermal barrier ceramic coatings.
- research to stabilise oxide coats formed during corrosion, to

seek an alternative to alumina.
- coating/substrate mechanical interactions causing strain in aerofoils.
- study of the role of Y in MCrAlY to promote adherence in cyclic exposures. Investigation of other elements and alloy systems to check or confirm 'monopoly' role of Y. Strategic importance of Y to be assessed.
- study of cyclic corrosion loss mechanisms.
- study of the effect Cr, Al and Ti:Al.
- study of erosion-corrosion resistance.
- effect of salt contamination on creep behaviour.
- investigation of duplex and multi-layer coats.
- behaviour of coatings on directionally solidified, PM and MAP alloys
- composite system investigation
- rapidly solidified metallic system assessment.
- metal-ceramic bonding and temperature monitoring coated devices
- cooler component temperatures and steeper thermal gradients designed for higher engine efficiency have to be accommodated, and coatings for internal cooling passages developed.

10.4.3. COATINGS FOR SUPERSONIC & AEROSPACE HARDWARE:

- improved coatings needed for Mo and Ta alloys above 1650°C and for W alloys above 1800°C.
- improved alloy development for Nb- and Zr- systems.
- coatings and composite systems for PM and MAP alloys.
- coatings and claddings match for the carbon-carbon composite.
- rapidly solidified material adaptation.
- metal-ceramic bonding and temperature monitoring coated devices

10.4.4. COATINGS FOR DIESEL ENGINES:

- more studies on plasma sprayed ZrO_2 coatings, and other types such as Mo and Cr carbides.
- denser and smoother wear resistant coatings for piston rings.
- coatings with controlled thermal conductivity.
- coatings for adiabatic diesel engines.
- erosion and fretting resistant coatings & seals.
- temperature monitoring coated devices.

10.4.5. COATINGS FOR COAL GASIFIERS:

FeCrAlY compositions have the lead as coating or cladding materials. Other candidate materials including those with dispersed oxides should be studied. A wider temperature range and more thermal cycling studies should be investigated.

Studies of component gas pressures and compositions in the fluidised bed combustor and studies which elucidate the role of deposits will support and clarify the development of coatings.

Studies to explain anomalies such as why Incolloy 800H is better in pressurised than in 1 atmosphere fluidised beds and other mechanistic studies are neccessary to provide clarifications for the development of future coating compositions.

10.4.6. COATINGS FOR NUCLEAR REACTORS:

- improved coatings for fuel cladding materials.
- improvements in borides and carbide coatings.
- further development in wear-resistant seals.
- further work on oxidation and carburization resistant barriers.

10.4.7. COATINGS FOR POWER PLANT SYSTEMS:

Development for-

- higher gas inlet temperatures.
- directionally solidified eutectics.
- refractory metal fibre reinforced superalloys.
- ceramic coatings like Si_3N_4 and SiC.
- higher ductility and toughness.
- develop coatings with chemical and mechanical compatibility with the substrate.
- combine ceramic coats and tailored cooling technology to allow $1500^{o}C$ to be exceeded with a capability of 100 N/m^2 stress to rupture in 10^5 hours.

10.4.8. COATINGS & SOLAR POWER:

Coatings are required for high temperature heat exchangers (gas cooled, liquid metal or salt cooled, steam cooled, oil cooled) and for mid-temperature solar absorbers. Coatings must tolerate daily thermal cycling. Bimetal claddings or overlays seem likely candidates; stainless steels or superalloys may have to be cost-justified. Absorber coatings of black Cr, Ni or Co with high selective absorbtion and low emissivity are required. Abrasion resistance would be a necessary feature.

10.5. COATING PRODUCTION METHODS: FUTURE WORK

10.5.1. EVAPORATION:

Process refinement is needed in EBPVD for :- avoidance of spits from the melt pool which degrade coatings, corrections for the occurrence of columnar defects, and, work on the kinetics of depositing atoms, its effect on coating quality, and laser sources for evaporation.